Energy Management Systems for Multi-Microgrid Networks Under Uncertainties

by

Carlos Ceja Espinosa

A thesis
presented to the University of Waterloo
in fulfillment of the
thesis requirement for the degree of
Doctor of Philosophy
in
Electrical and Computer Engineering

Waterloo, Ontario, Canada, 2023

Examining Committee Membership

The following served on the Examining Committee for this thesis. The decision of the Examining Committee is by majority vote.

Supervisor:	Claudio Cañizares University Professor Dept. of Electrical and Computer Engineering University of Waterloo
Supervisor:	Mehrdad Pirnia Lecturer Dept. of Management Sciences University of Waterloo
Internal Member:	Kankar Bhattacharya Professor Dept. of Electrical and Computer Engineering University of Waterloo
Internal Member:	Mehrdad Kazerani Professor Dept. of Electrical and Computer Engineering University of Waterloo
Internal-External Member:	Jessie Ma Assistant Professor Dept. of Systems Design Engineering University of Waterloo
External Examiner:	Bala Venkatesh Professor Dept. of Electrical, Computer and Biomedical Engineering Toronto Metropolitan University

Author's Declaration

I hereby declare that I am the sole author of this thesis. This is a true copy of the thesis, including any required final revisions, as accepted by my examiners.

I understand that my thesis may be made electronically available to the public.

Abstract

Environmental concerns have motivated a gradual transformation of power systems in recent years, mainly focused on replacing fossil fuel-based energy sources with Renewable Energy Sources (RESs) such as solar and wind energy. However, due to their variable nature, the large-scale integration of RESs poses several technical challenges for the safe and efficient operation of evolving power systems. The adoption of microgrids (MGs) has increased as a viable option to effectively integrate RESs into existing grids and reduce the dependency on conventional, centralized power stations, as well as enhancing the electrical supply resiliency. Furthermore, MGs can provide sustainable energy to remote areas in which a connection to the main power grid is not possible. In this context, the Energy Management System (EMS) of the MG, which is responsible for determining its optimal operation, is an important part of MG control. However, the variability of electricity demand and RESs within an MG complicates the adequate dispatch of the MG resources to maintain supply-demand balance. Hence, uncertainties inherent to an MG must be taken into account, which is one of the main topics of this thesis.

The coordinated operation of multiple MGs as a multi-microgrid (MMG) system has recently attracted attention due to the potential benefits that originate from a coordinated operation, as opposed to the individual and independent operation of each MG. The collective operation enables the possibility of power exchanges among MGs and the main grid, which can mitigate the unpredictability of RESs, as well as reduce the operational costs by taking advantage of the heterogeneity of load and generation profiles in each MG. Furthermore, differences in generation costs and grid buying/selling prices can incentivize power exchanges and ensure the maximum utilization of RESs. Therefore, it is important to design EMSs that adequately consider the collective operation of a set of MGs while taking uncertainties into account, which is the primary focus of this thesis.

In the first part of this thesis, a centralized MMG EMS model is proposed, which is formulated as a cost minimization problem that considers the operation of all MGs and their interactions among each other and the main grid as a single system. The model includes detailed operational constraints of thermal generation units and Energy Storage Systems (ESSs), as well as power capacity limits at the Point of Common Coupling (PCC) of each MG. A decomposition procedure based on Lagrangian relaxation is then applied, with the goal of separating the complete problem into subproblems corresponding to each MG, which can be solved independently with minimal information exchange through a subgradient-based distributed optimization algorithm. Demand and solar irradiance data from a realistic Active Distribution Network (ADN) in São Paulo, Brazil, are then used to design a system to test and validate the proposed models. The simulation results show

that the distributed algorithm converges to the optimal or a near-optimal solution of the centralized model, making the proposed approach a viable alternative for the implementation of a distributed MMG EMS. Furthermore, the advantages of an MMG system are demonstrated by showing that the operational costs of the system are significantly reduced when MGs are able to exchange power among each other and with the main grid, compared to their costs in individual operation.

In the second part of this thesis, the proposed centralized MMG EMS model is reformulated using an Affine Arithmetic (AA) optimization framework to consider uncertainties associated with electricity demand and renewable generation. First, the uncertainties are characterized by their affine forms, which are then used to redefine the variables, objective function, and constraints of the original model in the AA domain. Then, the linearization procedure of the absolute values introduced by the AA operators is explained in detail. The proposed AA model is validated through comparisons with the deterministic and Monte Carlo Simulation (MCS) solutions. The test system used in the aforementioned MMG distributed dispatch approach is utilized to show that the AA model is robust under a range of possible realizations of the uncertain parameters, and can be solved with lower computational burden and in shorter execution times with respect to an MCS approach, while considering the same range of uncertainties, which is one the main advantages of the proposed AA model. Furthermore, it is demonstrated that the affine forms of the solution variables can be used to find a dispatch for different realizations of demand and renewable generation, with no need to repeatedly solve the optimization problem.

Acknowledgements

I would like to first express my utmost gratitude to my supervisors, Professor Claudio Cañizares and Professor Mehrdad Pirnia, for supporting me throughout my graduate studies at the University of Waterloo. They are exemplary professionals and individuals, and I am truly fortunate to have had the opportunity of learning from them and work under their supervision. Without their invaluable help to overcome both academic and personal challenges, this thesis would have never come to fruition.

I would also like to thank the members of my Examination Committee for their insightful comments and observations: Professor Kankar Bhattacharya and Professor Mehrdad Kazerani from the Department of Electrical and Computer Engineering at the University of Waterloo; Professor Jessie Ma from the Department of Systems Design Engineering at the University of Waterloo; and Professor Bala Venkatesh from the Department of Electrical, Computer and Biomedical Engineering at the Toronto Metropolitan University.

I thankfully acknowledge the financial support provided by the *Consejo Nacional de Ciencia y Tecnología* (CONACYT) in Mexico, and the University of Waterloo, which made possible this research.

My earnest thanks go to the friends and colleagues I have met over the years at Waterloo: Sofía, Darío, Pablo, Matheus, Anshul, Hanwen, Felicitas, Steven, Hediyeh, Muhammad, Mauricio, Iván, Fabián, Diego, Mariano, William, Enrique, Chioma, Baheej, Walter, Fulong, Katarina, Samuel, Santiago, Dante, Jean-Michell, Chioma, Bharat, Ricardo and Renato. Sharing this journey with them has enriched my life beyond measure.

Special thanks go to my friends Osmar, Javier, Gerardo, Jacqueline and Paola, who, despite the distance, have been with me in one way or another when I needed them the most. I would also like to thank my friends Baldwin, Napoleón, and the memory of our late friend Gilberto, for all the shared experiences in our undergraduate and graduate studies, and their helpful words of support.

Finally, I wish to express my deepest gratitude to all my family for their unconditional love and support, in particular to my parents, Alejandro and Marina, and my brother, Alejandro, who have always encouraged me to pursue my goals.

Dedication

To my family and friends for believing in me, even when my own confidence faltered.

Contents

List of Figures

List of Tables

List of Abbreviations

AA	Affine Arithmetic
ADMM	Alternating Direction Method of Multipliers
ADN	Active Distribution Network
DER	Distributed Energy Resource
DNO	Distribution Network Operator
EC	Economic Dispatch
EMS	Energy Management System
ESS	Energy Storage System
IA	Interval Arithmetic
LP	Linear Programming
MCS	Monte Carlo Simulation
MG	Microgrid
MILP	Mixed-Integer Linear Programming
MINLP	Mixed-Integer Non-Linear Programming
MMG	Multi-Microgrid
MPC	Model Predictive Control

NLP	Nonlinear Programming
OPF	Optimal Power Flow
PCC	Point of Common Coupling
pdf	Probability Distribution Function
PV	Photovoltaic
RES	Renewable Energy Source
RHC	Receding Horizon Control
RO	Robust Optimization
SoC	State of Charge
SP	Stochastic Programming
UC	Unit Commitment

List of Symbols

Sets

G	Thermal generators.
M	Microgrids.
S	ESS units.
T	Periods in the optimization time span.

Indices

0	Center value of an affine form.
g	Thermal generator.
h	Partial deviation of an affine form.
m, n	Microgrid.
s	ESS unit.
t	Period in the optimization time span.

Parameters

α	Update step size for the subgradient method.
β	Coefficient of the power transfer cost function [\$/kW^{2}h].
Δt	Duration of periods in the optimization time span [h].
η^{ch}	Charging efficiency of ESS units.

η^{dch}	Discharging efficiency of ESS units.
$\overline{P^{ch}}$	Maximum charging power of ESS units [kW].
$\overline{P^{dch}}$	Maximum discharging power of ESS units [kW].
$\overline{P}$	Maximum power output of thermal generators [kW].
$\overline{SoC}$	Maximum state of charge of ESS units [kWh].
$\overline{T}$	Number of periods in the optimization time span.
ρ^{gb}	Grid buying price [$/kWh].
ρ^{gs}	Grid selling price [$/kWh].
$\underline{P^{ch}}$	Minimum charging power of ESS units [kW].
$\underline{P^{dch}}$	Minimum discharging power of ESS units [kW].
$\underline{P}$	Minimum power output of thermal generators [kW].
$\underline{SoC}$	Minimum state of charge of ESS units [kWh].
a	Coefficient of the quadratic term of the cost function of thermal generators [$/kW^{2}h].
b	Coefficient of the linear term of the cost function of thermal generators [$/kWh].
c	Coefficient of the constant term of the cost function of thermal generators [$/h].
C^{SD}	Shutdown cost of thermal generators [$].
C^{SU}	Startup cost of thermal generators [$].
D	Power demand [kW].
D^{lb}	Lower bound of uncertainty range for demand [kW].
D^{ub}	Upper bound of uncertainty range for demand [kW].
DT	Minimum down time of thermal generators [h].

DT^0	Number of periods that thermal generators have been down prior to the first period of the optimization time span [h].
f^{PV}	Derating factor of PV array.
$G^{T,STC}$	Solar radiation incident on PV array at standard test conditions [kW/m^2].
G^T	Solar radiation incident on PV array [kW/m^2].
L^D	Number of periods that thermal generators must be initially down due to their minimum down time requirement [h].
L^U	Number of periods that thermal generators must be initially up due to their minimum up time requirement [h].
M^b	Large constant for linearization of absolute values.
p^D	Number of noise symbols in the affine form of demand.
P^{PCC}	Maximum power transfer capacity through the PCC [kW].
$P^{r,lb}$	Lower bound of uncertainty range for renewable generation [kW].
$P^{r,ub}$	Upper bound of uncertainty range for renewable generation [kW].
P^r	Power generation from renewable energy sources [kW].
p^r	Number of noise symbols in the affine form of renewable generation.
RD	Ramp down limit of thermal generators [kW/h].
RU	Ramp up limit of thermal generators [kW/h].
UT	Minimum up time of thermal generators [h].
UT^0	Number of periods that thermal generators have been up prior to the first period of the optimization time span [h].
v^0	Initial commitment status of thermal generators.
w	Objective function weighting factor.
Y^{PV}	Power output of PV array [kW].

Variables

λ	Microgrid power selling price [$/kW].
Ω^G	Feasible region for thermal generators.
Ω^S	Feasible region for ESS units.
σ	Total power sold by a microgrid to all other microgrids [kW].
ε^D	Noise symbol associated with demand variations.
ε^r	Noise symbol associated with renewable generation variations.
$\widehat{\cdot}$	Affine form of an uncertain quantity.
P	Power output of thermal generators [kW].
P'	Auxiliary variable corresponding to the absolute value of power output of thermal units [kW].
P^{ch}	Charging power of ESS units [kW].
P^{dch}	Discharging power of ESS units [kW].
$P^{e'}$	Auxiliary variable corresponding to the absolute value of power exchange among microgrids [kW].
P^e	Power exchange among microgrids [kW].
$P^{gb'}$	Auxiliary variable corresponding to the absolute value of power bought by the main grid from microgrids [kW].
P^{gb}	Power bought by the main grid from microgrids [kW].
$P^{gs'}$	Auxiliary variable corresponding to the absolute value of power sold by the main grid to microgrids [kW].
P^{gs}	Power sold by the main grid to microgrids [kW].
SD	Shutdown decision for thermal generators.
SoC	State of charge of ESS units [kWh].

SU	Startup decision for thermal generators.
v	Commitment status of thermal generators.
x^D	Auxiliary binary variable for linearization of absolute values of partial deviations associated with demand variation.
x^r	Auxiliary binary variable for linearization of absolute values of partial deviations associated with renewable generation variation.
z^{ch}	Charging status of ESS units.
z^{dch}	Discharging status of ESS units.

Functions

γ	Power transfer cost [$/h].
C	Generation cost of thermal units [$/h].

Chapter 1

Introduction

This chapter presents the motivation behind this research, followed by a comprehensive literature review and a discussion on existing models and approaches for achieving optimal and reliable operations of Multi-Microgrid (MMG) systems. Finally, the research objectives and the outline of the thesis content are presented.

1.1 Motivation

In recent years, environmental concerns have motivated an ongoing global effort to reduce greenhouse gas emissions. To keep in line with the Paris Agreement of 2015, which aims at limiting the global temperature increase, significant carbon intensity reduction programs in all sectors of the economy are required. This calls for unparalleled work on several areas relevant to this research, such as the development of renewable energy technologies, and the transformation of existing power grids to accommodate such technologies [1].

The gradual transformation of power systems is focused on replacing traditional fossil fuel-based energy sources such as coal and natural gas, with Renewable Energy Sources (RESs) such as wind and solar energy. Furthermore, the integration of these RESs as a large number of Distributed Energy Resources (DERs) that supply renewable energy in a reliable and localized manner will also help to reduce the dependency on conventional power plants [2]. However, the large-scale integration of DERs into existing power systems poses several technical challenges that must be addressed to fully leverage the potential of RESs.

In the aforementioned context, the adoption of Microgrids (MGs) is an appealing approach to effectively harness RESs by enabling high penetration of DERs, as well as restructuring the existing conventional power grids to enhance their efficiency and reliability [3]. MGs are also of special interest due to their capability of providing sustainable energy to areas in which a connection to the main power grid is not possible or has been unexpectedly interrupted [4]. An MG is a cluster of DERs and loads operated in coordination to reliably supply electricity, capable of operating either in isolated or grid-connected modes, connected through the Point of Common Coupling (PCC) to the main power grid at the distribution level, thus enhancing the system resiliency and reducing power transmission utilization and losses [5, 6]. These features enable the possibility to schedule energy exchanges between the MG and the main grid that would be mutually beneficial, as well as addressing operational issues locally within the MG [7].

For example, hurricanes Irma and Maria severely damaged the centralized power grid of Puerto Rico in 2017, compromising 25% of the transmission towers and 40% of the island's substations, which led to the longest blackout in U.S. history. The majority of the population had to rely on diesel generators, which were expensive, polluting, and insufficient to satisfy the energy demand [8]. As reconstruction of the power grid began, the goal was to design a more resilient system that would heavily rely on MGs to integrate RESs and Energy Storage Systems (ESSs) [9]. The reliability of MGs in Puerto Rico was put to the test more recently, when a 6.4-magnitude earthquake struck in January of 2020. One of the main power plants was severely affected, disrupting 25% of the island's energy supply; however, ten schools which received energy from isolated MGs were able to continue operating normally, demonstrating the potential for enhancing the power grid resiliency [10].

There are, however, challenges associated with MG-based power grids. Thus, the variability of electricity demand and renewable energy sources within an MG results in unpredictable load and generation profiles, complicating the adequate dispatch of the MG resources and presenting stability and reliability problems [11]. To guarantee the reliable and economic operation of an MG, appropriate strategies and methods for its control must be implemented. In an MG, the optimal operation is determined by the Energy Management System (EMS), which solves optimization problems such as the Unit Commitment (UC) or Economic Dispatch (EC) problems. These traditionally deterministic problems must be reformulated to consider the uncertainties inherent to an MG, which is one of the main focuses of this thesis.

The coordinated operation of multiple MGs connected to form an MMG system has recently attracted significant attention due to the potential performance improvement of the overall system and the mutual benefits for all participating MGs, when compared

to their independent operation [12]. An MMG system can be described as a high-level structure, formed at the distribution system voltage level through the clustering of single interconnected MGs, which are geographically close to each other and can function as a single aggregated island from the main grid's perspective [13, 14, 15]. Through a coordinated operation with the main distribution grid, an MMG system enables optimal power exchanges that mitigate the undesirable effects of intermittent renewable energy sources, while benefiting from the heterogeneity of load and generation profiles in each MG [16]. Furthermore, differences in buying and selling prices can incentivize power exchanges that will ensure the maximum utilization of RESs and reduce the total operating costs [17]. With the growing integration of DER in distribution systems, the need and advantages of properly coordinating the collective operation of MGs are becoming apparent [18], and is thus the primary overall focus of this thesis.

In general, the existing literature related to MMG systems falls into the categories of system planning, voltage and frequency control, communication in power sharing, service restoration, stability enhancement, and optimal energy management. The presented research focuses on the last category, where most of the literature relates to coordination mechanisms, modeling of the EMS as centralized or distributed optimization problems, and the implementation of solution techniques for such problems [19].

The distinction between centralized, decentralized, and distributed control is particularly relevant in the area of MMG systems. While a centralized EMS model is mathematically easier to formulate and solve, and may result in the lowest operational cost for the MMG system, it has two main disadvantages: (1) the whole system is reliant on a centralized entity or controller, which severely compromises its reliability in the case of contingencies, and (2) the centralized controller requires complete knowledge of the generation costs, load profiles, and relevant parameters of DERs within each MG, which may pose privacy concerns if the MGs are operated by different utilities [20]. These issues are addressed by implementing decentralized or distributed approaches, which are characterized by local controllers in each MG that preserve their privacy [21].

Based on the aforementioned discussion, this research focuses on the development of a centralized, decomposable, and realistic EMS model for the optimal and coordinated operation of MMGs, and the subsequent implementation of a distributed solution algorithm. Thereafter, given the challenges encountered with the implementation and solution of the distributed MMG EMS problem, uncertainties associated with load and renewable generation are introduced in the centralized model only, through an Affine Arithmetic (AA) approach, to obtain a detailed MMG EMS model that is robust for a range of uncertainties and is significantly less computationally intensive than Monte Carlo Simulation (MCS).

1.2 Literature Review

A comprehensive literature review on MMG systems is presented in this section, with the goal of establishing the context for and justifying the development of this research, describing the state-of-the-art of related work and identifying relevant gaps or limitations addressed in this thesis. The focus will be on the EMS of MMGs, distributed optimization techniques applied to such systems, and different methods for considering uncertainties in centralized models.

1.2.1 Multi-Microgrid Centralized EMS

In [22], the authors present a model for the optimal operation of interconnected MGs with a centralized control structure. An evolutionary computation algorithm is applied to determine the optimal power exchanges, considering reliability indices for each MG. Results show that the reliability indices of the system improve, when comparing the interconnected and isolated operation of MGs. However, the proposed model requires the proper characterization of Probability Distribution Functions (pdfs) to account for uncertainties in load and renewable generation.

An optimal EMS for a cooperative MMG community is proposed in [23], which minimizes the operating costs of all MGs. A sequential coordinated procedure is proposed to distribute the computational burden of finding the optimal power exchange scheduling, carried out by a central controller. Results show that through power trading among each other, MGs can avoid unnecessary costs from external trading with the main grid, by adjusting their local generation. Nevertheless, the proposed model does not take uncertainties into account, and it lacks a detailed representation of the MG components.

A Model Predictive Control (MPC)-based global centralized control for a network of MGs is presented in [24], where the goal is to maximize the overall profit resulting from power exchanges among MGs and the main grid. Simulation results demonstrate that the cooperative operation has significant advantages for each participating MG, especially in terms of the total energy required from the main grid and the utilization of RESs. In [25], a general framework for reliability assessment of MMG systems is proposed, to investigate the impact of coordinated outage management strategies. A centralized control scheme is introduced for the operation of MMGs during outage events, which minimizes load curtailments based on an MPC approach. Results show that the proposed model improves the outage duration indices of the whole system. However, these MPC-based strategies rely on accurate forecasts of load and renewable generation.

1.2.2 Distributed Approaches

Due to the inherent characteristics of MMG systems, there are several benefits in implementing a distributed EMS model or solution approach. Since the concept of MMGs is relatively new, the application of distributed optimization techniques is currently a highly active research field.

In [26], the authors present a hierarchical power scheduling approach to manage the power trading and energy storage in a system consisting of a main grid supplying 400 users, and four cooperative MGs supplying 100 users each. A convex optimization problem is decomposed into a two-tier formulation; the first tier is related to the power distribution in the main grid, while the second tier is related to the cooperative power scheduling in the MGs. Results show that MGs may choose to import power from other MGs with lower transmission costs, instead of importing from the more expensive main grid. This is beneficial for the main grid as well, in which reductions of 43% peak generation and 13% overall generation are achieved. A drawback of this approach is that uncertainties associated with demand and renewable generation variability are considered through statistical distributions, which results in a method that is not as robust as other techniques such as Robust Optimization (RO) and AA.

A distributed MPC scheme for the coordinated stochastic energy management of MMGs is presented in [27]. Uncertainties associated with renewable generation and loads are handled though probabilistic forecasts. The proposed scheme is tested on a system composed of ten MGs, interconnected to the main distribution network. A two-layer EMS is implemented, with an upper layer that maintains the supply-demand balance in the distribution network, minimizing its operation cost and finding the optimal energy exchange with the transmission network, and a lower layer that coordinates the MGs to maintain their individual supply-demand balance, minimize their operation cost, and achieve the optimal energy exchange set by the upper layer controller. Results show that the total operation cost is reduced, with an enhanced trade-off between performance and computational feasibility, when compared to a non-cooperative operation. While the proposed approach coordinates multiple MGs adequately, it relies on probabilistic forecasts of load and renewable generation to find an optimal solution.

A decentralized control for MMGs is implemented in [28], where each MG is modeled as an inventory system, locally producing electricity from wind or solar sources. The costs of energy storage and power exchange among MG are minimized, while the storage levels in each MG are kept around a reference value through the power sharing among MGs. The proposed model has interesting features that make it useful to investigate the design of an MMG controller, such as scalability and robustness to changes in network topology;

however, uncertainties in load and renewable generation are not considered.

A distributed optimization framework for energy trading between MGs is presented in [29], which implements a subgradient-based algorithm that requires minimal information exchange, thus preserving the privacy of each MG. However, the proposed model does not take into account the power capacity limits at the PCC of each MG. In [30], the authors present a mechanism to incentivize energy trading among MGs, based on Nash bargaining theory. The bargaining problem is decomposed into two sequential problems, one for social cost minimization and one for trading benefit sharing, and a distributed solution using an Alternating Direction Method of Multipliers (ADMM) algorithm is implemented. Results show that the operational costs of all MGs that participate in energy trading are reduced; however, the PCC limits are also neglected.

In [31], a distributed and robust EMS for networked hybrid ac/dc MGs is proposed, which coordinates the energy sharing through the dc network, minimizing the power transmission losses. A distributed algorithm that preserves the privacy of each MG is implemented, also based on the ADMM principle, which is applicable to this model because MGs only need to update their energy exchange schedule with the dc network, and not other MGs. Thus, in the formulation, there are no terms representing power exchanges among MGs, which would couple the constraints of all MGs and result in a non-separable problem structure that is incompatible with ADMM algorithms.

A distributed energy management framework formulated as a bi-level quadratic optimization problem is developed in [32]. The upper level corresponds to the distribution system, and the lower level to each individual MG; the two levels are linked through the clearing price determined in the upper level optimization. Simulation results show that the operational cost of the distribution system significantly decreases, when compared with fixed pricing schemes. However, the coordination depends entirely on the clearing price set by the upper level problem, instead of being determined locally by the corresponding MGs in the lower level problems. In [33], the authors propose a three-stage distributed algorithm that coordinates the operation of MGs, using an MPC approach. The first stage performs local optimizations for each MG, followed by a coordination stage controlled by an aggregator, and a final stage that redistributes power deviations from the aggregator's energy profile. Simulation results show that the cooperative operation reduces the amount of energy exchanged with the main grid. A similar technique is proposed in [34], where a distributed MPC-based dispatch process is implemented, with an upper level optimizing the energy exchanges between the distribution network and the MGs, and a lower level guaranteeing the economic supply and demand balance. Results show that the coordinated operation benefits both the distribution network and MGs. However, these approaches have the drawbacks of MPC-based optimization techniques discussed in the next section.

A two-layer system that enables peer-to-peer electricity sharing is proposed in [35], where the first layer corresponds to a multi-agent electricity trading mechanism, and the second layer consists of a blockchain-based mechanism to securely settle the transactions agreed upon in the first layer. Results show that the proposed approach efficiently promotes energy sharing and enhances the overall energy efficiency of the distribution network. In [36], a peer-to-peer trading mechanism that uses locational marginal prices to compute network usage charges is presented, with a decentralized configuration that takes into account the preferences of each individual peer. An iterative price-adjusting process is implemented, which matches the seller and buyer prices for all energy trades. Results show that a peer-centric configuration reduces network usage charges. However, these abstract trading mechanisms disregard some practical considerations of MMG systems, such as PCC capacity limits and a detailed representation of MG components.

A nested day-ahead scheduling model for networked MGs is proposed in [37], in which MGs are nested based on load priority. The layered structure enhances the system resiliency, while keeping operational costs close to a centralized approach. However, this nested configuration significantly increases the complexity of the problem, which might limit its use in practical systems.

A decentralized framework based on an ADMM algorithm that coordinates power exchanges between the distribution system and MMG is presented in [38]. Each entity is modeled as a two-stage RO problem to account for uncertainties in renewable generation and demand, assuming that only one MG is connected to the distribution system; hence, the necessary information exchange only involves the distribution system and a single MG, which makes it possible to apply the ADMM algorithm. Similar approaches, with different models and modified versions of ADMM algorithms are presented in [39] and [40]. However, representing power exchanges between MGs not considered in the formulation, impedes the application of the proposed ADMM approach, due to the model constraints being strongly coupled.

1.2.3 Uncertainty Modeling

Different approaches to deal with uncertainties in the MG scheduling problem have been proposed in the literature. In [41], the authors propose a deterministic Mixed-Integer Linear Programming (MILP) formulation of the energy management problem, with the addition of reserve constraints to compensate for forecast errors in demand and renewable generation. An MG dispatch model with frequency-aware constraints which ensure the MG's capability to ride through unplanned islanding events is presented in [42]. Instead of

specifying the primary reserve requirements as fixed amounts, the proposed dispatch determines the reserve requirements by explicitly simulating under-frequency or over-frequency dynamics caused by potential islanding events. Since these approaches are based on the inclusion of reserve constraints, they do not take uncertainties into account directly, and the obtained solutions may be infeasible for certain scenarios, depending on the forecast accuracy.

Methods based on MPC and Receding Horizon Control (RHC) have been proposed in the literature to mitigate the impact of forecast errors in the optimal MG operation. The authors in [43] present a centralized EMS for isolated microgrids based on MPC and RHC. A two-stage approach is implemented to reduce the computation time; the first stage corresponds to the UC problem, and the second stage is a three-phase Optimal Power Flow (OPF) problem. A coordination strategy based on an online moving horizon optimization approach is proposed in [44], which seems effective in terms of technical performance and computation time, when applied to isolated power systems. Forecast errors are considered indirectly in these methods, but the uncertainty is not explicitly included in the problem formulation, which requires defining a reserve constraint as well. The amount of reserves is usually overestimated to avoid load curtailment; hence, a better representation of uncertainties is necessary to guarantee the reliable operation of an MG, since the supply-demand balance is critical due to its modular nature.

Classical approaches to handle uncertainties in MG scheduling problems include Stochastic Programming (SP) and MCS. In SP, uncertainties are represented by a set of scenarios, which are generated from pdfs, and multi-stage optimization problems are usually formulated to enable adjustments to the first-stage decisions in latter stages, based on the realizations of the uncertain parameters [45]. In MCS, the optimization problem is solved repeatedly, each time with different input data obtained through random sampling from a known distribution of the uncertain parameters, and a statistical analysis is then performed on the results. The precision of the expected values of the variables and their distribution shape improve as the number of simulation trials increases [46]. The main drawbacks of these approaches are the need to identify a pdf of the uncertain parameters, which requires a considerable amount of historical data, and the high computational burden of the repeated simulations.

In [47], a two-stage energy exchange scheduling strategy for an MMG system is presented, which considers electric vehicles as storage devices. Simulation results show that the two-stage scheduling strategy reduces the electricity cost and avoids frequent transitions between battery charging/discharging states. A limitation of this approach is the method used to represent the stochastic nature of wind generation and the state of electric vehicles. Thus, MCS is used to create a large number of scenarios from statistical distri-

butions; the number of scenarios is then reduced to avoid excessive computation times. In this process, possible critical scenarios may be discarded, compromising the reliability of the system under certain realizations of the uncertain quantities.

Stochastic formulations of the MG EMS problem are based on representing uncertainties by a set of scenarios, which are generated from pdfs of the random parameters. For example, in [45], the authors formulate a cost minimization problem that also reduces the power losses in an MG, while considering the intermittent nature of renewable energy sources. A two-stage formulation is adopted, with the first stage finding the optimal decisions for day-ahead energy transactions, which remain constant in the second stage, considering the variations in wind and solar generation. In [48], a two-stage stochastic formulation that minimizes the expected operational cost is implemented. Scenarios of renewable generation and day-ahead energy and reserve scheduling are created based on pdfs of the forecast errors, and results show that the stochastic model allowed lower reserve requirements, when compared with a conventional deterministic method. A two-stage SP planning model for the implementation of MMGs in Active Distribution Networks (ADNs) is presented in [49], which aims to benefit from interactions among MGs while considering uncertainties associated with electricity demand and renewable generation. The proposed model includes long-term purchase decisions and short-term operational constraints, and simulation results show that the SP model is less conservative than a deterministic model with reserve constraints, for a system of four MGs in an ADN located in São Paulo, Brazil. The main disadvantage of SP approaches is the need to identify accurate pdfs of the uncertain parameters, which requires a considerable amount of historic data. Furthermore, feasibility cannot be guaranteed for all the possible realizations of the uncertain parameters, since certain scenarios may be neglected due to scenario reduction techniques commonly applied to reduce the computation time.

To circumvent the disadvantages of SP and MCS, alternative methods such as RO and AA have been proposed, in which uncertainties are represented by predefined intervals, according to the expected variability of the random parameters, usually determined from historical data. The obtained solutions are robust for the considered range of uncertainty, while avoiding the need for finding accurate pdfs or to perform repeated calculations. When considering uncertainties in the MG EMS through RO, the goal is to minimize the worst-case scenario, thus ensuring that the MG can operate adequately for any realization of the uncertain parameters [50]. For instance, an RO approach for finding the optimal MG scheduling considering wind generation uncertainty is presented in [51]. The proposed RO approach yields lower operational costs than a deterministic model with predicted wind generation, as well as a stochastic model, for both isolated and grid-connected modes of operation. In [52], uncertainties associated with real-time market price signals, renewable

energy sources, and forecasted load values are handled using an RO method. Results show that the effect of the buying price uncertainty is more prominent than the effect of the selling price uncertainty. In [53], an EMS for isolated MGs based on RO is presented, which combines the solution of a UC problem in the first stage, with a detailed OPF in the second stage. The main drawback of RO formulations is that they produce highly conservative solutions for the uncertainty interval considered, which are more expensive than the solutions obtained with other range analysis techniques.

The combination of different approaches has also been explored in the literature. For example, in [54], the authors present a stochastic-predictive EMS for isolated MGs which considers uncertainties through a two-stage decision process, combining the stochastic UC solution of the first stage with an RHC OPF solution in the second stage. A stochastic MPC approach is proposed in [55], where forecasting uncertainties are represented by a set of typical scenarios obtained from MCS. In this case, a stochastic mixed-integer quadratic programming model is developed, which minimizes the MG operational cost and reduces the required spinning reserve. Results show that the proposed model performs better than a deterministic MPC model, as well as deterministic and stochastic day-ahead approaches. The main disadvantage of these methods is the need for statistical assumptions to generate a set of scenarios to account for uncertainties.

More recently, self-validated computation techniques have been proposed for dealing with uncertainties in power systems [56]. In a self-validated computation, the numerical algorithm keeps track of the accuracy of the computed quantities, as part of the computation process itself [57, 58]. The most simple self-validated computation model is Interval Arithmetic (IA), in which an unknown quantity is represented by an interval. Mathematical operations can be performed using these intervals, in such a way that the computed interval contains the actual value of the corresponding quantity. However, IA may not be suitable for certain applications because it can produce solution intervals which are much wider than the range of the computed quantity or function, especially in the case of chained or iterative computations, since the overestimation effect in each step will accumulate [59].

AA is a different self-validated computation model that has been proposed to overcome the overestimation effect of IA [60]. An AA framework for computing reliable solution intervals for the OPF problem considering uncertainties is presented in [61], where relational and minimization operators in AA form are defined to provide better approximations of the solution bounds, when compared to other AA methods that approximate the minimization operator through domain contraction techniques. Using the defined operators, equality and inequality constraints can be included in the AA formulation. Results show that the proposed model estimates accurate boundaries for the state variables, while drastically reducing the computation time when compared to other approaches, especially MCS.

In [62], an AA-based OPF formulation for MGs with uncertain load and renewable generation is presented. The state and control variables are expressed in affine form, resulting in an interval-based model with upper and lower bounds for each variable. The proposed model yields intervals that can be used to estimate the necessary reserves that the MG should maintain to ensure that the demand is satisfied under the range of uncertainties considered. In [63], an AA-based EMS for isolated MG is presented, which can produce appropriate dispatch solutions by computing the noise symbols of the affine forms obtained from the AA UC solution, based on the actual realizations of demand, renewable generation, and available reserves. Simulation results demonstrate that the proposed method achieves cost-effective solutions, compared to a deterministic model, as well as MPC and SP techniques. Furthermore, the AA model avoids the repeated simulations required in the MPC method, and the statistical characterization of uncertainties required in SP. The objective function of the AA UC problem is a weighted expression of the central value and the affine radius associated with the uncertainties, so that the resulting AA MILP problem can be properly solved, which allows controlling the degree of robustness of the obtained solution.

The authors in [64] formulate RO and AA optimization problems, minimizing the maintenance and operation costs of an MG, in a 24-hour time frame, and compare the results with a traditional deterministic model. It is shown that the RO approach yields the most expensive solution, since it considers the worst-case scenario of the MG operation; however, the budget of uncertainty can be changed to control the conservatism of the results. The resulting AA forms of the variables provide valuable information about the impact that each source of uncertainty has in each variable, which can be useful to perform sensitivity analyses. A scheduling model for an MMG system using AA to account for load and renewable generation uncertainty is presented in [65], and simulation results show that the AA model provides less conservative solutions than its IA counterpart; however, the proposed EMS model does not consider detailed generator constraints, and the power limits at the PCCs are not taken into account.

1.2.4 Discussion

Based on the preceding literature review, it is clear that the study and development of adequate EMS models and solution techniques for the optimal operation of MMGs systems is currently a prominent research area, as these systems allow an efficient and reliable large-scale integration of DERs. In this context, the existing research mainly focuses on the development of distributed optimization models or algorithms which are generally too abstract and mathematically complex to be viable alternatives for implementation in real

systems. Furthermore, unrealistic assumptions are usually made, particularly regarding the interconnection of MGs to the distribution system, and the practical characteristics of the MG components. Therefore, the MMG EMS model and distributed solution approach presented in this thesis address such issues.

Regarding the consideration of uncertainties in MG scheduling problems, existing models are usually based on SP and MPC, which have the drawback of requiring an adequate identification of pdfs of the uncertain parameters, and accurate load and renewable generation forecasts. To carry out such statistical characterization, a considerable amount of historical data is needed, which may be difficult to obtain for MMG systems since they are not yet commonplace in existing distribution grids. This lack of data may lead to inadequate pdfs, potentially yielding significant errors. To address these limitations, techniques based on range arithmetic, such as RO, IA, and AA have been proposed in the literature. However, since RO and IA models generally produce exceedingly conservative solution intervals, AA techniques have been proposed to address this shortcoming.

Finally, most of the existing works that take uncertainties into account are focused on the operation of a single MG, either in isolated or grid-connected modes, as opposed to the more complex case of MMGs. Only a few works discuss uncertainty issues in MMG models, usually with the caveats of impractical assumptions as previously highlighted, utilizing inefficient SP or MPC approaches. Furthermore, even fewer works report MMG EMS models using range arithmetic techniques for dealing with uncertainties, and none of these consider PCC capacity limits and detailed representations of the MG components. Hence, the uncertainties associated with demand and renewable generation present in the MMG EMS model proposed in this thesis have been formulated using an AA approach.

1.3 Research Objectives

Based on the preceding literature review and discussion on MMG EMS models, solution approaches, and uncertainty representation, the main objectives of this thesis are the following:

- Develop a centralized and decomposable EMS model for the optimal and coordinated operation of MMGs, which considers detailed representations of thermal generation units, renewable generation, and ESS units within each MG, including realistic operational constraints that account for power flow limits at the PCC of each MG, considering all power exchanges among the set of MGs and the ADN, which are ignored in the majority of MMG EMS models in the existing technical literature.

- Based on the developed EMS model, implement a distributed solution approach for the optimal scheduling of all participating MGs, which requires minimal information exchange and enables local optimization in each MG, while preserving their privacy and coordinating their cooperative operation.
- Formulate the proposed centralized MMG EMS model in the AA domain, to account for uncertainties in demand and renewable generation, using linearization techniques to overcome the nonlinear components introduced by the AA formulation. The dispatch procedure to determine the optimal power generation, energy storage and power exchanges from the AA solution is demonstrated for specific realizations of the uncertain parameters.
- Test and validate the proposed models using electricity demand and renewable generation data from a realistic ADN in São Paulo, Brazil, demonstrating the benefits of the collective operation of MMGs, the distributed solution approach, and the AA modeling approach for dealing with uncertainties.

1.4 Thesis Outline

The rest of this thesis is organized as follows: Chapter 2 presents a review of the concepts, topics, and theoretical background relevant to the development of this work. Thus, descriptions of MG and MMG systems are presented, focusing on their components, the EMS modeling, and the interconnection topologies. An overview of centralized and distributed optimization techniques is also presented, followed by the AA framework used to reformulate the deterministic MMG EMS problem to account for uncertainties.

Chapter 3 presents the deterministic, centralized, and decomposable MMG EMS model which includes detailed representations of thermal generation units, renewable generation, and ESS units within each MG, as well as constraints that account for power flow limits at the PCCs. The distributed solution approach is then described and implemented, followed by the analysis and discussion of simulation results for a realistic MMG test system.

Chapter 4 presents the detailed formulation of the centralized MMG EMS model in the AA domain, including the linearization of nonlinear terms associated with the absolute value operators introduced by the AA formulation. Simulation results in a realistic MMG system are analyzed and discussed, and the procedure to determine the optimal dispatch of the MMG system from the obtained AA solution is described.

Finally, Chapter 5 summarizes the thesis content, presenting the main conclusions and contributions of this research, and outlining the scope of possible future work.

Chapter 2

Background Review

This chapter provides an overview of relevant background topics and concepts used in the development of this thesis. First, a general description of individual MGs is presented, discussing their operation modes, common components, and control structure. Then, the concept of MMGs is reviewed, describing the existing topologies and the use of centralized and distributed approaches for ensuring their optimal operation, including the application of decomposition techniques for solving centralized optimization problems in a distributed fashion. Finally, the concept of AA within an optimization framework to account for uncertainties in the MMG EMS model is introduced.

2.1 Microgrids

As it was previously mentioned, an MG is a cluster of loads, DERs, and ESSs operated in coordination to reliably supply electricity, connected to the distribution grid at the PCC [5]. MGs must be able to operate in either grid-connected mode or stand-alone modes (also known as islanded or isolated mode). In grid-connected mode, power can be transmitted from the MG to the main grid and vice versa, depending on the power balance and other operating conditions. In stand-alone mode, the MG is isolated from the main distribution grid and power exchanges are not possible; thus, the total power generated by the MG must be in balance with the local demand at any time. Furthermore, an MG must be capable of executing a seamless transition between the two operating modes. This capability of operating in either mode is one of the key features that makes MGs appealing to evolving electricity distribution networks, since they can provide support to the main grid when needed, engage in mutually beneficial power exchanges, or disconnect when needed, thus

lessening the burden on the main grid and ensuring the reliable energy supply to local loads.

Figure 2.1 shows a high-level view of the structure of a generic MG, indicating the energy and information flow within the MG, and its connection to the distribution network. The specific components found within the MG vary for each MG depending on its characteristics, such as the locally available resources, the topology of the system, the geographic features of the installation site, or whether grid-connected and/or stand-alone operation modes should be prioritized. Sources such as Photovoltaic (PV) arrays and wind turbines require converter interfaces. Non-critical loads can be simply connected or disconnected with a conventional circuit breaker, or also interfaced with a power electronics converter that would allow a more flexible control, although these interfaces may increase the levels of undesired harmonics [66].

DERs are classified as dispatchable or non-dispatchable units, depending on their con-

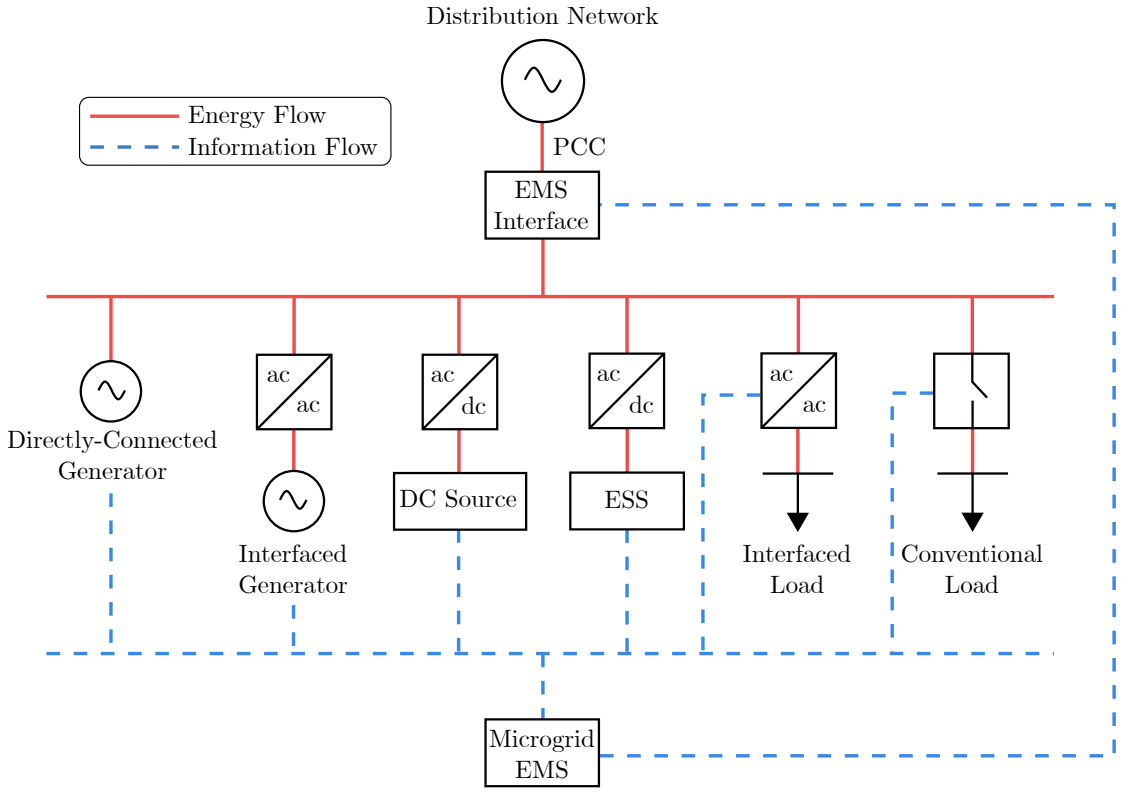

Figure 2.1: Generalized MG structure.

trollability. Fossil fuel generators, such as diesel generators, are an example of dispatchable units, whose power output can be controlled at any given time. On the other hand, DERs based on renewable energy sources have intermittent power output which cannot be controlled, and thus are usually operated at their maximum power output capacity at all times. However, a non-dispatchable unit combined with an ESS and an appropriate controller can operate as a dispatchable unit. The goal envisioned for future MGs is a complete departure from fossil fuel generation, and this challenging task can be accomplished with the proper coordination of charging and discharging of ESSs and demand response programs [67].

MGs usually have a hierarchical control structure divided in three levels: primary, secondary, and tertiary control [5]. Primary control refers to the control of the MG components, with the fastest response to local events (in the order of seconds or milliseconds), while ensuring adequate voltage and frequency levels, exclusively based on local measurements. Secondary control is associated with the MG EMS, which finds the optimal UC and dispatch of the available resources to ensure the reliable and economic operation of the MG, with a slower time frame than primary control (in the order of minutes). Longer term voltage and frequency deviations are restored in this level by determining the set points for the primary control. Tertiary control manages the power flow between the MG and the main grid at the PCC, providing signals to the secondary control to ensure the optimal operation of the joint system, in a time frame of several minutes. In the case of MMGs, the tertiary control is also responsible for the coordinated operation of all MGs and their interactions with the host grid [43, 68, 69]. Table 2.1 presents a summary of the control levels in an MG, and their associated functions. It is important to note that this classification varies slightly in the existing literature; in particular, functions related to the EMS and the coordination of power exchanges can be considered as secondary or tertiary control [70, 71].

To ensure the adequate operation of an MG, the control functions previously discussed can be implemented using centralized, decentralized, and distributed approaches. The focus in practice has been mainly on centralized structures, since this is the prevailing control architecture in conventional power grids. In a centralized approach, there is a central controller that monitors and controls all DERs and local loads; all calculations and decisions are made by the central controller, making the system vulnerable to single-point failures [5, 72]. In a decentralized approach, the MG control is physically distributed over a decentralized infrastructure, i.e., individual components are controlled by multiple local agents coordinated by the EMS. One advantage of the decentralized architecture is its scalability and reliability; new components can be added to the MG without disrupting its operation or updating the control algorithm, and the distributed structure makes the system immune to single-point failures. A distributed approach is similar to the decentralized structure,

Table 2.1: MG control levels and functions [5, 21].

Control Level	Timescale	Functions
Primary	Milliseconds, seconds	• Voltage and frequency control. • Active and reactive power sharing control. • Islanding detection.
Secondary	Seconds, minutes	• EMS. • Voltage and frequency deviation compensation. • Transition of grid-connected/isolated modes. • Demand side management.
Tertiary	Minutes, hours, days	• Coordination of grid/MGs power flow. • Coordination of clusters of MGs. • Ancillary services.

but it enables the coordination and cooperation of individual components [73, 74]. These control architectures will be further discussed in the following section, in the context of MMG systems.

The implementation and successful operation of single MGs is widespread nowadays, with numerous examples around the world of MGs designed to enhance the operation of different types of facilities, such as campus and community MGs, commercial or industrial MGs, and remote or emergency MGs. For example, the installation of an 8.1 MW MG was completed in October 2022, at the Chula Vista Elementary School District, located in the San Diego metropolitan area of California, United States. The system consists of 18,050 solar panels, complemented by battery storage, supplying energy for 28,000 students across 50 schools. The project is expected to save around $70 million over the next 25 years [75]. An MG at the Siemens corporate headquarters in Vienna, Austria, was officially completed in November 2020. The MG has PV arrays with a total capacity of 312 kW, and 500 kWh of battery storage, and is expected to provide flexibility services to Austria's transmission network, while generating additional income [76]. Another example is a dc MG installed at the Mbogo Valley Tea Factory, in the northwest of Nairobi, Kenya. The system includes PV arrays with a combined capacity of 403 kW, and 544 kWh of battery storage. The MG supports the factory's continuous operation when the connection to the main power grid is unstable or interrupted, which was a recurring issue due to the its remote location [77]. These examples showcase the capability of MGs to enhance the operational efficiency of diverse facilities, thus creating market opportunities for their continued development.

2.2 Multi-Microgrid Systems

As DERs continue to proliferate in electricity distribution networks, the interest in the implementation of MGs has increased as well, and the logical progression to further enhance their operation is the formation of MG clusters. As it was previously mentioned, the novel concept of MMG corresponds to a high-level structure, formed at the medium voltage level through the interconnection of MGs at their PCC. The MGs can be created by sectionalizing the existing distribution network, or by installing new DERs and ESSs to supply local loads, for example in areas not connected to the distribution networks such as remote communities.

MMGs can be also categorized according to the type of power they operate with, namely, ac MMGs, dc MMGs, and hybrid ac/dc MMGs. AC MMGs are the most commonly studied since they can be integrated more easily into existing distribution networks. However, the control of a dc MMGs is simpler than that of its ac counterpart, since reactive power management is not necessary, and there is no need to regulate the frequency. Adequate power converters are needed to interface dc MMGs with conventional distribution networks. Hybrid ac/dc MMGs can combine the advantages of both types, achieving a higher flexibility [78, 79].

The objective function of the MMG EMS optimization problem usually minimizes operational costs or maximizes the profits from power transactions, customer satisfaction, or utilization of renewable energy sources [19]. The operating costs can be minimized through the maximum utilization of available renewable generation, buying power at low prices and selling power at high prices, and taking advantage of the heterogeneity of load and generation profiles in each MG. These objectives are complementary and closely-related; hence, a common approach is to formulate a multi-objective problem that optimizes a combination of such objectives. The constraints considered largely depend on how the model is formulated. Thus, power and energy balance constraints are ubiquitous, but operating constraints of the MG components vary greatly, depending on the type of generation considered [80]. In this context, it is crucial to properly take into account the power transfer capacity limits through the PCC when considering power exchanges among MGs and the ADN, which has been ignored in most of the published research.

2.2.1 Topologies

As mentioned before, all MGs in an MMG system should be able to exchange energy among each other and with the main power grid, under the supervision of the distribution network

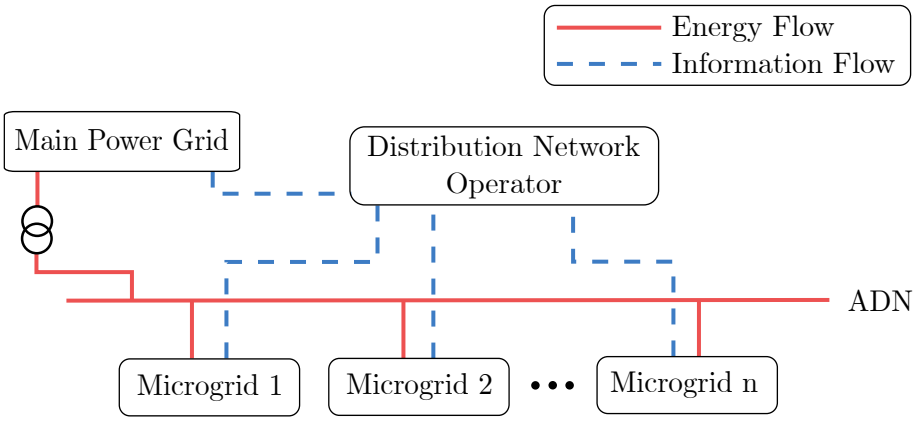

Figure 2.2: MMG system with radial topology.

operator. They should also be capable of operating in grid-connected or stand-alone modes. Based on these features, there are three common topologies of MMGs reported in the literature, as discussed next.

Radial Topology

In this configuration, each MG is connected directly to the main grid, forming a conventional radial topology in which the energy exchanges take place between each MG and the main grid through the distribution bus, as shown in Figure 2.2. Within individual MGs, there is information flow between each component and the MG EMS, whose objective is to optimally control all local resources. The distribution network operator requires information exchange with the main grid and all MGs since it is responsible for coordinating their operation [81, 82].

If an MG is unable to satisfy its demand, or has a surplus of renewable generation, the required energy exchange can only be made through the main grid, i.e., no energy exchanges directly among MGs are possible. Taking into account their geographical location and the physical connection of MGs to a distribution system, the radial topology is the most realistic configuration, from a practical implementation perspective.

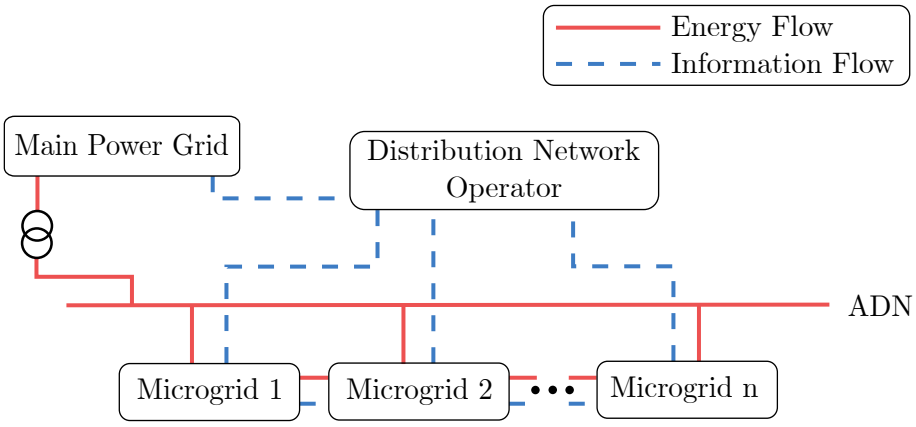

Figure 2.3: MMG system with daisy chain topology.

Daisy Chain Topology

In this topology, energy and information can be exchanged bidirectionally between adjacent MGs and between each MG and the main grid, as shown in Figure 2.3. The structure within each MG is the same as the one described in the radial topology. Such configuration causes a strong coupling of the energy schedules of all MGs, which requires additional network constraints. Furthermore, the EMS must be able to operate adequately using only non-critical information of the neighboring MGs, in order to preserve the users' privacy [26, 23].

Mesh Topology

In this configuration, all MGs are interconnected to each other and to the main grid directly, exchanging both energy and information, as shown in Figure 2.4, which is impractical. The mesh topology is commonly studied in the literature, for example in [24] and [83]. The formulation of this configuration allows a more straightforward implementation of distributed optimization algorithms [29], and therefore it has gained popularity in theoretical applications. However, such topologies are not existent nor expected to be implemented in practice.

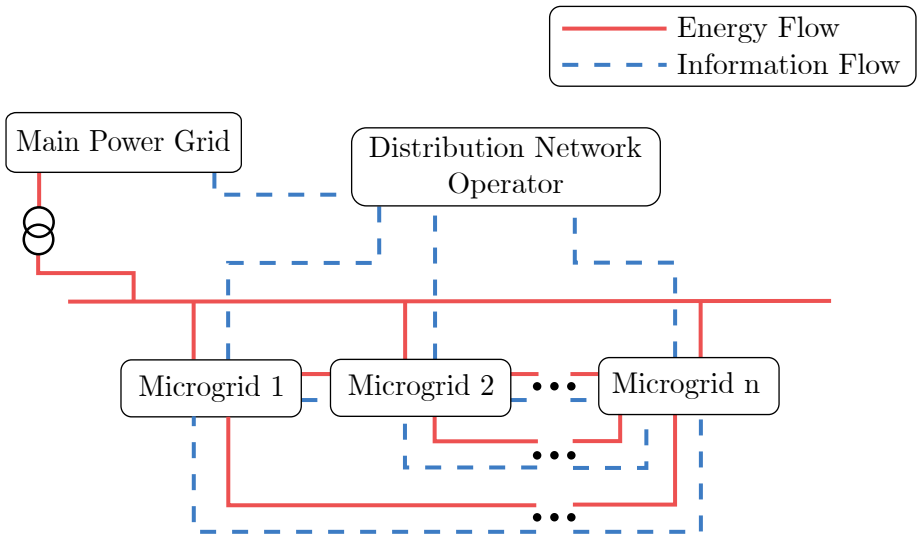

Figure 2.4: MMG system with mesh topology.

2.2.2 MMG EMS Architecture

The control structure for the EMS of single MGs, which was previously discussed, is also applicable to MMG systems. In some references, a nested hierarchical architecture is proposed, with MGs organized in multiple layers, requiring sequential information exchanges from bottom to top layers [84, 85]. However, such configuration is not realistic for practical MMG implementations. Thus, the review presented next only focuses on centralized, decentralized, and distributed approaches.

As the name implies, in the centralized EMS, the dispatchable units and controllable loads of all MGs are managed by a central controller, which is responsible for the interactions among MGs, the participation in market bidding, the transition between operating modes, and stability control functions [86]. The centralized MMG EMS optimizes the objective functions of all MGs, as a single lumped system. Such structure requires high computation power of the central controller, as the optimization problem increases in size with the addition of DERs. Although the coordination is simplified due to a single controller, this approach requires sharing sensitive information such as generation costs or load profiles with the central controller, which individual MGs may be unwilling to provide. Furthermore, the entire system depends on the adequate operation of the centralized controller, compromising the reliability in case of failure [23, 87]. For these reasons, a centralized EMS is not the best option for MMG systems.

In a fully decentralized EMS, each MG acts as an autonomous entity with a local controller, operating based on local information only, with no knowledge or awareness of the operation status of the other MGs. However, in this configuration, every MG seeks to optimize its own operation independently, which may lead to competition and negatively impact the overall system performance [88]. In the case of MMG systems with MGs owned by different entities, such configuration might be suitable.

Distributed approaches have been proposed to overcome the disadvantages of centralized and decentralized structures. While a distributed approach is more complex to implement, it resolves the aforementioned issues, as it does not depend on a centralized controller, it requires minimal information exchange among MGs to coordinate the power exchanges, and a global optimal state is achieved through the coordinated operation. Furthermore, in a distributed EMS, the addition of DERs in an MG only requires updating local parameters in the optimization problem of that MG, as opposed to updating a global centralized model, which may be problematic as the penetration level of DERs increases [89]. A drawback of a distributed control approach is the dependency on a communication network to coordinate the interactions among MGs, and the required infrastructure to enable frequent power transactions [88]. Table 2.2 shows a summary of the advantages and disadvantages of each one of the MMG EMS control structures.

Unlike the case of single MGs, which have already been widely adopted, real-world implementations of MMG systems are much more hard to find, mainly due to the increased complexity associated with such projects. A proper location is required, where multiple MGs are sufficiently close to interact with one another, and the owners or stakeholders of these MGs must be willing to heavily invest in the development of the project. A notable example is a project being developed in Chicago, United States, where the Bronzeville Community MG will be linked to the Illinois Institute of Technology MG. The Bronzeville MG consists of PV arrays with a total capacity of 750 kW, and 2 MWh of battery storage. It is adjacent to the Institute's MG, which has 12 MW of DERs, including dispatchable units such as gas turbines, and non-dispatchable units such as PV arrays and wind turbines. With the joint operation, it is expected that during an outage, both MGs are capable of isolating from the main grid, and share power with each other if necessary. This is an ongoing project that is attracting significant attention, and should be followed closely as a model for the implementation of MMGs in other locations [91, 92].

Table 2.2: Characteristics of MMG EMS structures [88, 90].

EMS Structure	Advantage	Disadvantage
Centralized	• Simpler implementation and coordination. • Reduced operation cost. • Efficient use of MG components.	• High computation burden. • Vulnerable to single-point failures. • Complete dependence on a central controller. • Limited flexibility to system modifications.
Decentralized	• Robust against single-point failures. • Privacy protection. • Strong plug-and-play functionality. • Reduced computational burden for local controllers.	• More complex implementation and coordination. • Higher operation cost. • Unawareness of system-level resources. • High energy exchanges between MGs and main grid.
Distributed	• Privacy protection. • High plug-and-play functionality. • Relatively low operation cost. • Reduced computational burden for central/local controllers.	• Disclosing of partial information required. • Coordinated operation still relies on a central controller. • High dependence on communication network.

2.3 Distributed Optimization

The development of communication technologies has resulted in the emergence of networked systems, in which interconnected subsystems cooperate to achieve a global objective which is beneficial for all subsystems. An MMG is a perfect example of such a system, with an inherent distributed structure that can be advantageously exploited. Several solution methods and algorithms based on distributed optimization techniques have been reported in the literature to solve such problems, such as approaches based on game theory, hierarchical decision-making, ADMM algorithms, consensus algorithms, heuristics, and dual decomposition, among others [89, 30].

It is important to note that a distributed optimization approach can only be applied if the problem in question has a decomposable structure, or can be mathematically transformed to attain such structure, i.e., if it can somehow be formulated to be solved by

blocks. For example, in the MMG EMS problem, a block would be each MG, and the goal is to decompose the complete problem into subproblems corresponding to each MG. These subproblems can then be solved locally, and by sharing minimal information, the optimal solution for all MGs can be obtained through an iterative algorithm. Depending on the type and structure of the optimization problem, the approach to implement a distributed solution algorithm changes. Thus, Linear Programming (LP), Nonlinear Programming (NLP), MILP, and Mixed-Integer Non-Linear Programming (MINLP) problems would be handled differently, while also considering whether their structure presents complicating variables or complicating constraints, i.e., variables or constraints which prevent a straightforward decomposition. Methods such as Benders decomposition and Dantzig-Wolfe decomposition (or some variation) are applied accordingly to each type of problem [93, 94]. A detailed description of these methods is beyond the scope of this thesis; however, it is important to mention them to provide some context.

The decomposition technique used in this research is known as dual decomposition (sometimes also referred to as Lagrangian relaxation). This technique has its basis on the dual ascent method, and is closely related to the method of multipliers and ADMM algorithms [95]. However, due to the coupled characteristic of the proposed MMG EMS model, the augmented Lagrangian is not separable across the partitioning of variables by MG, preventing decomposition using the ADMM approach. Thus, a generic description of dual decomposition, as presented in [96], is provided next, which supports the explanation of the decomposition procedure for the proposed MMG EMS model in Chapter 3.

The dual decomposition method has been widely applied to various optimization problems that benefit from a distributed solution [97]. Thus, consider the following optimization model:

$$\min_{\mathbf{x}} \quad \sum_{i=1}^{I} f_i(\mathbf{x}) \tag{2.1a}$$

$$\text{s.t.} \quad g_i(\mathbf{x}) \leq a_i \quad \forall\ i \tag{2.1b}$$

$$\sum_{i=1}^{I} h_i(\mathbf{x}) \leq b \tag{2.1c}$$

where the objective function $f_i(\mathbf{x})$ is a convex, quadratic, and separable function with respect to variables $\mathbf{x}$; $g_i(\mathbf{x})$ is a separable function across variables $\mathbf{x}$, representing a set of inequality constraints of the problem; $h_i(\mathbf{x})$ is a function corresponding to another set of constraints of the problem, but it is not separable across variables $\mathbf{x}$; and a_i and b are the corresponding right-hand side values of the inequality constraints. Based on these

properties, constraints (2.1b) are separable (one constraint for each i), but constraint (2.1c) is a complicating constraint, as it is not separable and prevents the decomposition of the problem among each i. In order to relax the complicating constraints, a dual decomposition procedure is applied by dualizing (2.1c), as follows [95]:

$$\max_{\lambda}\Bigg\{ \min_{\mathbf{x}} \quad \sum_{i=1}^{I} f_i(\mathbf{x}) + \lambda\Bigg[b - \sum_{i=1}^{I} h_i(\mathbf{x})\Bigg] \tag{2.2a}$$

$$\text{s.t.} \quad g_i(\mathbf{x}) \leq a_i \quad \forall i \Bigg\} \tag{2.2b}$$

This problem is not decomposable yet, due to the Lagrange multiplier (or dual variable) λ in the objective function. To solve this issue, the problem is relaxed by fixing λ to a constant value $\overline{\lambda}$, i.e., turning it into a parameter, with the relaxed problem being decomposable into the following i subproblems:

$$\min_{x_i} \quad f_i(x_i) - \overline{\lambda} h_i(x_i) \tag{2.3a}$$

$$\text{s.t.} \quad g_i(x_i) \leq a_i \tag{2.3b}$$

In dual decomposition, the maximization over λ is carried out through the iterative solution of the obtained subproblems, updating the fixed dual variable in each iteration with an appropriate technique, such as the subgradient or cutting plane methods [93]. While cutting plane methods may converge faster for certain problems, they have a significantly higher computational burden. The subgradient method is the most straightforward approach, based on the following update step:

$$\lambda^{k+1} = \lambda^k + \alpha^k s^k \tag{2.4}$$

where α is the step size, s is the subgradient of (2.3), and k is the iteration counter. The step size can be chosen according to different rules, as described in [98]. For a constant step size, the subgradient algorithm is guaranteed to converge within some range of the optimal value in a finite number of steps, depending on the step size. The iterative procedure starts by initializing the dual variable at some fixed value, solving each subproblem independently with the dual variable as parameter, and updating the dual variable with the obtained solutions using (2.4). The process is then repeated by solving the subproblems with the updated dual variables, until convergence is reached.

The subgradient algorithm is very sensitive to the chosen step size α because it progresses to the optimum in an oscillating fashion, which makes it very difficult to select

an adequate stopping criterion. Thus, the algorithm is typically stopped after a prespecified number of iterations. Variable step sizes may improve the convergence rate of the algorithm, depending on the specific problem. Furthermore, to reach convergence, the objective function must be convex with respect to the coupling variables of the problem [97, 93].

2.4 Affine Arithmetic

AA is a range analysis method suitable for handling multiple uncertainty sources, such as imprecise data, modeling errors, round-off errors, or truncation errors. It automatically keeps track of rounding or truncation errors for each computed quantity, as well as the correlations between those quantities [59]. In AA, a quantity x subject to uncertainty is represented by an affine form $\hat{x}$, which is a first-degree polynomial, as follows:

$$\hat{x} = x_0 + x_1\varepsilon_1 + \cdots + x_p\varepsilon_p = x_0 + \sum_{h=1}^{p} x_h\varepsilon_h \tag{2.5}$$

The coefficient x_0 is called the *central value* of the affine form, which represents the value that x is most likely to take. Coefficients x_h are called *partial deviations*, and define the magnitude of the corresponding uncertainty component. The symbolic real variables ε_h are called *noise symbols*, and have unknown values within the range [-1,1]. The number of noise symbols p depends on the uncertainties affecting variable x, and could be shared with other affine forms. Each noise symbol represents an independent component of the total uncertainty of quantity x, and the corresponding x_h coefficients set the magnitude of that component. A key feature of the AA model is that the same noise symbol may contribute to the uncertainty of two or more quantities, indicating partial dependency between them.

According to the fundamental Invariance Theorem of AA, for every AA operation there is a single assignment of values from the [-1,1] interval into each of the noise symbols that makes the value of every affine form equal to the true value of the corresponding variable [59]. Thus, the actual value of quantity x is guaranteed to lie in the interval given by:

$$[\hat{x}] = [x_0 - \mathrm{rad}(\hat{\mathrm{x}}),\ x_0 + \mathrm{rad}(\hat{\mathrm{x}})] \tag{2.6}$$

$$\mathrm{rad}(\hat{x}) = \sum_{i=1}^{p} |x_i| \tag{2.7}$$

Note that $[\hat{x}]$ is the smallest interval that contains all possible values of x. This conversion

discards any correlation between computed quantities present in their affine forms. The quantity $\mathrm{rad}(\hat{x})$ is called the *total deviation* or *radius* of the affine form $\hat{x}$, around its center value x_0.

2.4.1 AA Operations

The first step to perform AA computations is to extend elementary operations and functions to the affine domain; then, these affine operations can be combined to compute arbitrarily complex functions. For example, without loss of generality, consider a generic function of two variables, $f(x, y)$. If the function is linear, the corresponding affine function can be obtained by expanding and rearranging the original noise symbols $\varepsilon_h \; \forall \, h \in (1, \cdots, p)$ of the affine forms of the variables $\hat{x}$ and $\hat{y}$. For instance, given any real numbers a, b, and c, the operation $g = ax + by + c$ carried out in the affine domain is:

$$\hat{g} = a\hat{x} + b\hat{y} + c = (ax_0 + by_0 + c) + (ax_1 + by_1)\,\varepsilon_1 + \cdots + (ax_p + by_p)\,\varepsilon_p \tag{2.8}$$

Except for round-off errors, the affine form $\hat{g}$ captures all the information about quantities x, y, and g that can be deduced from the given affine forms. However, if $f(x, y)$ is a nonlinear function, the corresponding affine extension cannot be expressed exactly as an affine combination of the original noise symbols; in this case, an affine function that approximates the original function must be identified, and an additional term to account for the approximation error is introduced. For instance, the product of two variables in affine form is given by:

$$\hat{x}\hat{y} = x_0 y_0 + \sum_{h=1}^{p} (x_0 y_h + y_0 x_h)\,\varepsilon_h + \sum_{h=1}^{p} x_h \varepsilon_h \sum_{h=1}^{p} y_h \varepsilon_h \tag{2.9}$$

The last term on the right-hand side of (2.9) is nonlinear, and it represents the approximation error. Rewriting this term as $z_{p+1}\varepsilon_{p+1}$, the product becomes:

$$\hat{x} \cdot \hat{y} = x_0 y_0 + \sum_{h=1}^{p} (x_0 y_h + y_0 x_h)\,\varepsilon_h + z_{p+1}\varepsilon_{p+1} \tag{2.10}$$

where

$$|z_{p+1}| \geq \left| \sum_{h=1}^{p} x_h \varepsilon_h \sum_{h=1}^{p} y_h \varepsilon_h \right| \tag{2.11}$$

is an upper bound for the approximation error. The most simple and conservative affine approximation can be computed as:

$$z_{p+1} = \sum_{h=1}^{p} |x_h| \sum_{h=1}^{p} |y_h| \tag{2.12}$$

The new noise symbol ε_{p+1} is introduced by the non-affine operation, hence describing an endogenous uncertainty, as opposed to the noise symbols $\varepsilon_1, \cdots, \varepsilon_p$, which describe exogenous uncertainties. This approximation of the product of affine forms is straightforward, but there is a loss of information because the noise symbol ε_{p+1} is assumed to be completely independent from the original noise symbols, which is not true. More accurate approximations may be used, such as the Chebyshev approximation, at the cost of higher computational burden [58].

2.4.2 AA Optimization

Based on the previous description of affine extensions, a deterministic optimization problem can be reformulated to account for data uncertainties, according to the theoretical framework introduced in [61]. The goal is to solve the following constrained optimization problem in the presence of data uncertainties represented as affine forms:

$$\begin{aligned} \min_{\hat{\mathbf{z}}} \quad & \hat{f}(\hat{\mathbf{z}}) \\ \text{s.t.} \quad & \hat{g}_j(\hat{\mathbf{z}}) = 0 \quad \forall\ j \in (1, \cdots, n) \\ & \hat{h}_k(\hat{\mathbf{z}}) < 0 \quad \forall\ k \in (1, \cdots, m) \end{aligned} \tag{2.13}$$

where $\hat{\mathbf{z}}$ is the vector of unknown affine forms of the state variables, which includes dependent and control variables; $\hat{f}$ is the continuous and differentiable affine objective function; and $\hat{g}_j(\hat{\mathbf{z}})$ and $\hat{h}_k(\hat{\mathbf{z}})$ are continuous and differentiable affine functions that represent the j-th equality and k-th inequality constraints, respectively.

To solve (2.13), the minimization and comparison operators must be extended into the affine domain, as proposed in [61]. These operators are fundamental for the affine formulation of the EMS problem described in Chapter 4, and thus their definitions are presented next.

Similarity Operator

Two affine forms defined as $\hat{x} = x_0 + \sum_{h=1}^{p+p^{na}} x_h \varepsilon_h$ and $\hat{y} = y_0 + \sum_{h=1}^{p+p^{na}} y_h \varepsilon_h$ are similar with an approximation degree $L_{x,y}$, i.e., $\hat{x} \overset{A}{\simeq} \hat{y}$, if and only if:

$$\{x_h = y_h,\ \forall\ h \in (0, \cdots, p)\} \wedge \left\{ L_{x,y} = \sum_{h=p+1}^{p+p^{na}} (|x_h| + |y_h|) \right\} \tag{2.14}$$

The noise symbols $\varepsilon_{p+1}, \cdots, \varepsilon_{p+p^{na}}$ describe the endogenous uncertainties, which are generated by the approximation of p^{na} non-affine functions such as multiplications and other nonlinear operations; the partial deviations $x_{p+1}, \cdots, x_{p+p^{na}}$ are the upper bounds of the corresponding approximation errors. This operator is useful when the radius of the uncertain variables is the only available information.

Inequality Operator

Given two affine forms defined as $\hat{x} = x_0 + \sum_{h=1}^{p^x} x_h \varepsilon_h^x$ and $\hat{y} = y_0 + \sum_{h=1}^{p^y} y_h \varepsilon_h^y$, then $\hat{x} \overset{A}{<} \hat{y}$, if and only if:

$$x_0 + \sum_{h=1}^{p^x} |x_h| < y_0 - \sum_{h=1}^{p^y} |y_h| \tag{2.15}$$

This definition simply states that the upper bound of $\hat{x}$, i.e., the maximum value that the uncertain variable x can take, is less than the lower bound of $\hat{y}$, i.e., the minimum value that the uncertain variable y can take.

Minimization Operator

Given a differentiable, nonlinear function f and the affine form $\hat{x} = x_0 + \sum_{h=1}^{p} x_h \varepsilon_h$, the AA-based minimization problem

$$\min_{\hat{x}} \quad \hat{f}(\hat{x}) = f_0(\hat{x}) + \sum_{h=1}^{p} f_h(\hat{x}) \varepsilon_h + \sum_{h=p+1}^{p+p^{na}} f_h(\hat{x}) \varepsilon_h \tag{2.16}$$

is equivalent to the deterministic multi-objective programming problem

$$\min_{x_0, x_1, \cdots, x_p} \quad \left\{ f_0(x_0, x_1, \cdots, x_p), \sum_{h=1}^{p+p^{na}} |f_h(x_0, x_1, \cdots, x_p)| \right\} \tag{2.17}$$

The minimization of the affine central value $f_0(x_0, x_1, \cdots, x_p)$ seeks the optimal solution without considering the uncertainties represented by the noise symbols, while the minimization of the affine radius $\sum_{h=1}^{p+p^{na}} |f_h(x_0, x_1, \cdots, x_p)|$ seeks the most robust solution with the lowest tolerance to data uncertainty.

Using these operators, the solution of problem (2.13) is obtained by solving the following deterministic multi-objective constrained optimization problem:

$$\begin{aligned} \min_{\hat{\mathbf{z}}} \quad & \left\{ f_0(\hat{\mathbf{z}}), \sum_{h=1}^{p+p^{na}} |f_h(\hat{\mathbf{z}})| \right\} \\ \text{s.t.} \quad & \hat{g}_j(\hat{\mathbf{z}}) \overset{A}{\simeq} 0 \quad \forall\ j \in (1, \cdots, n) \\ & \hat{h}_k(\hat{\mathbf{z}}) \overset{A}{<} 0 \quad \forall\ k \in (1, \cdots, m) \end{aligned} \tag{2.18}$$

2.5 Summary

This chapter presented a review of the main background topics relevant to the development of this thesis. A description of single MGs was provided, discussing their common components and control levels. Then, the concept of MMG systems was introduced, describing their main features, topologies, and EMS architectures. A brief description of distributed optimization and dual decomposition was presented next. Finally, the core elements, concepts, and operators of the AA optimization framework for considering uncertainties were defined.

Chapter 3

A Centralized and Distributed EMS for Multi-Microgrid Systems

This chapter presents a distributed optimization approach for the solution of the MMG EMS problem. First, the centralized EMS model is formulated as a cost minimization problem that considers the operation of all MGs and their interactions among each other and the main grid as a single, centralized system. Then, a decomposition procedure is described, which transforms the central problem into subproblems that can be solved separately by each MG. A distributed optimization algorithm is then presented, which finds the optimal or near-optimal solution of the entire system through the iterative solution of the MG subproblems, while preserving the privacy of each MG. Finally, case studies are presented and discussed, testing and validating the proposed MMG EMS models.

3.1 Centralized EMS

In this section, the formulation of the UC problem for MMGs is described in detail. A single-node model of the MG is considered, in which all the nonlinear power flow constraints are replaced by a single supply-demand balance equation, because in MGs, feeders can be neglected without significantly affecting the EMS results, while improving computational performance [99]. The UC problem is a mathematical optimization problem whose solution yields the optimal operation of the system in a defined period, according to a specific target, such as minimizing operational costs or maximizing generation revenue, while satisfying a set of system constraints.

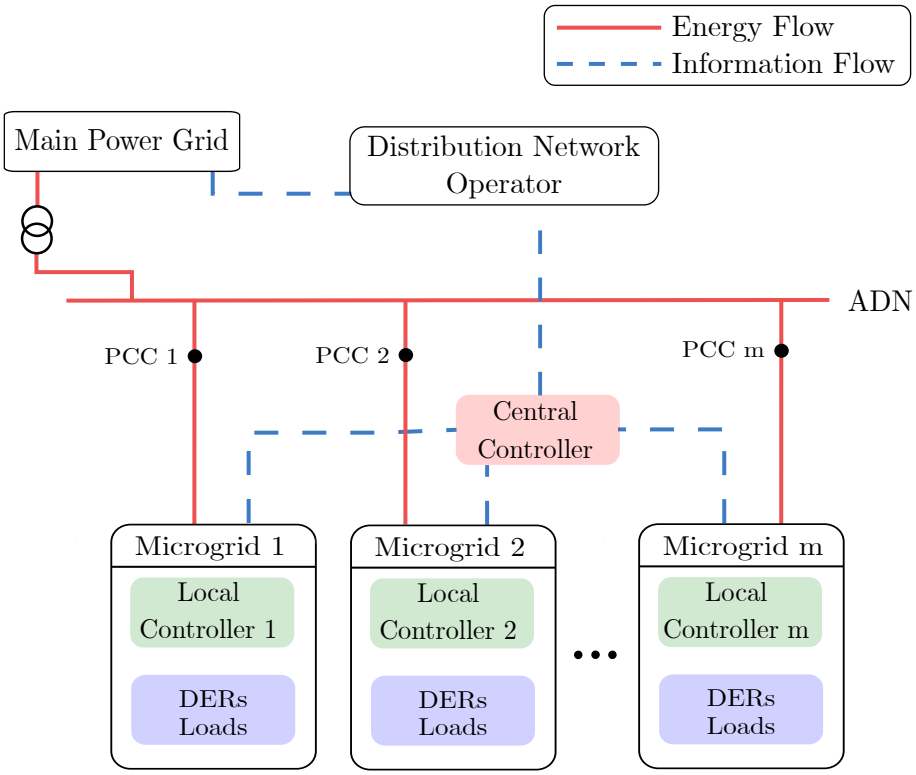

Figure 3.1: Overview of an MMG system.

The MMG system considered in this work is comprised of m MGs connected to the ADN, as shown in Figure 3.1. It is assumed that each MG can exchange power with the ADN and with all other MGs. The power exchanges between MGs take place through the main grid and their corresponding PCCs, as per the most realistic MMG radial topology. Each MG has a local controller which is responsible for the management of local resources, while the central controller coordinates the interactions between individual MGs and the ADN. The optimization period is defined by the set of hours T, with each hour represented by the index t. In this system, it is important to consider the capacity limits of the connection of each MG; furthermore, information exchange is necessary to coordinate the power exchanges among MGs. The focus of the proposed model is the application of a distributed optimization technique; therefore, for the sake of simplicity, the distribution and communication networks are not explicitly considered.

Each MG has a set of thermal generators G_m, such as diesel units, with each generator represented by index g, as well as a set of ESS units S_m, with units represented by the

index s. The conventional quadratic cost function of thermal generators is assumed, as follows:

$$C(P_{m,g,t}) = a_{m,g}P_{m,g,t}^2 + b_{m,g}P_{m,g,t} + c_{m,g}v_{m,g,t} \quad \forall\ m \in M,\ g \in G_m,\ t \in T \tag{3.1}$$

where $a_{m,g}$, $b_{m,g}$ and $c_{m,g}$ are the quadratic, linear, and constant coefficients of the cost function of generator g in MG m, respectively, $P_{m,g,t}$ is the power output of the generator at time t, and $v_{m,g,t}$ is a binary variable indicating the status of the generator, equal to 1 when the generator is up, and 0 otherwise.

Based on (3.1), the objective function, which minimizes the operational cost for the whole MMG system, can be formulated as follows:

$$\begin{aligned} \min \quad & \sum_{t\in T}\sum_{m\in M}\Bigg[\sum_{g\in G_m}\left(C(P_{m,g,t})\Delta t + C_{m,g}^{SD}SD_{m,g,t} + C_{m,g}^{SU}SU_{m,g,t}\right) \\ & + \left(\rho_m^{gs}P_{m,t}^{gs} - \rho_m^{gb}P_{m,t}^{gb}\right)\Delta t\Bigg] \end{aligned} \tag{3.2}$$

where $C_{m,g,t}$ is the cost function given by (3.1); Δt is the duration of each period in the optimization time span, which allows considering shorter periods by taking fractional values; $C_{m,g}^{SD}$ and $C_{m,g}^{SU}$ are the shutdown and startup costs of generator g in MG m, respectively; and $SD_{m,g,t}$ and $SU_{m,g,t}$ are the shutdown and startup decisions for each generator at time t, respectively, equal to 1 if the unit is scheduled for shutdown or startup, and 0 otherwise. The selling and buying prices of the main grid to and from each MG are denoted by ρ_m^{gs} and ρ_m^{gb}, respectively, and the power sold and bought by the main grid to and from each MG are represented by P_m^{gs} and P_m^{gb}, respectively. The first term in the objective function corresponds to the operational cost of the MG, and the second term corresponds to the cost or profit resulting from power exchanges with the main grid. The minimization is done over all MGs, which makes it a centralized formulation. It is assumed here that there is no cost for the use of ESSs; however, such costs can be readily added to (3.2) to reflect ESS degradation (e.g. [79]).

The supply-demand balance constraint ensures that the total generation in each MG is equal to its total demand at all hours, taking into account the power exchanges between

MGs and the main grid, and can be formulated as follows:

$$\sum_{g\in G_m} P_{m,g,t} + P^r_{m,t} + \sum_{s\in S_m}(P^{dch}_{m,s,t} - P^{ch}_{m,s,t}) + \sum_{n\in M\backslash m} P^e_{n,m,t} + P^{gs}_{m,t} = D_{m,t} + \sum_{n\in M\backslash m} P^e_{m,n,t} + P^{gb}_{m,t} \quad \forall\ m\in M,\ t\in T \tag{3.3}$$

where $P^r_{m,t}$ is the renewable generation power in MG m at time t, and $P^{dch}_{m,s,t}$ and $P^{ch}_{m,s,t}$ are the discharging and charging powers of ESS unit s in MG m at time t, respectively. $P^e_{n,m,t}$ is the power exchange from MG n to MG m at time t, where $n \in M\backslash m$, i.e., the index n denotes each MG in the set M different than MG m, to account for all possible combinations of power exchanges between MGs. $D_{m,t}$ is the power demand in MG m at time t.

The following constraints impose the minimum and maximum power output of thermal units:

$$v_{m,g,t}\underline{P}_{m,g} \le P_{m,g,t} \le \overline{P}_{m,g} v_{m,g,t} \quad \forall\ m\in M,\ g\in G_m,\ t\in T \tag{3.4}$$

where $\underline{P}_{m,g}$ and $\overline{P}_{m,g}$ are the minimum and maximum power outputs, respectively. The product of each limit and the binary variable ensures that the generated power is zero when the unit is down. Ramping limits of thermal units are also considered and represented by:

$$P_{m,g,t} - P_{m,g,t+1} \le RD_{m,g}\Delta t + SD_{m,g,t+1}\underline{P}_{m,g} \quad \forall\ m\in M,\ g\in G_m,\ t, t+1\in T \tag{3.5}$$

$$P_{m,g,t+1} - P_{m,g,t} \le RU_{m,g}\Delta t + SU_{m,g,t+1}\underline{P}_{m,g} \quad \forall\ m\in M,\ g\in G_m,\ t, t+1\in T \tag{3.6}$$

where $RD_{m,g}$ and $RU_{m,g}$ are the ramp down and ramp up limits of generator g in MG m, respectively. The first term on the right-hand side in (3.5) and (3.6) ensures that the change in power from period t to period $t+1$ does not exceed the maximum ramp value, if the unit status does not change in period $t+1$. In the ramp down constraints, the second term on the right-hand side ensures that $P_{m,g,t}$ can reach zero if the unit is shutdown in period $t+1$. Similarly, in the ramp up constraints, the second term on the right-hand side ensures that $P_{m,g,t}$ can change from zero to the required value if the unit is started up in period $t+1$.

The following constraints coordinate the shutdown and startup decisions with the generator status variables, as well as ensuring that each unit is not shut down and started up at the same period:

$$SU_{m,g,t} - SD_{m,g,t} = v_{m,g,t} - v_{m,g,t-1} \quad \forall\ m\in M,\ g\in G_m,\ t, t-1\in T \tag{3.7}$$

$$SU_{m,g,t} + SD_{m,g,t} \leq 1 \quad \forall\ m \in M,\ g \in G_m,\ t \in T \tag{3.8}$$

The minimum downtime requirements of thermal units are imposed by the following constraints [100]:

$$\sum_{t=1}^{L^D_{m,g}} v_{m,g,t} = 0 \quad \forall\ m \in M,\ g \in G_m,\ L^D_{m,g} \geq 1 \tag{3.9}$$

$$\sum_{t'=t}^{t+DT_{m,g}-1} (1 - v_{m,g,t'}) \geq DT_{m,g} SD_{m,g,t} \quad \forall\ m \in M,\ g \in G_m, \quad t = (L^D_{m,g} + 1), \cdots, (\overline{T} - DT_{m,g} + 1) \tag{3.10}$$

$$\sum_{t'=t}^{\overline{T}} (1 - v_{m,g,t'} - SD_{m,g,t}) \geq 0 \quad \forall\ m \in M,\ g \in G_m,\ t = (\overline{T} - DT_{m,g} + 2), \cdots, \overline{T} \tag{3.11}$$

where $L^D_{m,g} = \min\{\overline{T}, (DT_{m,g} - DT^0_{m,g})(1 - v^0_{m,g})\}$ is the number of periods that generator g in MG m must be down after considering its downtime before solving the problem; $\overline{T}$ is the number of periods in the optimization time span; $DT_{m,g}$ is the minimum downtime of generator g in MG m; $DT^0_{m,g}$ is the number of periods that the generator has been down prior to the first period of the optimization time span; and $v^0_{m,g}$ is the initial commitment status, equal to 1 if the unit is up, and 0 otherwise. Constraint (3.9) ensures that the unit satisfies its minimum downtime at the beginning of the optimization time span, and is only included when $L^D_{m,g} \geq 1$, i.e., when the unit is initially down and the number of periods it has been down prior to the first period is less than its minimum down time requirement. Constraint (3.10) enforces the downtime requirement for all subsequent sets of consecutive periods of size $DT_{m,g}$ that come after period $L^D_{m,g}$, and is only included if $(L^D_{m,g} + 1) < (\overline{T} - DT_{m,g} + 1)$ and $DT_{m,g} > 1$. Constraint (3.11) enforces the minimum downtime for the last $(DT_{m,g} - 1)$ periods, i.e., if the unit is shutdown at one of these periods, it will remain down until the last period of the entire time span. Similarly, the following set of constraints guarantee that the minimum uptime requirements of thermal generators are fulfilled [100]:

$$\sum_{t=1}^{L^U_{m,g}} (1 - v_{m,g,t}) = 0 \quad \forall\ m \in M,\ g \in G_m,\ L^U_{m,g} \geq 1 \tag{3.12}$$

$$\sum_{t'=t}^{t+UT_{m,g}-1} v_{m,g,t'} \geq UT_{m,g} SU_{m,g,t} \quad \forall\ m \in M,\ g \in G_m, \\ t = (L^U_{m,g}+1), \cdots, (\overline{T} - UT_{m,g} + 1) \tag{3.13}$$

$$\sum_{t'=t}^{\overline{T}} (v_{m,g,t'} - SU_{m,g,t}) \geq 0 \quad \forall\ m \in M,\ g \in G_m,\ t = (\overline{T} - UT_{m,g} + 2), \cdots, \overline{T} \tag{3.14}$$

where $L^U_{m,g} = \min\{\overline{T}, (UT_{m,g} - UT^0_{m,g}) v^0_{m,g}\}$ is the number of periods that generator g in MG m must be up after considering its uptime before solving the problem; $UT_{m,g}$ is the minimum uptime of generator g in MG m; $UT^0_{m,g}$ is the number of periods that the generator has been up prior to the first period of the optimization time span. Constraint (3.12) ensures that the unit satisfies its minimum uptime at the beginning of the optimization time span, and is only included when $L^U_{m,g} \geq 1$, i.e., when the unit is initially up and the number of periods it has been up prior to the first period is less than its minimum uptime requirement. Constraint (3.13) enforces the uptime requirement for all subsequent sets of consecutive periods of size $UT_{m,g}$ that come after period $L^U_{m,g}$, and is only included if $(L^U_{m,g}+1) < (\overline{T} - UT_{m,g} + 1)$ and $UT_{m,g} > 1$. Constraint (3.14) enforces the minimum uptime for the last $(UT_{m,g}-1)$ periods, i.e., if the unit is started up in one of these periods, it will remain up until the last period of the entire time span.

The following expressions impose the energy balance, status coordination, and operating limits of the ESS units:

$$SoC_{m,s,t+1} - SoC_{m,s,t} = [P^{ch}_{m,s,t} \eta^{ch}_{m,s} - P^{dch}_{m,s,t} / \eta^{dch}_{m,s}] \Delta t \quad \forall\ m \in M,\ s \in S_m, \\ t, t+1 \in T \tag{3.15}$$

$$\underline{SoC}_{m,s} \leq SoC_{m,s,t} \leq \overline{SoC}_{m,s} \quad \forall\ m \in M,\ s \in S_m,\ t \in T \tag{3.16}$$

$$\underline{P^{ch}}_{m,s} z^{ch}_{m,s,t} \leq P^{ch}_{m,s,t} \leq \overline{P^{ch}}_{m,s} z^{ch}_{m,s,t} \quad \forall\ m \in M,\ s \in S_m,\ t \in T \tag{3.17}$$

$$\underline{P^{dch}}_{m,s} z^{dch}_{m,s,t} \leq P^{dch}_{m,s,t} \leq \overline{P^{dch}}_{m,s} z^{dch}_{m,s,t} \forall\ m \in M,\ s \in S_m,\ t \in T \tag{3.18}$$

$$z^{ch}_{m,s,t} + z^{dch}_{m,s,t} \leq 1 \quad \forall\ m \in M,\ s \in S_m,\ t \in T \tag{3.19}$$

where $SoC_{m,s,t}$ is the State of Charge (SoC) of ESS unit s in MG m at time t, with $\underline{SoC}_{m,s}$ and $\overline{SoC}_{m,s}$ representing its minimum and maximum limits, respectively; $\eta^{ch}_{m,s}$ and $\eta^{dch}_{m,s}$ are the charging and discharging efficiencies, respectively; $\underline{P^{dch}}_{m,s}$ and $\overline{P^{dch}}_{m,s}$ are the minimum and maximum discharging power limits, respectively; $\underline{P^{ch}}_{m,s}$ and $\overline{P^{ch}}_{m,s}$ are the minimum and maximum charging power limits, respectively; and $z^{ch}_{m,s,t}$ and $z^{dch}_{m,s,t}$ are

binary variables representing the charging and discharging status, respectively, equal to 1 if the unit is charging/discharging, and 0 otherwise. Constraint (3.15) guarantees the energy balance for ESS units at all periods; constraint (3.16) enforces the minimum and maximum SoC limits; constraints (3.17) and (3.18) set the minimum and maximum boundaries for charging and discharging power, respectively; and constraint (3.19) ensures that the ESS units are never charging and discharging simultaneously.

The limits of power transfer capacity through the PCC of each MG, as shown in Figure 3.1, are enforced by the following constraints:

$$\sum_{n \in M \backslash m} P^{e}_{m,n,t} + P^{gb}_{m,t} \leq P^{PCC}_{m} \quad \forall\ m \in M,\ t \in T \tag{3.20}$$

$$\sum_{n \in M \backslash m} P^{e}_{n,m,t} + P^{gs}_{m,t} \leq P^{PCC}_{m} \quad \forall\ m \in M,\ t \in T \tag{3.21}$$

$$P^{e}_{m,n,t} P^{e}_{n,m,t} = 0 \quad \forall\ m \in M,\ n \in M \backslash m,\ t \in T \tag{3.22}$$

where P^{PCC}_{m} is the maximum power transfer capacity through the PCC of MG m. Constraint (3.20) ensures that the power outflow from MG m to the other n MGs and to the main grid is within the required limits, and (3.21) ensures that the power inflow from all n MGs and the main grid to MG m is within the required limits. Simultaneous power exchanges in opposite directions between MGs are prevented by (3.22), which is a nonlinear expression that can be linearized through methods such as McCormick envelopes [101]. Finally, the following constraints define the model's binary and nonnegative variables:

$$v_{m,g,t},\ SD_{m,g,t},\ SU_{m,g,t},\ z^{ch}_{m,s,t},\ z^{dch}_{m,s,t} \in \{0,1\} \quad \forall\ m \in M,\ g \in G_m,\ s \in S_m,\ t \in T \tag{3.23}$$

$$P^{e}_{m,n,t},\ P^{gs}_{m,t},\ P^{gb}_{m,t} \geq 0 \quad \forall\ m \in M,\ n \in M \backslash m,\ t \in T \tag{3.24}$$

3.2 Distributed EMS

Once the proposed centralized MMG EMS model has been described, the goal is to obtain a distributed model from the centralized model, which can be solved with minimum information exchange through a central entity. The first step is applying a decomposition approach to separate the complete problem into subproblems that can be solved locally by each MG. To keep notation compact in the following explanation of the decomposition

procedure, all operational constraints associated with thermal generators and ESS units within a single MG are represented as follows:

$$\{P_{m,g,t},\ SD_{m,g,t},\ SU_{m,g,t},\ v_{m,g,t}\} \in \Omega^{G}_{m,g,t} \quad \forall\ m \in M,\ g \in G_m,\ t \in T \tag{3.25}$$

$$\{SoC_{m,s,t},\ P^{ch}_{m,s,t},\ P^{dch}_{m,s,t},\ z^{ch}_{m,s,t},\ z^{dch}_{m,s,t}\} \in \Omega^{S}_{m,s,t} \quad \forall\ m \in M,\ s \in S_m,\ t \in T \tag{3.26}$$

where $\Omega^{G}_{m,g,t}$ is the feasible region for thermal generators, defined by constraints (3.4)–(3.14), and $\Omega^{S}_{m,s,t}$ is the feasible region for ESS units, defined by constraints (3.15)–(3.19). This representation is introduced because these constraints only deal with internal variables in each MG, and thus require no modifications for applying the decomposition procedure.

According to [95], to apply a distributed optimization algorithm, the objective function of the problem must be convex with respect to the coupling variables, which, in this case, are the variables representing power exchanges among MGs. However, the objective function (3.2) is not convex with respect to the P^e variables, causing convergence issues when solving the dual problem with the iterative procedure described in Section 2.3. Therefore, a power transfer cost function is added in the objective function to resolve this issue. This new term, which is assumed quadratic to fulfill the convexity requirement, represents the cost of power transfer for the use of the distribution network, which should be paid to the distribution network operator, and may be defined as follows to guarantee convexity and convergence, instead of a typical nonconvex linear function:

$$\gamma(P^{e}_{n,m}) = \beta(P^{e}_{n,m})^2 \tag{3.27}$$

where β is a scalar chosen as small as possible to reduce the impact of this term in the objective function value, considering that the cost of power transfer is low. The range of adequate values for β to ensure convexity of the objective function depends on the parameters of the optimization problem, and can be determined through trial and error.

With this modification, the centralized EMS model can be rewritten as:

$$\min \quad \sum_{t\in T}\sum_{m\in M}\Bigg[\sum_{g\in G_m}\big(C(P_{m,g,t})\Delta t + C^{SD}_{m,g}SD_{m,g,t} + C^{SU}_{m,g}SU_{m,g,t}\big) + \big(\rho^{gs}_m P^{gs}_{m,t} - \rho^{gb}_m P^{gb}_{m,t}\big)\Delta t + \sum_{n\in M\setminus m}\gamma(P^e_{n,m,t})\Delta t\Bigg] \tag{3.28a}$$

$$\text{s.t.} \quad \sum_{g\in G_m} P_{m,g,t} + P^r_{m,t} + \sum_{s\in S_m}(P^{dch}_{m,s,t} - P^{ch}_{m,s,t}) + \sum_{n\in M\setminus m} P^e_{n,m,t} + P^{gs}_{m,t} = D_{m,t} + \sum_{n\in M\setminus m} P^e_{m,n,t} + P^{gb}_{m,t} \quad \forall\, m\in M,\ t\in T \tag{3.28b}$$

$$\{P_{m,g,t},\ SD_{m,g,t},\ SU_{m,g,t},\ v_{m,g,t}\} \in \Omega^G_{m,g,t} \quad \forall\, m\in M,\ g\in G_m,\ t\in T \tag{3.28c}$$

$$\{SoC_{m,s,t},\ P^{ch}_{m,s,t},\ P^{dch}_{m,s,t},\ z^{ch}_{m,s,t},\ z^{dch}_{m,s,t}\} \in \Omega^S_{m,s,t} \quad \forall\, m\in M,\ s\in S_m,\ t\in T \tag{3.28d}$$

$$\sum_{n\in M\setminus m} P^e_{m,n,t} + P^{gb}_{m,t} \le P^{PCC}_m \quad \forall\, m\in M,\ t\in T \tag{3.28e}$$

$$\sum_{n\in M\setminus m} P^e_{n,m,t} + P^{gs}_{m,t} \le P^{PCC}_m \quad \forall\, m\in M,\ t\in T \tag{3.28f}$$

$$v_{m,g,t},\ SD_{m,g,t},\ SU_{m,g,t},\ z^{ch}_{m,s,t},\ z^{dch}_{m,s,t} \in \{0,1\} \quad \forall\, m\in M,\ g\in G_m, s\in S_m,\ t\in T \tag{3.28g}$$

$$P^e_{m,n,t},\ P^{gs}_{m,t},\ P^{gb}_{m,t} \ge 0 \quad \forall\, m\in M,\ n\in M\setminus m,\ t\in T \tag{3.28h}$$

Notice that the bilinear constraint (3.22) is no longer needed in the model because the added power transfer cost function in the objective function has the effect of preventing simultaneous power exchanges in opposite directions between MGs. This key observation allows decomposing the problem by MGs, as (3.22) is a complicating constraint that couples all MGs.

The problem is still not decomposable, due to the power exchange variables $P^e_{m,n}$ present in (3.28b) and (3.28e). Thus, to decompose the problem, an auxiliary variable σ is introduced, to represent the total power sold by MG m to all other MGs at time t, defined as follows:

$$\sigma_{m,t} = \sum_{n\in M\setminus m} P^e_{m,n,t} \quad \forall\, m\in M,\ t\in T \tag{3.29}$$

Then, the centralized problem (3.28) is modified by adding (3.29) to its set of constraints, and substituting the auxiliary variable in (3.28b) and (3.28e), which results in the following constraints:

$$\sum_{g \in G_m} P_{m,g,t} + P^r_{m,t} + \sum_{s \in S_m} (P^{dch}_{m,s,t} - P^{ch}_{m,s,t}) + \sum_{n \in M \setminus m} P^e_{n,m,t} + P^{gs}_{m,t} = D_{m,t} + \sigma_{m,t} + P^{gb}_{m,t} \quad \forall\ m \in M,\ t \in T \tag{3.30}$$

$$\sigma_{m,t} + P^{gb}_{m,t} \leq P^{PCC}_m \quad \forall\ m \in M,\ t \in T \tag{3.31}$$

With these modifications, (3.29) is now the only complicating constraint, and therefore a decomposition method such as the dual decomposition method described in Chapter 2 can be applied. Thus, after dualizing (3.29) and replacing (3.28b) and (3.28e) with (3.30) and

(3.31), respectively, the Lagrangian dual problem of (3.28) can be expressed as follows:

$$\max_{\lambda_m}\Bigg\{ \min \quad \sum_{t\in T}\sum_{m\in M}\Bigg[\sum_{g\in G_m}\big(C(P_{m,g,t})\Delta t + C^{SD}_{m,g}SD_{m,g,t} + C^{SU}_{m,g}SU_{m,g,t}\big)$$

$$+\big(\rho^{gs}_m P^{gs}_{m,t} - \rho^{gb}_m P^{gb}_{m,t}\big)\Delta t + \sum_{n\in M\backslash m}\gamma(P^{e}_{n,m,t})\Delta t \tag{3.32a}$$

$$+\lambda_{m,t}\Bigg(\sum_{n\in M\backslash m} P^{e}_{m,n,t} - \sigma_{m,t}\Bigg)\Bigg] \tag{3.32b}$$

$$\text{s.t.} \quad \sum_{g\in G_m} P_{m,g,t} + P^{r}_{m,t} + \sum_{s\in S_m}(P^{dch}_{m,s,t} - P^{ch}_{m,s,t}) + \sum_{n\in M\backslash m} P^{e}_{n,m,t} + P^{gs}_{m,t}$$

$$= D_{m,t} + \sigma_{m,t} + P^{gb}_{m,t} \quad \forall\ m\in M,\ t\in T \tag{3.32c}$$

$$\{P_{m,g,t},\ SD_{m,g,t},\ SU_{m,g,t},\ v_{m,g,t}\} \in \Omega^{G}_{m,g,t}$$

$$\forall\ m\in M,\ g\in G_m,\ t\in T \tag{3.32d}$$

$$\{SoC_{m,s,t},\ P^{ch}_{m,s,t},\ P^{dch}_{m,s,t},\ z^{ch}_{m,s,t},\ z^{dch}_{m,s,t}\} \in \Omega^{S}_{m,s,t}$$

$$\forall\ m\in M,\ s\in S_m,\ t\in T \tag{3.32e}$$

$$\sigma_{m,t} + P^{gb}_{m,t} \le P^{PCC}_{m} \quad \forall\ m\in M,\ t\in T \tag{3.32f}$$

$$\sum_{n\in M\backslash m} P^{e}_{n,m,t} + P^{gs}_{m,t} \le P^{PCC}_{m} \quad \forall\ m\in M,\ t\in T \tag{3.32g}$$

$$v_{m,g,t},\ SD_{m,g,t},\ SU_{m,g,t},\ z^{ch}_{m,s,t},\ z^{dch}_{m,s,t} \in \{0,1\}$$

$$\forall\ m\in M,\ g\in G_m, s\in S_m,\ t\in T \tag{3.32h}$$

$$P^{e}_{m,n,t},\ P^{gs}_{m,t},\ P^{gb}_{m,t},\ \sigma_{m,t} \ge 0 \quad \forall\ m\in M,\ n\in M\backslash m,\ t\in T\Bigg\} \tag{3.32i}$$

The internal minimization problem in (3.32) now has a separable structure, and can thus be decomposed into subproblems corresponding to each MG. To carry out the decomposition, the power exchange variables $P_{n,m,t}$ and $\sigma_{m,t}$ are allocated to the subproblem of MG m, while variables $P_{m,n,t}$ belong to the subproblems of the other n MGs. This means that MG m will optimize its operation in terms of the individual power received from each one of the other n MGs, the total power it sends to all other MGs, and the rest of its local variables. To clarify this allocation procedure of power exchange variables, Table 3.1 shows which variables belong to each subproblem, in the case of a three-MG system.

Based on the previous procedure, the complicating constraint, which was moved to the objective function with its corresponding Lagrange multiplier, can now be separated,

Table 3.1: Allocation of power exchange variables for decomposition.

Subproblem	Allocated Power Exchange Variables
MG1	$P^e_{2,1,t}$, $P^e_{3,1,t}$, $\sigma_{1,t}$
MG2	$P^e_{1,2,t}$, $P^e_{3,2,t}$, $\sigma_{2,t}$
MG3	$P^e_{1,3,t}$, $P^e_{2,3,t}$, $\sigma_{3,t}$

resulting in the following subproblem for MG m:

$$\min \quad \sum_{t\in T}\Bigg[\sum_{g\in G_m}\big(C(P_{m,g,t})\Delta t + C^{SD}_{m,g}SD_{m,g,t} + C^{SU}_{m,g}SU_{m,g,t}\big) + \big(\rho^{gs}_m P^{gs}_{m,t} - \rho^{gb}_m P^{gb}_{m,t}\big)\Delta t$$
$$+ \sum_{n\in M\backslash m}\gamma(P^e_{n,m,t})\Delta t + \sum_{n\in M\backslash m}\lambda_{n,t}P^e_{n,m,t} - \lambda_{m,t}\sigma_{m,t}\Bigg] \tag{3.33a}$$

$$\text{s.t.} \quad \sum_{g\in G_m}P_{m,g,t} + P^r_{m,t} + \sum_{s\in S_m}(P^{dch}_{m,s,t} - P^{ch}_{m,s,t}) + \sum_{n\in M\backslash m}P^e_{n,m,t} + P^{gs}_{m,t}$$
$$= D_{m,t} + \sigma_{m,t} + P^{gb}_{m,t} \quad \forall\, t\in T \quad : \lambda_{m,t} \tag{3.33b}$$

$$\{P_{m,g,t},\ SD_{m,g,t},\ SU_{m,g,t},\ v_{m,g,t}\} \in \Omega^G_{m,g,t} \quad \forall\, g\in G_m,\ t\in T \tag{3.33c}$$

$$\{SoC_{m,s,t},\ P^{ch}_{m,s,t},\ P^{dch}_{m,s,t},\ z^{ch}_{m,s,t},\ z^{dch}_{m,s,t}\} \in \Omega^S_{m,s,t} \quad \forall\, s\in S_m,\ t\in T \tag{3.33d}$$

$$\sigma_{m,t} + P^{gb}_{m,t} \le P^{PCC}_m \quad \forall\, t\in T \tag{3.33e}$$

$$\sum_{n\in M\backslash m}P^e_{n,m,t} + P^{gs}_{m,t} \le P^{PCC}_m \quad \forall\, t\in T \tag{3.33f}$$

$$v_{m,g,t},\ SD_{m,g,t},\ SU_{m,g,t},\ z^{ch}_{m,s,t},\ z^{dch}_{m,s,t} \in \{0,1\}$$
$$\forall\, g\in G_m, s\in S_m,\ t\in T \tag{3.33g}$$

$$P^e_{n,m,t},\ P^{gs}_{m,t},\ P^{gb}_{m,t},\ \sigma_{m,t} \ge 0 \quad \forall\, n\in M\backslash m,\ t\in T \tag{3.33h}$$

Note that (3.33) is now a local problem that can be solved by each MG m independently. Furthermore, the dual variable $\lambda_{m,t}$ of the supply-demand balance constraint can be interpreted as the power selling price among MGs.

To solve the dual problem defined in (3.32), i.e., to carry out the maximization over the multipliers, the subgradient method [98] is used, which is implemented through the iterative procedure described in Algorithm 1. The first step is choosing initial values for the selling prices $\lambda_{m,t}$, which can be determined from existing and/or expected exchange prices. Then, these prices must be shared among MGs, which are needed by each MG for solving its own local optimization problem. Once a solution is found, MGs share the

Algorithm 1 Solution of the Dual Problem

1: Initialize selling prices $\lambda_{m,t}$
2: **repeat**
3: MGs share $\lambda_{m,t}$ with each other
4: MGs solve (3.33) independently
5: MGs share $P^{e}_{n,m,t}$ at the current $\lambda_{m,t}$
6: MGs update their selling prices:

$$\lambda_{m,t} \leftarrow \lambda_{m,t} + \alpha \left(\sum_{n \in M \setminus m} P^{e}_{m,n,t} - \sigma_{m,t} \right) \tag{3.34}$$

7: **until** Convergence criterion is satisfied

power they are willing to buy from each other ($P^{e}_{n,m,t}$), at the current selling price. With this information, each MG can update its own selling price locally. The updated prices are shared again, and the process is repeated until a convergence criterion is satisfied. The multiplier update step performed in (3.34) corresponds to the basic subgradient method, and a constant step size α was chosen, which yielded better results than different rules of variable step sizes. As discussed in Section 2.3, the subgradient algorithm is sensitive to the chosen step size α, complicating the selection of an appropriate stopping criterion. Thus, the algorithm is typically stopped after a prespecified number of iterations, and an appropriate step size can be determined through trial and error, since it depends on the problem parameters, which was the approach taken in this work.

3.3 Results and Discussion

In this section, results of the proposed centralized and distributed EMS models are presented, focusing on comparisons of the power dispatches for thermal units, ESSs, and power exchanges, with the goal of demonstrating the application of the distributed approach. To test the proposed models, a system comprised of three connected MGs was analyzed. Each MG has different demand and renewable generation profiles, considering a 24-hour optimization period. Only PV generation is considered in the model, but other RESs such as wind turbines can be readily included. Furthermore, each MG contains a set of three thermal units with distinct generation cost functions and operating limits, and a set of two ESS units.

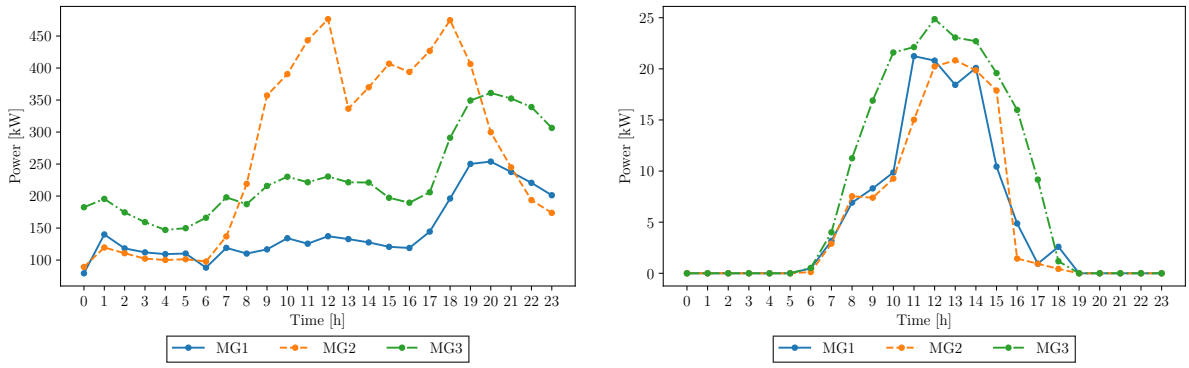

(a) Demand profiles.

(b) PV generation profiles.

Figure 3.2: Demand and PV generation profiles of all MGs.

3.3.1 Test System

The electricity demand and PV generation profiles of each MG were obtained from measured data in an ADN located in the state of São Paulo, Brazil, where the medium voltage grid was clustered to identify potential independent MGs [49]. The demand profiles are obtained directly from the available measurements of active power, with no data processing needed. However, in the case of renewable generation, which in this case is solely from PV panels, the available data corresponds to irradiance values, which are used to obtain the required profiles according to the following expression:

$$P^{r}_{m,t} = Y^{PV}_{m} f^{PV}_{m} \left(\frac{G^{T}_{m}}{G^{T,STC}_{m}} \right) \tag{3.35}$$

where Y^{PV}_{m} is the power output of the PV array in MG m under standard test conditions, assumed to be 24 kW for each MG, based on the characteristics of the system; f^{PV}_{m} is the PV panel derating factor, assumed to be equal to 1; G^{T}_{m} is the solar radiation incident on the PV array, i.e., the available measurements; $G^{T,STC}_{m}$ is the incident radiation at standard test conditions, also assumed to be equal to 1 [102]. The resulting profiles are shown in Figure 3.2. All the other parameters in the model are presented in Tables 3.2–3.4, which were adapted from various references, such as [31, 32, 103], and adjusted to be adequate for the available demand and renewable generation profiles. Note that, for simplicity, the grid's power selling and buying prices are assumed constant at all time periods; however, variable time rates can be readily incorporated into the formulation.

Table 3.2: Parameters of thermal units [31, 32, 103].

	MG1			MG2			MG3		
Parameter	G1	G2	G3	G1	G2	G3	G1	G2	G3
a [\$/kW^{2}h]	0.0002	0.0003	0.0002	0.0005	0.0007	0.0005	0.0003	0.0006	0.0004
b [\$/kWh]	0.2440	0.2876	0.2881	0.3042	0.4525	0.3554	0.2537	0.2913	0.4301
c [\$/h]	10.5	25.5	15.0	27.3	45.4	25.3	30.0	23.4	35.7
$\overline{P}$ [kW]	80	110	90	150	210	150	110	120	140
$\underline{P}$ [kW]	10	15	10	25	30	25	15	15	30
RD [kW/h]	70	95	80	125	180	125	95	105	110
RU [kW/h]	70	95	80	125	180	125	95	105	110
C^{SD} [\$]	2.00	2.75	2.25	3.75	5.25	3.75	2.75	3.00	3.50
C^{SU} [\$]	12.0	16.5	13.5	22.5	31.5	22.5	16.5	18.0	21.0
DT [h]	1	2	1	1	2	1	1	2	1
UT [h]	1	1	1	1	1	1	1	1	1
DT^0 [h]	0	0	0	0	0	0	0	0	0
UT^0 [h]	1	1	1	1	1	1	1	1	1
v^0	1	1	1	1	1	1	1	1	1

Table 3.3: Parameters of ESS units.

	MG1		MG2		MG3	
Parameter	ESS1	ESS2	ESS1	ESS2	ESS1	ESS2
η^c	0.9	0.9	0.9	0.9	0.9	0.9
η^d	0.9	0.9	0.9	0.9	0.9	0.9
$\overline{P^{ch}}$ [kW]	50.0	70.0	30.0	60.0	85.0	55.0
$\underline{P^{ch}}$ [kW]	0.0	0.0	0.0	0.0	0.0	0.0
$\overline{P^{dch}}$ [kW]	50.0	70.0	30.0	60.0	85.0	55.0
$\underline{P^{dch}}$ [kW]	0.0	0.0	0.0	0.0	0.0	0.0
$\overline{SoC}$ [kWh]	50.0	70.0	30.0	60.0	85.0	55.0
$\underline{SoC}$ [kWh]	0.0	0.0	0.0	0.0	0.0	0.0

Table 3.4: Parameters related to MG and grid interactions, with prices reflecting electricity prices in the state of São Paulo, Brazil [104].

Parameter	MG1	MG2	MG3
ρ^{gs} [\$/kWh]	0.221	0.221	0.221
ρ^{gb} [\$/kWh]	0.05	0.05	0.05
P^{PCC} [kW]	100	200	100

The solution of the centralized EMS model is used as reference to validate the proposed distributed approach. All simulations were performed on a server with dual Intel Xeon Silver 4214 processors with a base speed of 2.20 GHz, and implemented using the Pyomo optimization modeling language. The Gurobi 10.0.1 solver was used for solving the presented models [105].

3.3.2 Base Case

The base case corresponds to the data presented in Tables 3.2–3.4. In order to have a fair comparison between the centralized and distributed approaches, results of the original centralized problem, the modified centralized problem (3.28), which includes the power transfer cost function, and the iterative procedure for solving the decomposed subproblems (3.33) are analyzed next.

An update step α for the subgradient method of 0.0025 and a scaling factor β for the power transfer cost function of 0.1 were chosen through trial and error, with the goal of making the power transfer cost as small as possible, while retaining the convexity properties required by the distributed algorithm. The objective function values and costs corresponding to thermal unit generation and power transfer among MGs for the base case are presented in Table 3.5. For this particular case, there are no power exchanges among MGs in the optimal solutions; therefore, the objective function values of the centralized, modified centralized, and distributed problems are equal. These matching cost values indicate that the distributed algorithm is successfully converging to the optimal solution of the centralized problem. While the solutions will not be identical for all variables at all periods, due to the iterative nature of the distributed algorithm, the overall objective function value is similar, which demonstrates that the optimal solution is found, even if there are differences in some of the solution variables.

For example, Figure 3.3 shows a comparison of the power dispatch of thermal units in all MGs, obtained from the centralized and distributed models. As can be seen, the resulting profiles are practically identical. On the other hand, the power dispatch profiles

Table 3.5: Base Case costs.

	Centralized	Modified Centralized	Distributed
Objective function [$]	6,703.3	6,703.3	6,703.3
Generator's cost function [$]	4,901.7	4,901.7	4,901.7
Transfer cost function [$]	–	0.00	0.00

of ESS units, obtained as the difference of discharging and charging powers and shown in Figure 3.4, present differences between the centralized and distributed models. In this figure, negative values indicate that the unit is being charged, consuming power, while positive values indicate a discharge, providing power. While they follow a similar pattern, variations can be seen at different hours, which can be the case for similar optimal objective function values. The reason for these differences is that there is no cost associated with the usage or degradation of ESS units in the objective function, and thus the specific time of charge/discharge will not directly affect the objective function value.

Figure 3.5 shows the power exchanges between MGs and the main grid, from the centralized and distributed models. Once again, the resulting profiles for all MGs are practically identical, for the power sold by the main grid, while the power bought by the main grid is zero at all times, in both models. This indicates that, in this case, it is more beneficial for MGs to only buy power from the main grid, rather than sell, due to their own generation cost functions and load and PV generation profiles.

Figure 3.6 shows the behavior of the dual objective function value and duality gap through the iterations of the distributed algorithm. A fixed number of iterations was chosen here to show the convergence of the subgradient algorithm; however, as can be observed, the dual objective function value and duality gap converge in fewer iterations, and the algorithm could be stopped considering a convergence criterion such as the percent change in the dual objective function value from one iteration to the next, which in this case would require less iterations. Figure 3.6b shows the duality gap (the difference between the objective function values of the centralized and distributed models) which converges to zero, as expected.

The iterative algorithm is relatively fast, considering the complexity of the model, which has a significant number of binary variables. It requires approximately 7 min to complete 500 iterations, which is reasonable since the scheduling period is assumed here to be hourly and expected to be repeated in practice every 5-15 min based on an MPC approach to deal with forecasting inaccuracies [99]. The time may be reduced if, as mentioned before, a different convergence criterion is considered. The selling prices could also be initialized at different values, if a previous solution is known, which would improve the convergence rate of the algorithm. However, since these values may not always be available, it is important to verify the convergence of the algorithm with arbitrary initial values.

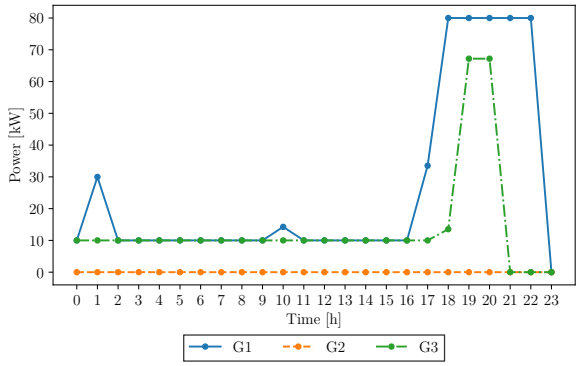

(a) MG1 centralized.

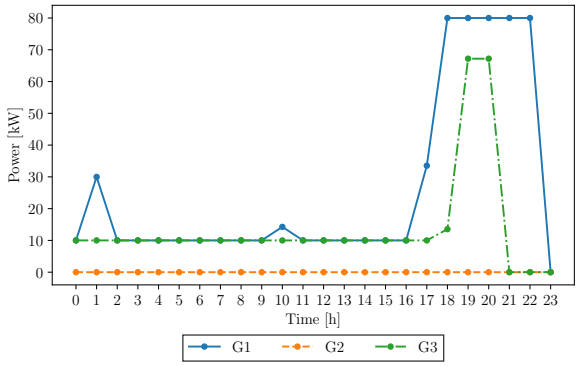

(b) MG1 distributed.

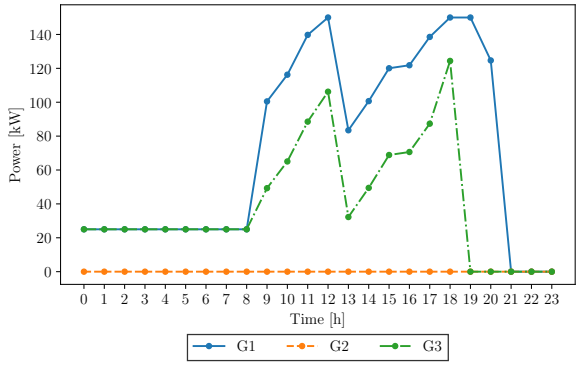

(c) MG2 centralized.

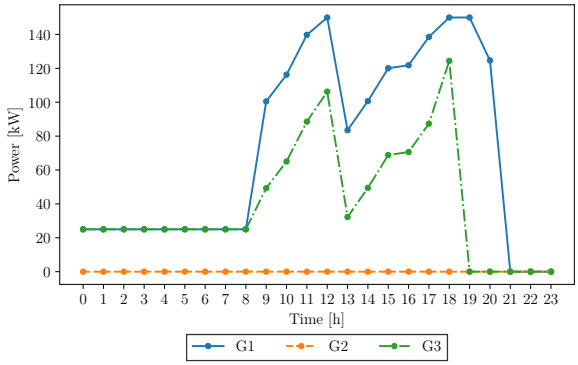

(d) MG2 distributed.

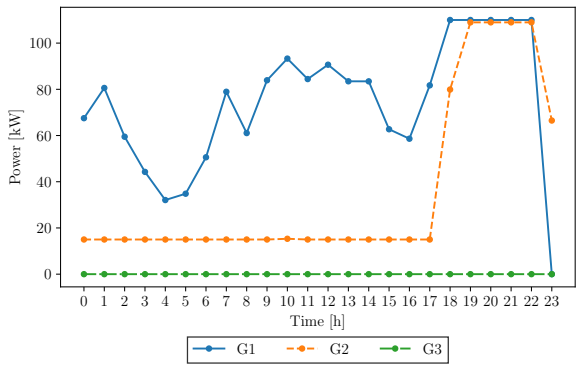

(e) MG3 centralized.

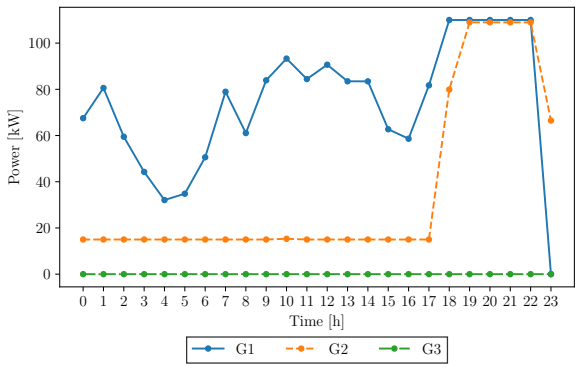

(f) MG3 distributed.

Figure 3.3: Power dispatch of thermal units for the Base Case from centralized and distributed models.

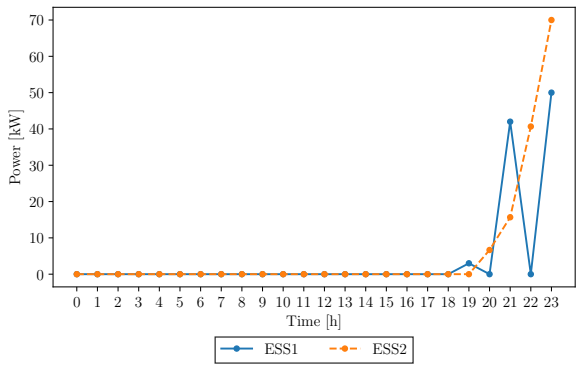

(a) MG1 centralized.

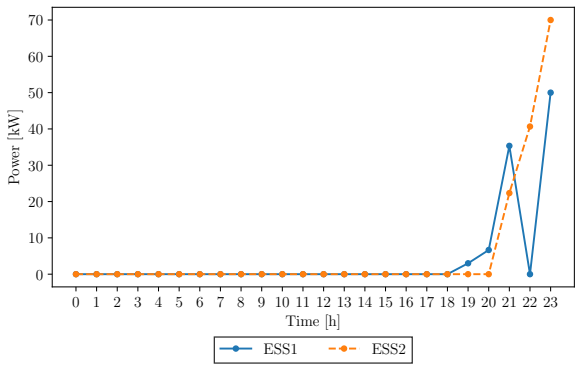

(b) MG1 distributed.

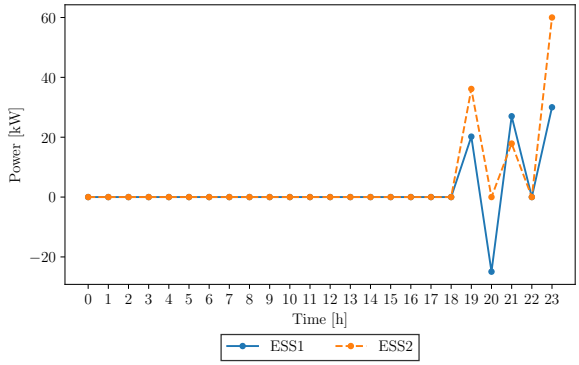

(c) MG2 centralized.

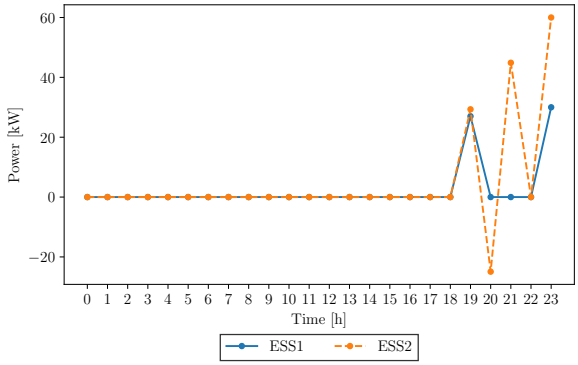

(d) MG2 distributed.

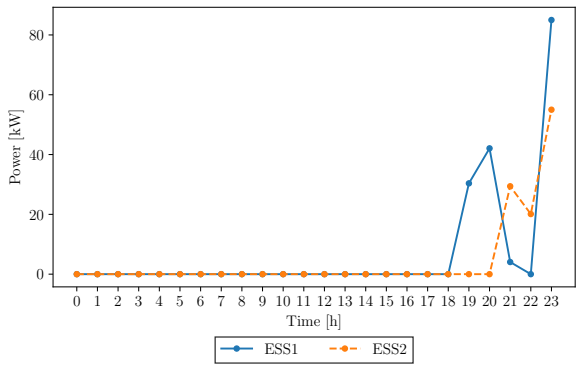

(e) MG3 centralized.

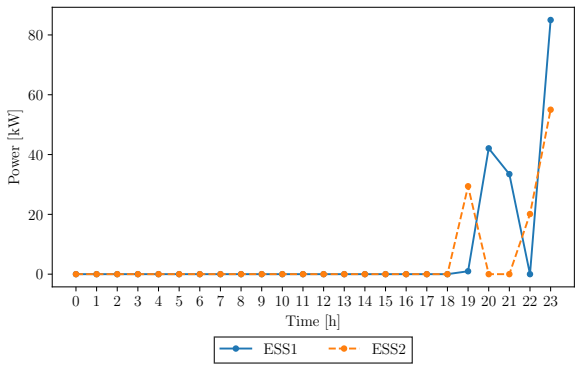

(f) MG3, distributed.

Figure 3.4: Power dispatch of ESS units for the Base Case from centralized and distributed models.

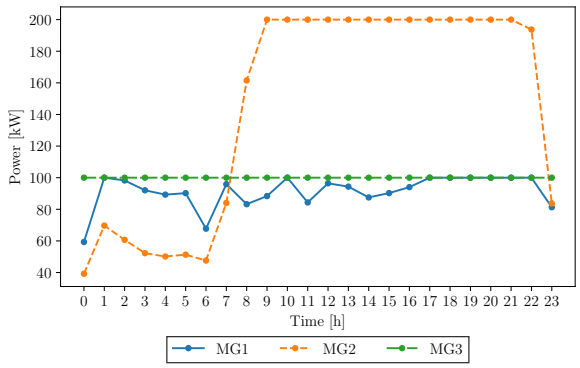

(a) Power sold by the main grid to MGs, centralized.

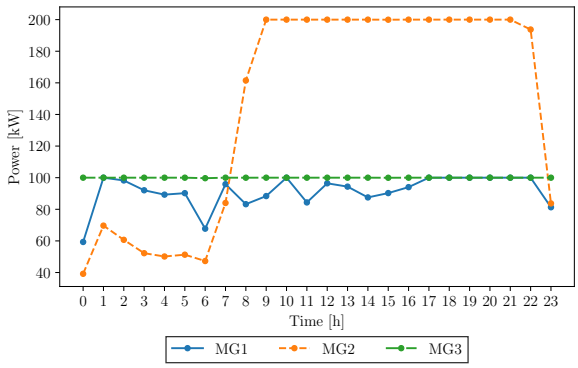

(b) Power sold by the main grid to MGs, distributed.

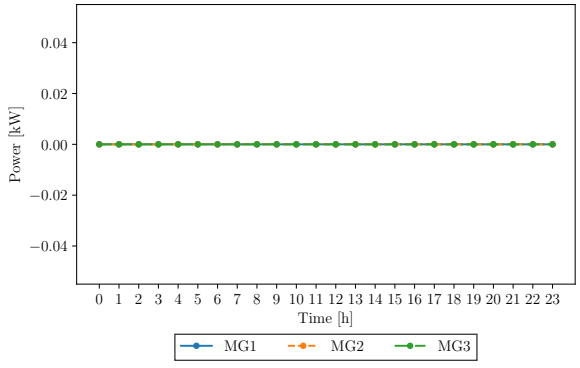

(c) Power bought by the main grid from MGs, centralized.

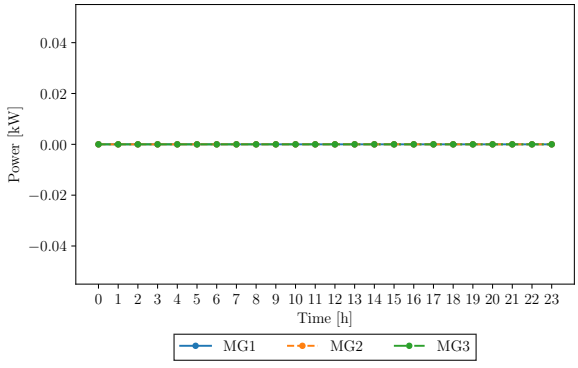

(d) Power bought by the main grid from MGs, distributed.

Figure 3.5: Power exchanges between MGs and main grid for the Base Case from centralized and distributed models.

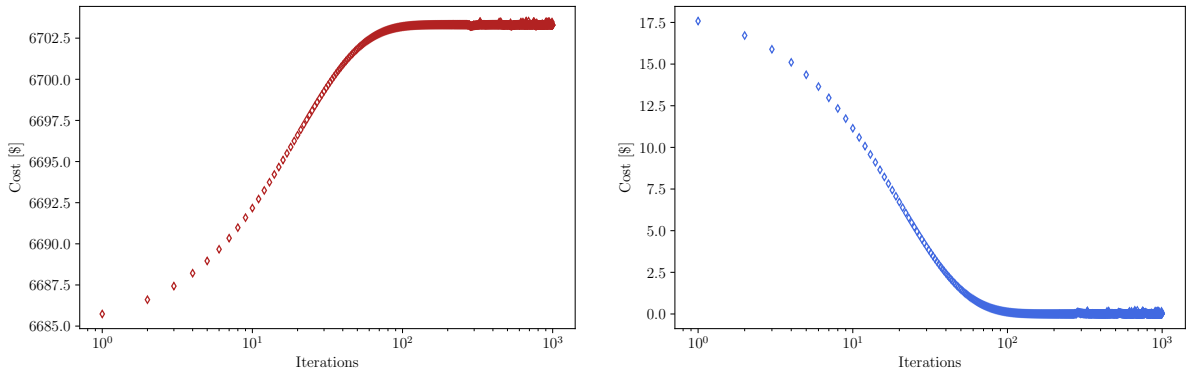

(a) Dual objective function value.

(b) Duality gap.

Figure 3.6: Iterations of the distributed algorithm for the Base Case.

3.3.3 Stressed Case

Once the distributed model has been validated against its centralized counterpart, a different case study is presented, in which the parameters are modified to put stress on one of the MGs, i.e., create conditions that will force it to buy power from the other MGs and the main grid to meet its local demand. Thus, the following modifications to the data were made: the demand profile of MG2 was scaled up by a factor of 1.5, and its PV generation profile was scaled down by a factor of 0.9. Then, the maximum generation limits of thermal units in MG2 were decreased to limit its local capacity, which would not be able to supply the MG load. To compensate this capacity reduction, the limits of thermal units in MG1 and MG3 were increased. Furthermore, the linear cost coefficients of thermal units in MG2 were also increased, to make its local generation more expensive. The grid selling prices were drastically increased, from 0.221 \$/kWh to 50 \$/kWh, to incentivize exchanges among MGs instead. Finally, the PCC limits of all MGs must be increased, to ensure that the stressed MG2 can receive the required power from the others, and that the others can send that power as well. If the PCC limits are not increased accordingly, there would be a bottleneck that would render the problem infeasible as the demand of MG2 would not be fully supplied, even if the total generation of the system is sufficient to meet its total demand. Thus, for this case, the PCC limits of all MGs were increased by a factor of 3.

Figure 3.7 shows the power dispatch of thermal units, for the centralized and distributed solutions. The resulting profiles reflect the conditions of the Stressed Case as expected: since MG2 has an increased demand, and the grid selling price is too high, MG2 must increase its local generation, despite having higher generation costs than in the Base Case

Table 3.6: Stressed Case costs.

	Centralized	Modified Centralized	Distributed
Objective function [$]	12,400.2	23,160.4	23,511.8
Total generators' cost [$]	12,400.2	19,424.6	20,106.6
Total transfer cost [$]	-	3,735.8	3,405.2

(notice how G2 in MG2 was off throughout the entire optimization period in the Base Case, but in the Stressed Case it is on for most of the hours). Furthermore, generation in MG1 and MG3 also increases to allow MG2 to supply its local demand. The centralized and distributed solutions present similar profiles with slight differences for MG2 and MG3, and more significant differences for MG1, which can be expected from the distributed algorithm.

The power exchanges among MGs, obtained from the centralized and distributed models are shown in Figure 3.8. As can be seen, MG1 and MG3 are now sending power to MG2, while MG2 uses all its local generation, as expected from the problem conditions. Figure 3.9 shows the charging/discharging power of ESS units, which support the operation of all MGs. For example, at hour 18, when the demand in MG2 is at its highest, both of its ESS units are discharging power, contributing to the MG's power balance.

Figure 3.10 shows the power exchanges between MGs and the main grid, from the centralized and distributed models. In this case, the grid selling price was set very high so that the cost of buying from the main grid is higher than the generation cost of thermal units, which results in no power exchanges with the main grid. If the grid selling price was lower, all MGs would import as much power as possible from the grid at all times. This condition was enforced in this case only to ensure power exchanges among the MGs, when power from expensive thermal units is the main source of energy in the MG. With a high enough penetration of RESs, this artificial restriction on power bought from the main grid would not be necessary, since there is no cost associated with renewable generation, and the power exchanged would originate from the excess renewable energy in each MG.

The objective function values and costs corresponding to the thermal generation and power transfer functions are presented in Table 3.6. As expected, the power transfer cost is now higher because MG2 is receiving a significant amount of power from the other MGs; this cost could be regarded as the tradeoff for attaining a decomposable problem suitable for solution with the distributed algorithm. Table 3.7 shows the operating costs and the revenues resulting from power exchanges in each MG, for the distributed model. In this case, there is no power being bought by the main grid from the MGs; therefore, the revenue originates solely from the power exchanges among MGs. These results are consistent with

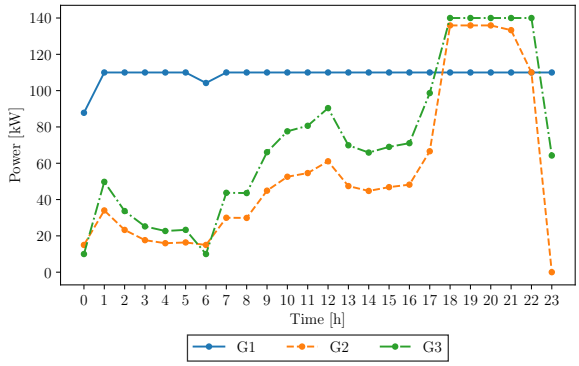

(a) MG1 centralized.

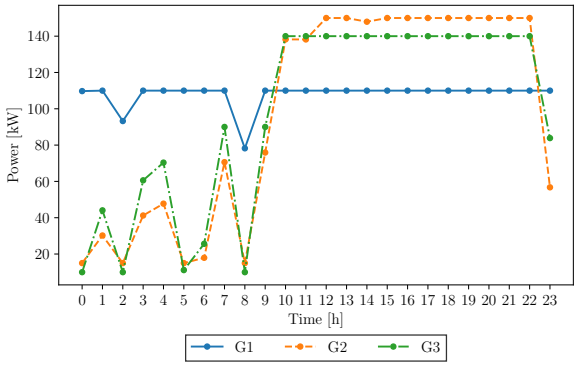

(b) MG1 distributed.

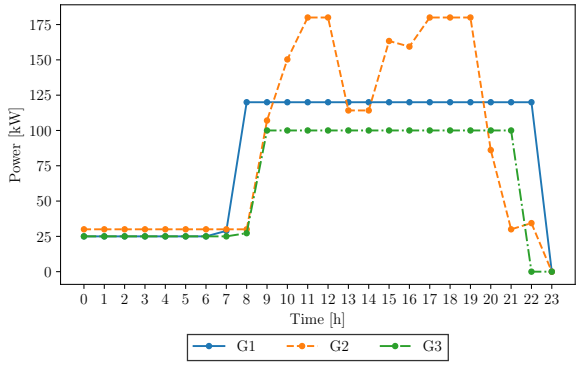

(c) MG2 centralized.

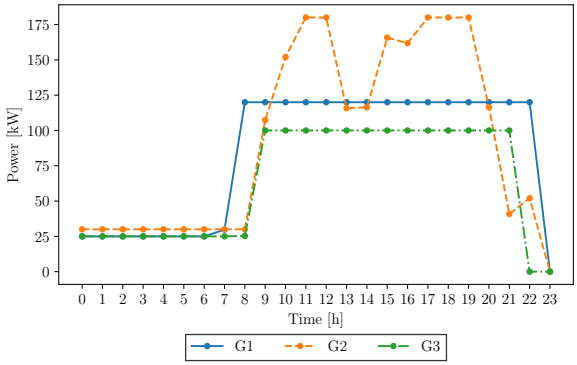

(d) MG2 distributed.

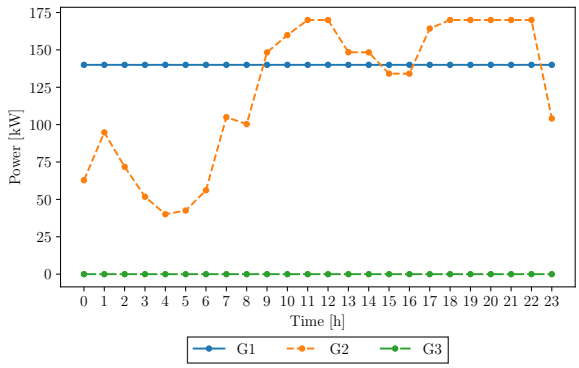

(e) MG3 centralized.

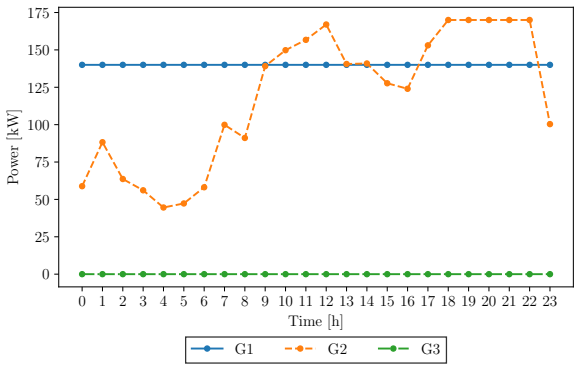

(f) MG3 distributed.

Figure 3.7: Power dispatch of thermal units for the Stressed Case from centralized and distributed models.

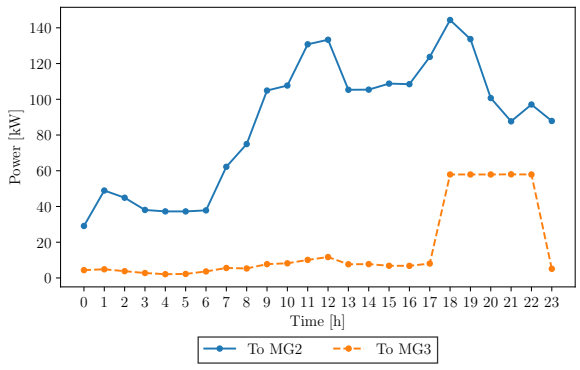

(a) MG1 centralized.

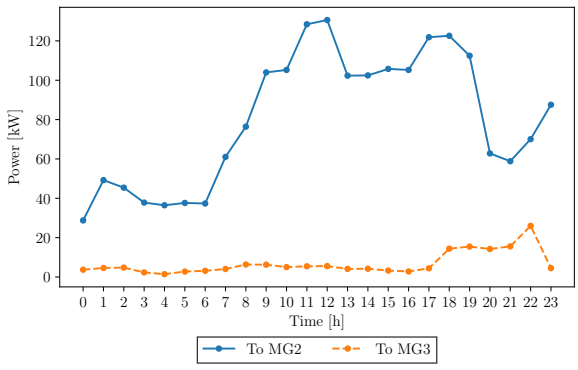

(b) MG1 distributed.

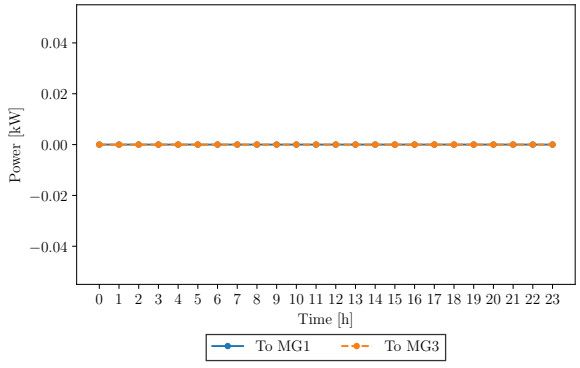

(c) MG2 centralized.

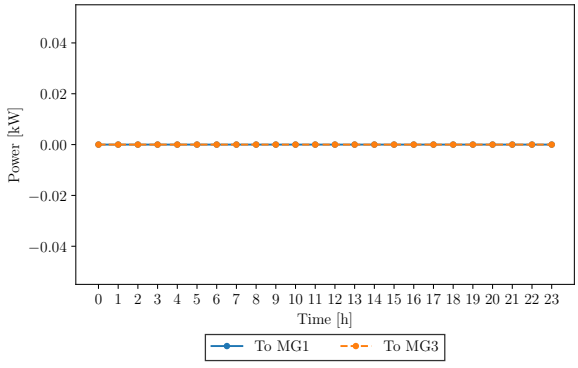

(d) MG2 distributed.

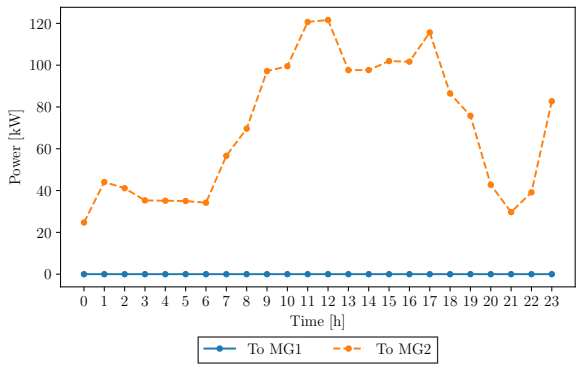

(e) MG3 centralized.

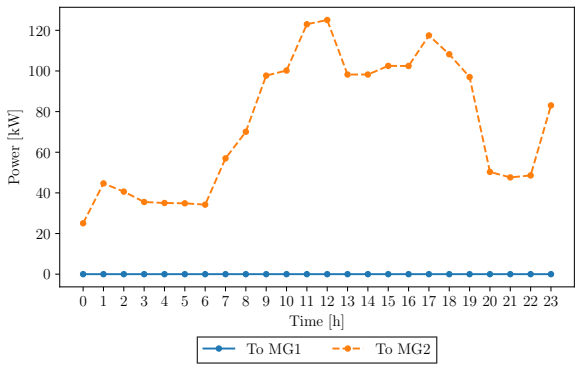

(f) MG3 distributed.

Figure 3.8: Power exchanges between MGs for the Stressed Case from centralized and distributed models.

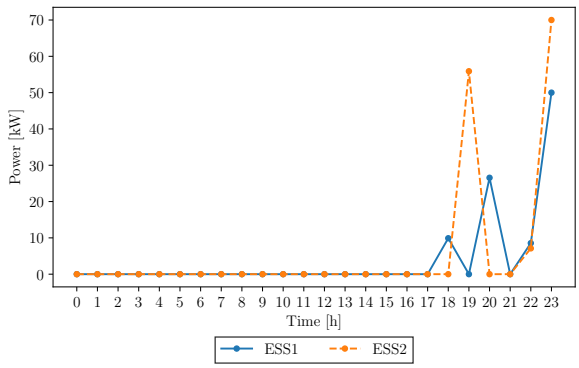

(a) MG1 centralized.

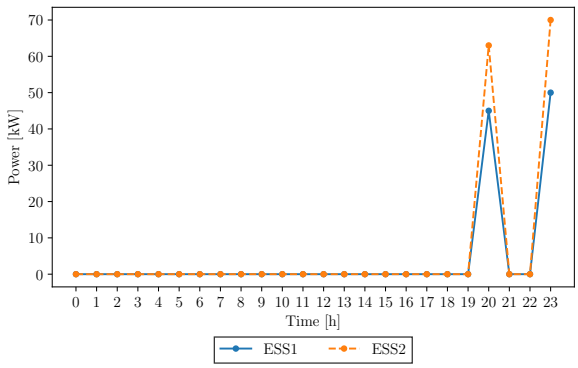

(b) MG1 distributed.

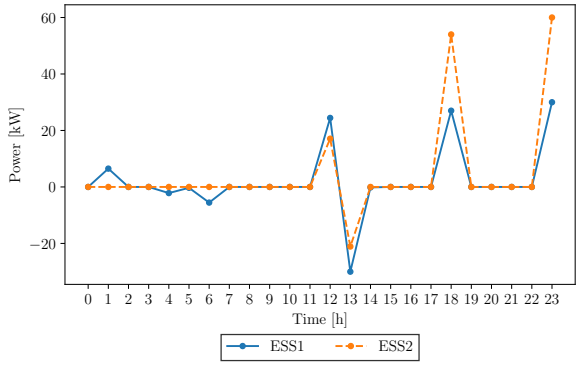

(c) MG2 centralized.

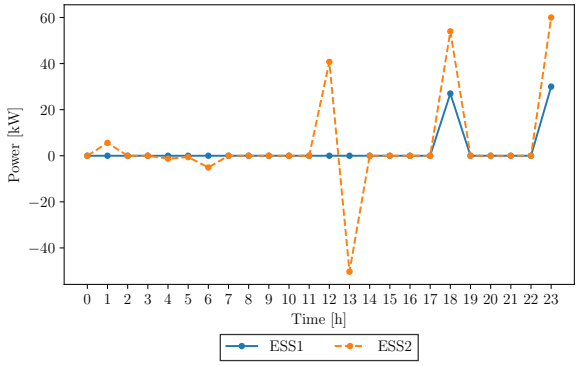

(d) MG2 distributed.

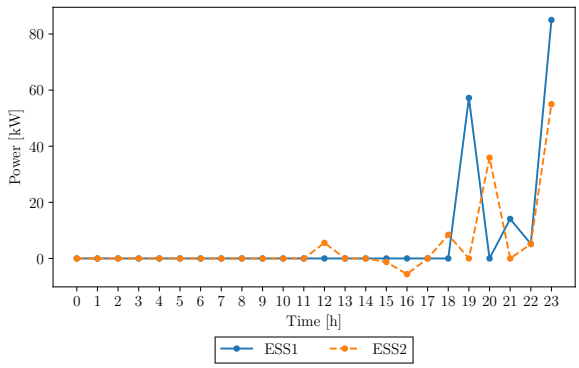

(e) MG3 centralized.

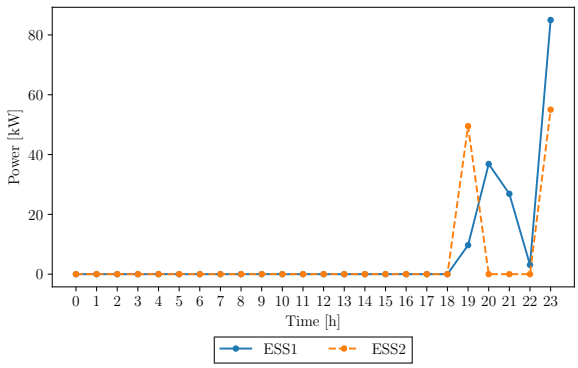

(f) MG3 distributed.

Figure 3.9: Power dispatch of ESS units for the Stressed Case from centralized and distributed models.

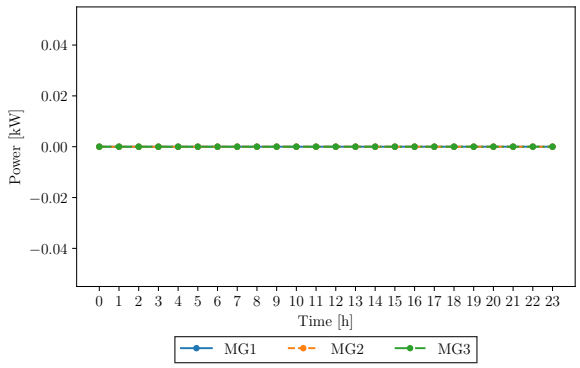

(a) Power sold by the main grid to MGs, centralized.

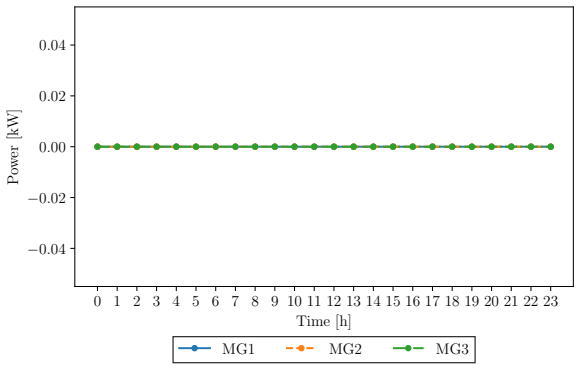

(b) Power sold by the main grid to MGs, distributed.

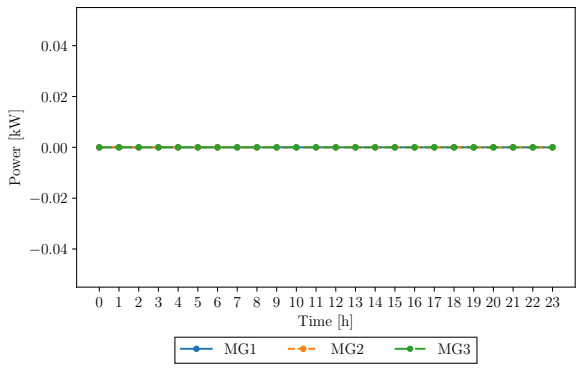

(c) Power bought by the main grid from MGs, centralized.

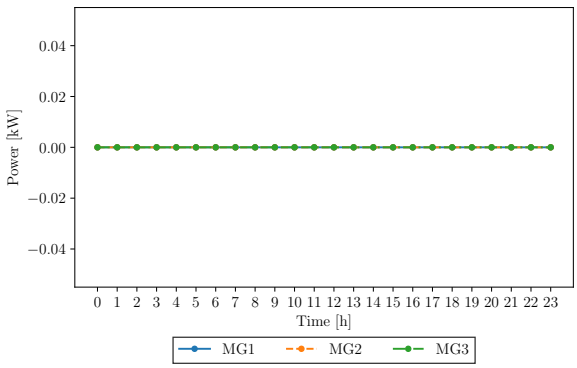

(d) Power bought by the main grid from MGs, distributed.

Figure 3.10: Power exchanges between MGs and main grid for the Stressed Case from centralized and distributed models.

Table 3.7: Operating costs and revenues from power exchanges in the distributed model, Stressed Case.

	Operating Cost [$]	Selling Revenue [$]	Total Cost [$]
MG1	3,400.5	1,120.9	2,279.6
MG2	16,752.0	-2,126.5	18,878.5
MG3	3,359.3	1,005.6	2,353.7
Total	23,511.8	0.0	23,511.8

the profiles shown in Figure 3.8, which indicate that MG1 is selling power to MG2 and MG3, charging $1,001.6 and $119.3, respectively; MG2 is buying from MG1 and MG3, paying $1,001.6 and $1,124.9, respectively; and MG3 is buying from MG1 and selling to MG2, paying and charging $119.3 and $1,124.9, respectively. The total costs in Table 3.7, which result from subtracting the selling revenue from the operating cost, show how MG1 and MG3 benefit from supporting the operation of MG2.

3.3.4 Individual and Cooperative Operation

A final experiment was carried out to compare the costs of MGs operating on their own, with no power exchanges, against the cost when there are power exchanges. Data from the Stressed Case was used for this comparison, and to create the individual operation condition, the PCC limits of all MGs were set to zero. Furthermore, to ensure feasibility under this scenario, the maximum generation capacity of thermal units in each MG was increased, especially for MG2, which has the most critical conditions.

The results are presented in Table 3.8, where the first column shows the operation costs of each MG and the total cost for the complete system, when operating individually, and the second column shows the operation costs when power exchanges are enabled. The third column shows the revenue of each MG from power sold to the other MGs in the cooperative operation mode, and the fourth column shows the total cooperative operating cost, i.e., the cost in the second column minus the revenue in the third column. Note that in this case, MG1 and MG3 must increase their operating cost when power exchanges are enabled because they need to support MG2, which had a very high cost due to its increased demand and expensive local generation. As a consequence of the exchanges, the total cost of the system decreased from $22,498.5 to $18,625.4 (by around 17%). This was not beneficial for MG1 and MG3 individually, in terms of their operating cost; however, there is a cost associated with the power transfer received by MG2 from the other MGs, and this payment from MG2 can be redistributed among the supplying MGs according to the amount of power provided, which results in the selling revenue shown in the third column in Table 3.8.

Table 3.8: Operating costs of MGs in individual and cooperative mode.

	Individual [$]	Cooperative [$]	Selling Revenue [$]	Cooperative Total [$]
MG1	1,112.6	1,696.9	1,191.6	505.3
MG2	19,048.3	14,067.9	-2,100.7	16,168.6
MG3	2,337.6	2,860.6	909.1	1,951.5
Total	22,498.5	18,625.4	0.0	18,625.4

Considering this revenue, the total operating cost of each MG in cooperative mode, shown in the fourth column, is reduced with respect to the corresponding individual operation cost shown in the first column, which indicates that all MGs benefit from supporting the operation of MG2, which incentivizes their participation in the cooperative operation. The overall degree of improvement will depend on the generation costs of each MG, their demand, the costs of buying and selling electricity from and to the main grid, and the PCC limits.

3.4 Summary

This chapter presented a centralized model for the optimal operation of an MMG system that considers power exchanges among a set of MGs and the main grid, including detailed constraints for thermal generation units and ESS units within each MG. It was assumed that the interaction among MGs occurs through the main grid, and therefore the MGs PCC could limit the amount of power exchange. Simulation results show that the centralized model yields the optimal dispatch of the MMG resources for the considered cases.

The centralized model was then decomposed using Lagrangian relaxation and solved through an iterative distributed procedure based on a subgradient method to find the solution of the corresponding dual problem. The distributed algorithm only requires the exchange of minimal information to coordinate the operation of the complete system, keeping the local parameters and demand profiles of each MG private.

Demand, solar irradiance, and price data from a realistic ADN in São Paulo, Brazil, was used to design a test system for the proposed models. Results showed that the distributed algorithm converges to the optimal or near-optimal solution in a reasonable execution time, considering the time frame of the EMS problem, making the proposed model a viable alternative for the implementation of a distributed EMS in an MMG system. Furthermore, it was demonstrated that the operation costs of the MMG system significantly reduces when MGs engage in power exchanges, as opposed to their individual operation.

Chapter 4

An Affine Arithmetic-Based EMS for Multi-Microgrid Systems

This chapter presents an AA-based MMG EMS model to consider uncertainties associated with demand and renewable generation variability, based on the centralized EMS model proposed in Chapter 3. An AA approach was chosen in favor of SP and MCS because the solutions of an AA model are robust for a range of variations of the uncertain parameters while avoiding the need for finding accurate pdfs or performing repeated simulations, thus reducing the computational burden. Note that SP or RO models were not considered for comparison, as AA has been shown to be superior to these techniques in [63] and [64], respectively.

First, the uncertainties are characterized by their affine forms, which are used to redefine the variables, objective function, and constraints of the original EMS model in the AA domain. The linearization procedure of absolute values introduced by AA operators is described in detail, followed by a brief explanation of the MCS carried out for comparison purposes. Finally, simulation results on the same sample system used in Chapter 3 are performed to test and validate the proposed AA-based MMG EMS model, and an example of a dispatch procedure to determine the optimal solution for a specific realization of uncertain parameters from the AA model is presented.

4.1 AA-Based MMG EMS Model

Based on the AA principles and operators introduced in Section 2.4, the parameters, variables, objective function, and constraints of the centralized EMS model are formulated in

affine form in the following subsections.

4.1.1 Characterization of Uncertainty in AA

The AA formulation first requires characterizing the uncertain parameters in affine form. Thus, the uncertainties associated with variations in power demand and renewable generation can be respectively represented in the AA domain as follows:

$$\widehat{D}_{m,t} = D_{0,m,t} + \sum_{h=1}^{p^D} D_{h,m,t}\varepsilon^D_{h,m,t} \quad \forall\ m \in M,\ t \in T \tag{4.1}$$

$$\widehat{P}^r_{m,t} = P^r_{0,m,t} + \sum_{h=1}^{p^r} P^r_{h,m,t}\varepsilon^r_{h,m,t} \quad \forall\ m \in M,\ t \in T \tag{4.2}$$

where $D_{0,m,t}$ and $P^r_{0,m,t}$ are the central values of the affine forms of demand and renewable generation in MG m at hour t, respectively; $D_{h,m,t}$ and $P^r_{h,m,t}$ are the h-th partial deviations of the corresponding affine forms at hour t; and $\varepsilon^D_{h,m,t}$ and $\varepsilon^r_{h,m,t}$ are the h-th noise symbols associated with demand and renewable generation variations in MG m at hour t, respectively. Parameters p^D and p^r are the number of noise symbols in the affine forms of the demand and renewable generation, respectively. It is realistically assumed that the sources of uncertainty are independent, and thus a single and distinct noise symbol for each parameter is used. It is also assumed for simplicity that there is only one renewable generation lumped source per MG, which is a reasonable and practical assumption given the relatively small geographical area covered by each MG, and the fact that renewable generation in MGs in urban ADNs primarily consists of solar PV generators, as this is where MMG systems are most likely to develop. However, the model can be readily modified to consider multiple and independent renewable generation sources, which would make the problem unnecessarily more complex in practice. Hence, the affine parameters defined by (4.1) and (4.2) become:

$$\widehat{D}_{m,t} = D_{0,m,t} + D_{1,m,t}\varepsilon^D_{m,t} \quad \forall\ m \in M,\ t \in T \tag{4.3}$$

$$\widehat{P^r}_{m,t} = P^r_{0,m,t} + P^r_{1,m,t}\varepsilon^r_{m,t} \quad \forall\ m \in M,\ t \in T \tag{4.4}$$

4.1.2 Affine Variables

Once the uncertain parameters have been expressed in their affine form, all the continuous variables in the centralized EMS model defined by (3.2)–(3.24) are formulated to include terms corresponding to each one of the noise symbols appearing in the parameters, as follows:

$$\widehat{P}_{m,g,t} = P_{0,m,g,t} + P_{1,m,g,t}\varepsilon^{D}_{m,t} + P_{2,m,g,t}\varepsilon^{r}_{m,t} \quad \forall\ m \in M,\ g \in G_m,\ t \in T \tag{4.5}$$

$$\widehat{P^{gs}}_{m,t} = P^{gs}_{0,m,t} + P^{gs}_{1,m,t}\varepsilon^{D}_{m,t} + P^{gs}_{2,m,t}\varepsilon^{r}_{m,t} \quad \forall\ m \in M,\ t \in T \tag{4.6}$$

$$\widehat{P^{gb}}_{m,t} = P^{gb}_{0,m,t} + P^{gb}_{1,m,t}\varepsilon^{D}_{m,t} + P^{gb}_{2,m,t}\varepsilon^{r}_{m,t} \quad \forall\ m \in M,\ t \in T \tag{4.7}$$

$$\widehat{P^{e}}_{m,n,t} = P^{e}_{0,m,n,t} + P^{e}_{1,m,n,t}\varepsilon^{D}_{m,t} + P^{e}_{2,m,n,t}\varepsilon^{r}_{m,t} \quad \forall\ m \in M,\ n \in M \backslash m,\ t \in T \tag{4.8}$$

$$\widehat{SoC}_{m,s,t} = SoC_{0,m,s,t} + SoC_{1,m,s,t}\varepsilon^{D}_{m,t} + SoC_{2,m,s,t}\varepsilon^{r}_{m,t} \quad \forall\ m \in M,\ s \in S_m,\ t \in T \tag{4.9}$$

$$\widehat{P^{ch}}_{m,s,t} = P^{ch}_{0,m,s,t} + P^{ch}_{1,m,s,t}\varepsilon^{D}_{m,t} + P^{ch}_{2,m,s,t}\varepsilon^{r}_{m,t} \quad \forall\ m \in M,\ s \in S_m,\ t \in T \tag{4.10}$$

$$\widehat{P^{dch}}_{m,s,t} = P^{dch}_{0,m,s,t} + P^{dch}_{1,m,s,t}\varepsilon^{D}_{m,t} + P^{dch}_{2,m,s,t}\varepsilon^{r}_{m,t} \quad \forall\ m \in M,\ s \in S_m,\ t \in T \tag{4.11}$$

where $\widehat{P}_{m,g,t}$ is the affine form of the power output of thermal units; $\widehat{P^{gs}}_{m,t}$ and $\widehat{P^{gb}}_{m,t}$ are the affine forms of the power sold and bought by the main grid to and from each MG, respectively; $\widehat{P^{e}}_{m,n,t}$ is the affine form of the power exchanges among MGs; and $\widehat{SoC}_{m,s,t}$, $\widehat{P^{ch}}_{m,s,t}$, and $\widehat{P^{dch}}_{m,s,t}$ are the affine forms of the SoC, charging power, and discharging power of ESS units. In all variables, the first term is the central value, the second term is the partial deviation due to demand uncertainty, and the third term is the partial deviation due to renewable generation uncertainties.

4.1.3 Affine Objective Function

The conventional quadratic cost function of thermal generators (3.1) used in the deterministic model is replaced here with the following linear cost function:

$$C(\widehat{P}_{m,g,t}) = b_{m,g}\widehat{P}_{m,g,t} + c_{m,g}v_{m,g,t} \quad \forall\ m \in M,\ g \in G_m,\ t \in T \tag{4.12}$$

where $b_{m,g}$ and $c_{m,g}$ are the linear and constant coefficients of the cost function, $\widehat{P}_{m,g,t}$ is the power output of the generator in affine form, and $v_{m,g,t}$ is the binary variable representing its operation status. The quadratic cost coefficient of diesel units is usually very small,

relative to the linear and constant coefficients, and can be neglected without significantly affecting the results [106]; thus, this linear cost function is used to simplify the formulation of the AA optimization problem proposed here.

According to the definition of the AA minimization operator in [61], the AA MMG EMS problem can be formulated as a multi-objective optimization problem that minimizes the affine central value and the affine radius. To solve this problem, a possible approach is to decompose the problem in two subsequent stages: The first stage finds the optimal central values, assuming a "nominal state" of the system in which the uncertainties are not considered; and the second stage finds the optimal values of the partial deviations, corresponding to a "perturbed state" of the system in which uncertainties are taken into account [61]. However, the binary variables and intertemporal constraints present in the MMG EMS problem do not allow such decomposition, because the solution of one stage may be infeasible for the other; hence, the objective function is instead formulated as a weighted function of both the center values and the affine radius [63], as follows:

$$\begin{aligned}\min \quad & \sum_{t\in T}\sum_{m\in M}\Bigg\{ w\Bigg[\sum_{g\in G_m}\left[(b_{m,g}P_{0,m,g,t}+c_{m,g}v_{m,g,t})\Delta t + C^{SD}_{m,g}SD_{m,g,t}+C^{SU}_{m,g}SU_{m,g,t}\right] \\ & \qquad + \left(\sum_{n\in M\setminus m}\beta P^{e}_{0,n,m,t}+\rho^{gs}_{m}P^{gs}_{0,m,t}-\rho^{gb}_{m}P^{gb}_{0,m,t}\right)\Delta t\Bigg] \\ & + (1-w)\Bigg[\Bigg(\sum_{g\in G_m} b_{m,g}(|P_{1,m,g,t}|+|P_{2,m,g,t}|)+\sum_{n\in M\setminus m}\beta(|P^{e}_{1,n,m,t}|+|P^{e}_{2,n,m,t}|) \\ & \qquad + \rho^{gs}_{m}(|P^{gs}_{1,m,t}|+|P^{gs}_{2,m,t}|)-\rho^{gb}_{m}(|P^{gb}_{1,m,t}|+|P^{gb}_{2,m,t}|)\Bigg)\Delta t\Bigg]\Bigg\}\end{aligned} \tag{4.13}$$

where w is a weighting factor that can be chosen in the range [0,1] according to the desired conservativeness of the solution with respect to uncertainties. For example, a weighting factor closer to 1 leads to cost-effective solutions that are sensitive to uncertainties, i.e., the AA objective function approximates the deterministic model more closely, while a value close to 0 leads to solutions that are more expensive but less sensitive to uncertainties, i.e., larger solution intervals.

The first term in square brackets in (4.13) is the operating cost associated with the affine central values, which includes the dispatch cost of thermal generators, the shutdown and startup costs, the power transfer cost, and the cost or revenue resulting from power exchanges with the main grid. Note that a linear power transfer cost function was assumed

here, to prevent the appearance of products of noise symbols. The second term in square brackets corresponds to the affine radius of objective function, which comprises the costs of the partial deviations of thermal units dispatch, power transfer, and power exchanges with the main grid. Note that no term related to shutdown and startup costs appears in the affine radius term, since these are not defined by continuous variables.

4.1.4 Affine Generator UC Constraints

Expanding the affine forms of the UC constraints of the centralized EMS model introduced in Chapter 3, and collecting terms corresponding to the central values and partial deviations of variables and parameters, produces the constraints presented next.

Power Balance

The supply-demand balance constraint (3.3) is formulated in the AA domain by applying the AA similarity operator defined in Section 2.4. Thus, based on (2.14) and (4.5)–(4.11), (3.3) is transformed as follows:

$$\begin{aligned}\sum_{g\in G_m} P_{0,m,g,t} + P^r_{0,m,t} + \sum_{s\in S_m}(P^{dch}_{0,m,s,t} - P^{ch}_{0,m,s,t}) + \sum_{n\in M\setminus m} P^e_{0,n,m,t} + P^{gs}_{0,m,t} \\ = D_{0,m,t} + \sum_{n\in M\setminus m} P^e_{0,m,n,t} + P^{gb}_{0,m,t} \quad \forall\ m\in M,\ t\in T\end{aligned} \tag{4.14}$$

$$\begin{aligned}\sum_{g\in G_m} P_{1,m,g,t} + \sum_{s\in S_m}(P^{dch}_{1,m,s,t} - P^{ch}_{1,m,s,t}) + \sum_{n\in M\setminus m} P^e_{1,n,m,t} + P^{gs}_{1,m,t} \\ = D_{1,m,t} + \sum_{n\in M\setminus m} P^e_{1,m,n,t} + P^{gb}_{1,m,t} \quad \forall\ m\in M,\ t\in T\end{aligned} \tag{4.15}$$

$$\begin{aligned}\sum_{g\in G_m} P_{2,m,g,t} + P^r_{1,m,t} + \sum_{s\in S_m}(P^{dch}_{2,m,s,t} - P^{ch}_{2,m,s,t}) + \sum_{n\in M\setminus m} P^e_{2,n,m,t} + P^{gs}_{2,m,t} \\ = \sum_{n\in M\setminus m} P^e_{2,m,n,t} + P^{gb}_{2,m,t} \quad \forall\ m\in M,\ t\in T\end{aligned} \tag{4.16}$$

Note that the single power balance constraint (3.3) in the deterministic problem has been replaced here by the following three constraints: (4.14) for the central values, (4.15) for the partial deviations associated with the demand uncertainty, and (4.16) for the partial

deviations associated with the renewable generation uncertainty. In general, the number of sources of uncertainty will determine the number of additional equality constraints required to enforce the supply-demand balance in the AA formulation.

Generator Limits

According to the AA inequality operator (2.15), the generation limit constraints (3.4) are reformulated based on the minimum and maximum values that the affine forms $\widehat{P}_{m,g,t}$ can reach, as follows:

$$P_{0,m,g,t} - |P_{1,m,g,t}| - |P_{2,m,g,t}| \geq \underline{P}_{m,g} v_{m,g,t} \quad \forall\ m \in M,\ g \in G_m,\ t \in T \tag{4.17}$$

$$P_{0,m,g,t} + |P_{1,m,g,t}| + |P_{2,m,g,t}| \leq \overline{P}_{m,g} v_{m,g,t} \quad \forall\ m \in M,\ g \in G_m,\ t \in T \tag{4.18}$$

Similarly, the ramping constraints (3.5) and (3.6) in AA form can be reformulated as:

$$\begin{aligned} P_{0,m,g,t} + |P_{1,m,g,t}| + |P_{2,m,g,t}| \leq P_{0,m,g,t+1} + RD_{m,g}\Delta t + SD_{m,g,t+1}\underline{P}_{m,g} \\ - |P_{1,m,g,t+1}| - |P_{2,m,g,t+1}| \quad \forall\ m \in M,\ g \in G_m,\ t, t+1 \in T \end{aligned} \tag{4.19}$$

$$\begin{aligned} P_{0,m,g,t+1} + |P_{1,m,g,t+1}| + |P_{2,m,g,t+1}| \leq P_{0,m,g,t} + RU_{m,g}\Delta t + SU_{m,g,t+1}\underline{P}_{m,g} \\ - |P_{1,m,g,t}| - |P_{2,m,g,t}| \quad \forall\ m \in M,\ g \in G_m,\ t, t+1 \in T \end{aligned} \tag{4.20}$$

Constraints (3.7)–(3.14), which correspond to the status coordination and minimum uptime/downtime of thermal units, only involve binary variables and are thus unaffected by the formulation of continuous variables as affine forms. Hence, these constraints do not need modifications to be included in the AA model.

4.1.5 Affine ESS Constraints

Energy Balance

Constraints (3.15), which are intertemporal equality constraints, are strictly equal in their AA form only if the noise symbols at time t are equal to the same noise symbols at time $t+1$, which is not likely to be the case for realizations of the uncertain parameters; thus, these types of constraints are approximated in the AA domain by equalizing the central values and affine radius, based on the similarity operator (2.14) defined in Section 2.4, as

follows:

$$SoC_{0,m,s,t+1} = SoC_{0,m,s,t} + [P^{ch}_{0,m,s,t}\eta^{ch}_{m,s} - P^{dch}_{0,m,s,t}/\eta^{dch}_{m,s}]\Delta t \quad \forall\ m \in M,\ s \in S_m,\ t, t+1 \in T \tag{4.21}$$

$$|SoC_{1,m,s,t+1}| + |SoC_{2,m,s,t+1}| = |SoC_{1,m,s,t}| + |SoC_{2,m,s,t}| + \big[(|P^{ch}_{1,m,s,t}| + |P^{ch}_{2,m,s,t}|)\eta^{ch}_{m,s} - (|P^{dch}_{1,m,s,t}| + |P^{dch}_{2,m,s,t}|)/\eta^{dch}_{m,s}\big]\Delta t \quad \forall\ m \in M,\ s \in S_m,\ t, t+1 \in T \tag{4.22}$$

This will not guarantee equality between the affine forms for all possible values of the noise symbols, since the affine radius defined by all partial deviations is being equalized, rather than the individual partial deviations. However, this will ensure that the operating limits are enforced for any noise symbol value at all times, even in the extreme cases corresponding to -1 and 1 values.

ESS Limits

The operational limits of ESS units, defined by (3.16)–(3.18), are formulated in the AA domain according to the minimum and maximum values that the affine forms can take, as follows:

$$SoC_{0,m,s,t} - |SoC_{1,m,s,t}| - |SoC_{2,m,s,t}| \geq \underline{SoC}_{m,s} \quad \forall\ m \in M,\ s \in S_m,\ t \in T \tag{4.23}$$

$$SoC_{0,m,s,t} + |SoC_{1,m,s,t}| + |SoC_{2,m,s,t}| \leq \overline{SoC}_{m,s} \quad \forall\ m \in M,\ s \in S_m,\ t \in T \tag{4.24}$$

$$P^{ch}_{0,m,s,t} - |P^{ch}_{1,m,s,t}| - |P^{ch}_{2,m,s,t}| \geq \underline{P^{ch}}_{m,s} z^{ch}_{m,s,t} \quad \forall\ m \in M,\ s \in S_m,\ t \in T \tag{4.25}$$

$$P^{ch}_{0,m,s,t} + |P^{ch}_{1,m,s,t}| + |P^{ch}_{2,m,s,t}| \leq \overline{P^{ch}}_{m,s} z^{ch}_{m,s,t} \quad \forall\ m \in M,\ s \in S_m,\ t \in T \tag{4.26}$$

$$P^{dch}_{0,m,s,t} - |P^{dch}_{1,m,s,t}| - |P^{dch}_{2,m,s,t}| \geq \underline{P^{dch}}_{m,s} z^{dch}_{m,s,t} \quad \forall\ m \in M,\ s \in S_m,\ t \in T \tag{4.27}$$

$$P^{dch}_{0,m,s,t} + |P^{dch}_{1,m,s,t}| + |P^{dch}_{2,m,s,t}| \leq \overline{P^{dch}}_{m,s} z^{dch}_{m,s,t} \quad \forall\ m \in M,\ s \in S_m,\ t \in T \tag{4.28}$$

Constraint (3.19) can be included without modifications in the AA model since it only involves binary variables.

4.1.6 Affine Power Exchange Constraints

Based on the minimum and maximum values that the affine forms of the power exchange variables can take, the PCC limit constraints (3.20) and (3.21) can be reformulated as

follows:

$$\sum_{n\in M\setminus m}(P^{e}_{0,m,n,t}+|P^{e}_{1,m,n,t}|+|P^{e}_{2,m,n,t}|)+P^{gb}_{0,m,t}+|P^{gb}_{1,m,t}|+|P^{gb}_{2,m,t}|\leq P^{PCC}_{m}\quad\forall\ m\in M,\ t\in T \tag{4.29}$$

$$\sum_{n\in M\setminus m}(P^{e}_{0,n,m,t}+|P^{e}_{1,n,m,t}|+|P^{e}_{2,n,m,t}|)+P^{gs}_{0,m,t}+|P^{gs}_{1,m,t}|+|P^{gs}_{2,m,t}|\leq P^{PCC}_{m}\quad\forall\ m\in M,\ t\in T \tag{4.30}$$

To include (3.22) in the AA model, which is a nonlinear constraint preventing simultaneous power exchanges between two MGs, it is assumed that the product of two noise symbols in the expansion of the affine operation is equal to 1, which is a conservative approximation of the non-affine operation that provides more protection against internal sources of error and allows a more straightforward implementation. This results in the following expression:

$$\sum_{h=0}^{2}P^{e}_{h,n,m,t}(P^{e}_{0,m,n,t}+P^{e}_{1,m,n,t}+P^{e}_{2,m,n,t})=0\quad\forall\ m\in M,\ n\in M\setminus m,\ t\in T \tag{4.31}$$

4.1.7 Affine Nonnegativity Constraints

Finally, the nonnegativity constraints (3.24) are reformulated to ensure that the minimum value that the affine forms can take is greater than zero, as follows:

$$P^{e}_{0,m,n,t}-|P^{e}_{1,m,n,t}|-|P^{e}_{2,m,n,t}|\geq 0\quad\forall\ m\in M,\ n\in M\setminus m,\ t\in T \tag{4.32}$$

$$P^{gb}_{0,m,t}-|P^{gb}_{1,m,t}|-|P^{gb}_{2,m,t}|\geq 0\quad\forall\ m\in M,\ t\in T \tag{4.33}$$

$$P^{gs}_{0,m,t}-|P^{gs}_{1,m,t}|-|P^{gs}_{2,m,t}|\geq 0\quad\forall\ m\in M,\ t\in T \tag{4.34}$$

4.1.8 Linearization of Absolute Values

In order to solve the AA-based MMG EMS model with existing optimization solvers, the absolute value functions introduced by the AA operators must be linearized. The linearization procedure involves the inclusion of auxiliary variables and constraints for each absolute value appearing in the objective function and constraints of the problem [107], as described next.

Linearization of Objective Function

To remove the absolute values associated with the thermal units generation cost in (4.13), the term:

$$\sum_{g \in G_m} b_{m,g}(|P_{1,m,g,t}| + |P_{2,m,g,t}|)\Delta t \tag{4.35}$$

is replaced with:

$$\sum_{g \in G_m} b_{m,g}(P'_{1,m,g,t} + P'_{2,m,g,t})\Delta t \tag{4.36}$$

where $P'_{1,m,g,t}$ and $P'_{2,m,g,t}$ are auxiliary variables that will take on the absolute value of the corresponding variable. Furthermore, the following constraints must be added:

$$\pm P_{1,m,g,t} \leq P'_{1,m,g,t} \quad \forall\ m \in M,\ g \in G_m,\ t \in T \tag{4.37}$$

$$\pm P_{2,m,g,t} \leq P'_{2,m,g,t} \quad \forall\ m \in M,\ g \in G_m,\ t \in T \tag{4.38}$$

The $\pm$ notation means that two constraints are being considered, one where the variable has a positive sign, and one where the variable has a negative sign. Thus, (4.37) and (4.38) represent two new sets of constraints each. This procedure has the desired effect of making the auxiliary variables equal to the absolute values of the original variables because the terms are being minimized and have positive coefficients, making the auxiliary variables as small as possible in the optimal solution. The two sets of constraints ensure that the original variables will not be greater than the minimized auxiliary variables, regardless of their sign (one set of constraints will be redundant, depending on the actual sign of the variable).

The term corresponding to the grid selling power has the same structure as the thermal unit generation cost (variables with positive coefficients being minimized). Thus, a similar logic applies, replacing the term:

$$\rho^{gs}_m(|P^{gs}_{1,m,t}| + |P^{gs}_{2,m,t}|) \tag{4.39}$$

with:

$$\rho^{gs}_m(P^{gs'}_{1,m,t} + P^{gs'}_{2,m,t}) \tag{4.40}$$

and adding the following constraints:

$$\pm P^{gs}_{1,m,t} \leq P^{gs'}_{1,m,t} \quad \forall\ m \in M,\ g \in G_m,\ t \in T \tag{4.41}$$

$$\pm P^{gs}_{2,m,t} \leq P^{gs'}_{2,m,t} \quad \forall\ m \in M,\ g \in G_m,\ t \in T \tag{4.42}$$

where $P^{gs'}_{1,m,t}$ and $P^{gs'}_{2,m,t}$ are the auxiliary variables that represent the corresponding absolute values.

The term associated with the power transfer cost function also consists of variables with positive coefficients being minimized. Thus, applying a similar logic, the term:

$$\sum_{n \in M \setminus m} \beta(|P^{e}_{1,n,m,t}| + |P^{e}_{2,n,m,t}|) \tag{4.43}$$

is replaced with:

$$\sum_{n \in M \setminus m} \beta(P^{e'}_{1,n,m,t} + P^{e'}_{2,n,m,t}) \tag{4.44}$$

and the following constraints are added:

$$\pm P^{e}_{1,m,t} \leq P^{e'}_{1,m,t} \quad \forall\ m \in M,\ g \in G_m,\ t \in T \tag{4.45}$$

$$\pm P^{e}_{2,m,t} \leq P^{e'}_{2,m,t} \quad \forall\ m \in M,\ g \in G_m,\ t \in T \tag{4.46}$$

where $P^{e'}_{1,m,t}$ and $P^{e'}_{2,m,t}$ are the auxiliary variables that represent the corresponding absolute values.

The term corresponding to the grid buying power has a different structure, with minimization of variables with a negative coefficient, where the absolute value will tend to be as large as possible in the optimal solution. In this case, the following constraints are required:

$$P^{gb}_{1,m,t} + M^b x^D_{m,t} \geq P^{gb'}_{1,m,t} \quad \forall\ m \in M,\ t \in T \tag{4.47}$$

$$-P^{gb}_{1,m,t} + M^b (1 - x^D_{m,t}) \geq P^{gb'}_{1,m,t} \quad \forall\ m \in M,\ t \in T \tag{4.48}$$

$$\pm P^{gb}_{1,m,t} \leq P^{gb'}_{1,m,t} \quad \forall\ m \in M,\ t \in T \tag{4.49}$$

$$P^{gb}_{2,m,t} + M^b x^r_{m,t} \geq P^{gb'}_{2,m,t} \quad \forall\ m \in M,\ t \in T \tag{4.50}$$

$$-P^{gb}_{2,m,t} + M^b (1 - x^r_{m,t}) \geq P^{gb'}_{2,m,t} \quad \forall\ m \in M,\ t \in T \tag{4.51}$$

$$\pm P^{gb}_{2,m,t} \leq P^{gb'}_{2,m,t} \quad \forall\ m \in M,\ t \in T \tag{4.52}$$

where M^b is a very large number which ensures that a constraint is always satisfied, and $x^D_{m,t}$ and $x^r_{m,t}$ are binary variables that control which auxiliary constraint is active, in conjunction with M^b. The combined effect of these constraints makes the auxiliary variables equal to the absolute values of the original variables.

Linearization of Constraints

To remove the absolute values in the thermal unit generation limit constraints, (4.17) and (4.18) are replaced with:

$$\pm P_{1,m,g,t} \pm P_{2,m,g,t} \leq P_{0,m,g,t} - \underline{P}_{m,g} v_{m,g,t} \quad \forall\ m \in M,\ g \in G_m,\ t \in T \tag{4.53}$$

$$\pm P_{1,m,g,t} \pm P_{2,m,g,t} \leq \overline{P}_{m,g} v_{m,g,t} - P_{0,m,g,t} \quad \forall\ m \in M,\ g \in G_m,\ t \in T \tag{4.54}$$

Considering all possible sign combinations, (4.53) and (4.54) introduce four sets of constraints each. Only one set of constraints will be active, depending on the actual signs of the variables; the others will be redundant, but they are needed to account for all possible sign combinations of the variables with absolute value. It is assumed that the right-hand side of the inequalities are nonnegative, which is the case in this problem since the intervals for these variables should not have negative values. Following the same logic, the ramping constraints (4.19) and (4.20) are replaced with:

$$\begin{aligned}\pm P_{1,m,g,t} \pm P_{2,m,g,t} \pm P_{1,m,g,t+1} \pm P_{2,m,g,t+1} \leq RD_{m,g}\Delta t + SD_{m,g,t+1}\underline{P}_{m,g} \\ +P_{0,m,g,t+1} - P_{0,m,g,t} \quad \forall\ m \in M,\ g \in G_m,\ t, t+1 \in T\end{aligned} \tag{4.55}$$

$$\begin{aligned}\pm P_{1,m,g,t+1} \pm P_{2,m,g,t+1} \pm P_{1,m,g,t} \pm P_{2,m,g,t} \leq RU_{m,g}\Delta t + SU_{m,g,t+1}\underline{P}_{m,g} \\ +P_{0,m,g,t} - P_{0,m,g,t+1} \quad \forall\ m \in M,\ g \in G_m,\ t, t+1 \in T\end{aligned} \tag{4.56}$$

Constraints (4.22)–(4.28), associated with the operation of ESS units, are replaced with the following set of constraints:

$$\begin{aligned}\pm SoC_{1,m,s,t+1} \pm SoC_{2,m,s,t+1} = \pm SoC_{1,m,s,t} \pm SoC_{2,m,s,t} + \big[(\pm P^{ch}_{1,m,s,t} \pm P^{ch}_{2,m,s,t})\eta^{ch}_{m,s} \\ -(\pm P^{dch}_{1,m,s,t} \pm P^{dch}_{2,m,s,t})/\eta^{dch}_{m,s}\big]\Delta t \quad \forall\ m \in M,\ s \in S_m,\ t, t+1 \in T\end{aligned} \tag{4.57}$$

$$\pm SoC_{1,m,s,t} \pm SoC_{2,m,s,t} \leq SoC_{0,m,s,t} - \underline{SoC}_{m,s} \quad \forall\ m \in M,\ s \in S_m,\ t \in T \tag{4.58}$$

$$\pm SoC_{1,m,s,t} \pm SoC_{2,m,s,t} \leq \overline{SoC}_{m,s} - SoC_{0,m,s,t} \quad \forall\ m \in M,\ s \in S_m,\ t \in T \tag{4.59}$$

$$\pm P^{ch}_{1,m,s,t} \pm P^{ch}_{2,m,s,t} \leq P^{ch}_{0,m,s,t} - \underline{P^{ch}}_{m,s} z^{ch}_{m,s,t} \quad \forall\ m \in M,\ s \in S_m,\ t \in T \tag{4.60}$$

$$\pm P^{ch}_{1,m,s,t} \pm P^{ch}_{2,m,s,t} \leq \overline{P^{ch}}_{m,s} z^{ch}_{m,s,t} - P^{ch}_{0,m,s,t} \quad \forall\ m \in M,\ s \in S_m,\ t \in T \tag{4.61}$$

$$\pm P^{dch}_{1,m,s,t} \pm P^{dch}_{2,m,s,t} \leq P^{dch}_{0,m,s,t} - \underline{P^{dch}}_{m,s} z^{dch}_{m,s,t} \quad \forall\ m \in M,\ s \in S_m,\ t \in T \tag{4.62}$$

$$\pm P^{dch}_{1,m,s,t} \pm P^{dch}_{2,m,s,t} \leq \overline{P^{dch}}_{m,s} z^{dch}_{m,s,t} - P^{dch}_{0,m,s,t} \quad \forall\ m \in M,\ s \in S_m,\ t \in T \tag{4.63}$$

The PCC constraints (4.29) and (4.30) are substituted by the following expressions:

$$\sum_{n \in M \setminus m} (\pm P^{e}_{1,m,n,t} \pm P^{e}_{2,m,n,t}) \pm P^{gb}_{1,m,t} \pm P^{gb}_{2,m,t} \leq P^{PCC}_{m} - \sum_{n \in M \setminus m} P^{e}_{0,m,n,t} - P^{gb}_{0,m,t} \quad \forall\ m \in M,\ t \in T \tag{4.64}$$

$$\sum_{n \in M \setminus m} (\pm P^{e}_{1,n,m,t} \pm P^{e}_{2,n,m,t}) \pm P^{gs}_{1,m,t} \pm P^{gs}_{2,m,t} \leq P^{PCC}_{m} - \sum_{n \in M \setminus m} P^{e}_{0,n,m,t} - P^{gs}_{0,m,t} \quad \forall\ m \in M,\ t \in T \tag{4.65}$$

Finally, constraints (4.32)–(4.34), which ensure that the AA forms of the power exchange variables can only take nonnegative values, are substituted by the following constraints:

$$\pm P^{e}_{1,m,n,t} \pm P^{e}_{2,m,n,t} \leq P^{e}_{0,m,n,t} \quad \forall\ m \in M,\ n \in M \setminus m,\ t \in T \tag{4.66}$$

$$\pm P^{gb}_{1,m,t} \pm P^{gb}_{2,m,t} \leq P^{gb}_{0,m,t} \quad \forall\ m \in M,\ t \in T \tag{4.67}$$

$$\pm P^{gs}_{1,m,t} \pm P^{gs}_{2,m,t} \leq P^{gs}_{0,m,t} \quad \forall\ m \in M,\ t \in T \tag{4.68}$$

As can be seen, the process of linearizing the absolute values introduced by the AA formulation significantly increases the number of variables and constraints of the problem, in proportion to the number MGs and sources of uncertainty considered.

4.2 Results and Discussion

To test the proposed AA model, the same test system described in Section 3.3 was used, comprised of three MGs, each one with distinct demand and renewable generation profiles, containing a set of three thermal units and a set of two ESS units, considering a 24-hour optimization period. For this system, if two sources of uncertainty are considered per MG, the number of constraints is 40,464; if an additional source of uncertainty is considered, the number of constraints significantly increases to 708,016, due to the linearization of absolute values. The AA model was implemented using the open-source modeling package Pyomo, and solved using the Gurobi 10.0.1 solver, running in a server with dual Intel Xeon Silver 4214 processors with a base speed of 2.20 GHz.

4.2.1 Comparative Analysis

MCS Results

To validate the proposed AA model, comparisons of the deterministic solution, MCS, and the AA solution intervals are presented next, assuming the data corresponding to the Base Case presented in Section 3.3. To carry out the MCS, upper and lower bounds for the uncertain parameters are first defined, considering ±10% for demand, and ±25% for renewable PV generation, which are typical variation ranges for these parameters, as follows:

$$D^{lb}_{m,t} = D_{m,t} - 0.1D_{m,t} \tag{4.69}$$

$$D^{ub}_{m,t} = D_{m,t} + 0.1D_{m,t} \tag{4.70}$$

$$P^{r,lb}_{m,t} = P^{r}_{m,t} - 0.25P^{r}_{m,t} \tag{4.71}$$

$$P^{r,ub}_{m,t} = P^{r}_{m,t} + 0.25P^{r}_{m,t} \tag{4.72}$$

Then, a set of random profiles within the defined bounds are created, assuming a uniform distribution of the uncertain parameters. Figure 4.1 shows the random profiles for each MG for a total of 1,000 generated profiles, which were found to be enough for convergence of the objective function and all variables through trial and error. Thus, Figure 4.2 shows the convergence of the power dispatch of thermal generation and ESS units in each MG, for a single hour of the optimization period, after 1,000 simulations. In this case, the power dispatches of all thermal units in all MGs stabilize relatively quickly, with very slight variations after 200 simulations; however, the power dispatch of ESS units require more simulations to reach convergence.

Figure 4.3 shows the distribution of a few variables of the MCS, for a single hour of the optimization period. These histograms show the relative frequency of power dispatch solutions for certain generators in each MG; the relative frequency is the number of solutions whose value fall within the interval defined by each bin in the histogram, divided by the total number of solutions. Thus, a relative frequency of 1.0 means that the variable had a value within the interval defined by the corresponding bin in all the optimal solutions found in the MCS. The least probable solutions are the ones with the lowest relative frequency values. For example, the histogram of the power dispatch solutions for thermal unit G1 in MG1 at hour 20 (Figure 4.3a) shows that all solutions in the MCS yield a value of 80 kW, which is corroborated by the corresponding trace in Figure 4.2a. Such strong dominance of a single solution indicates that the variable must take this value in the optimal solution of the EMS problem, regardless of the realization of the uncertain parameters within the

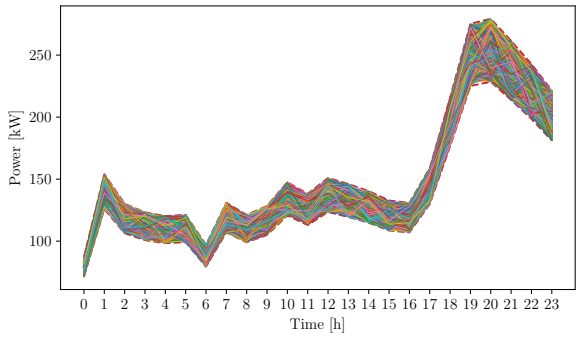

(a) Demand profiles for MG1.

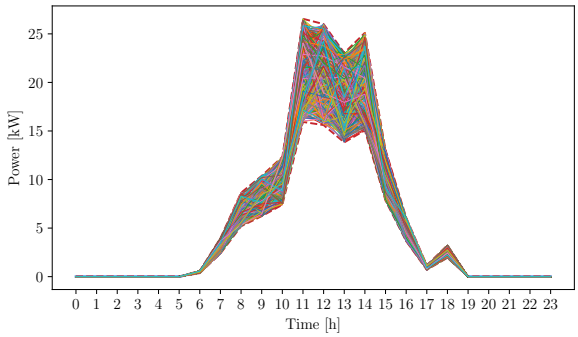

(b) PV generation profiles for MG1.

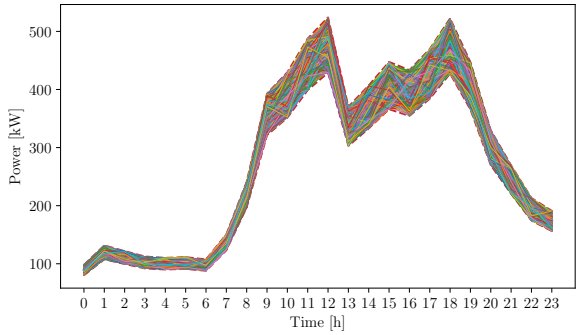

(c) Demand profiles for MG2.

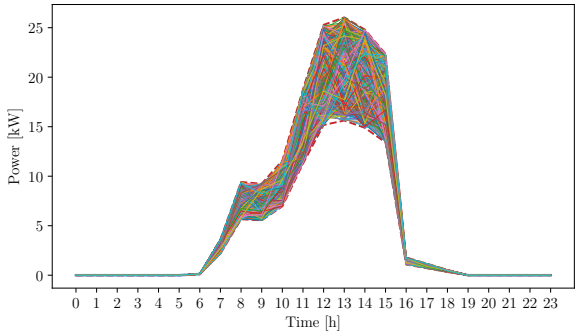

(d) PV generation profiles for MG2.

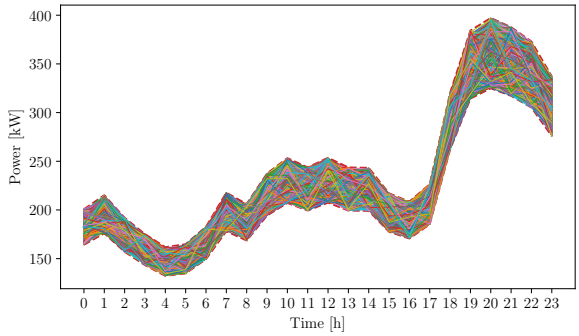

(e) Demand profiles for MG3.

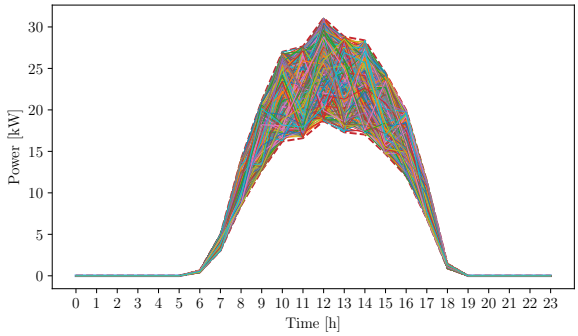

(f) PV generation profiles for MG3.

Figure 4.1: Random demand and PV generation profiles for MCS.

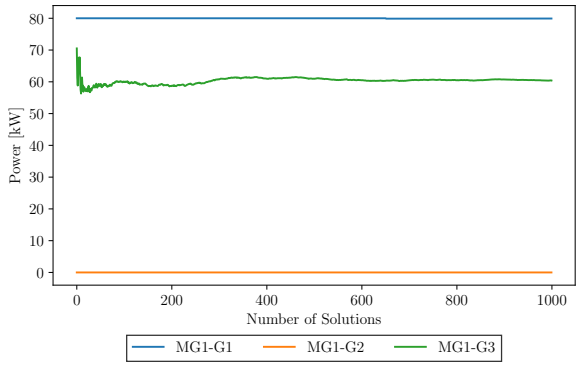

(a) Power dispatch of thermal units in MG1.

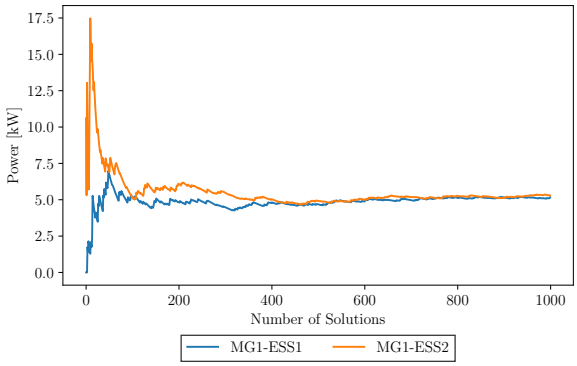

(b) Power dispatch of ESS units in MG1.

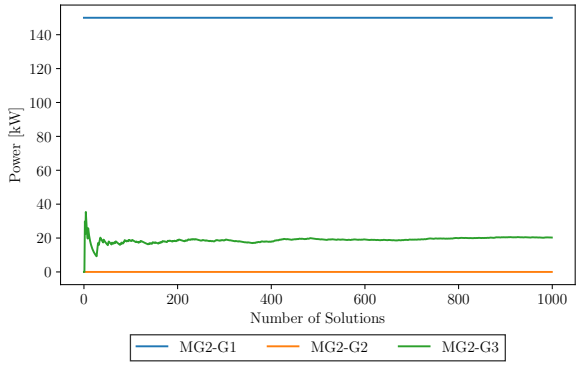

(c) Power dispatch of thermal units in MG2.

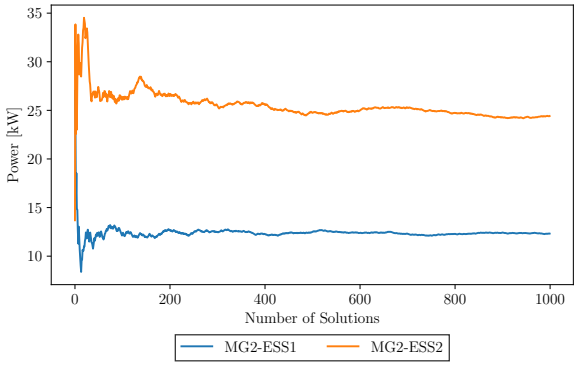

(d) Power dispatch of ESS units in MG2.

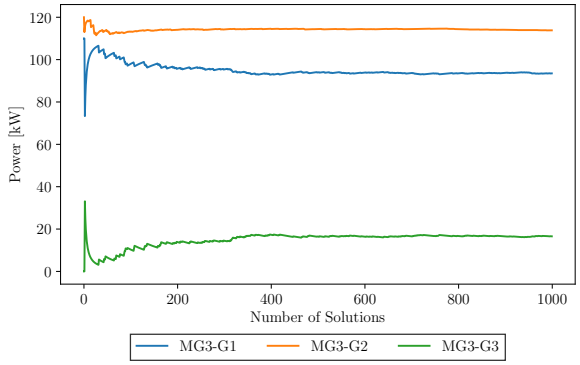

(e) Power dispatch of thermal units in MG3.

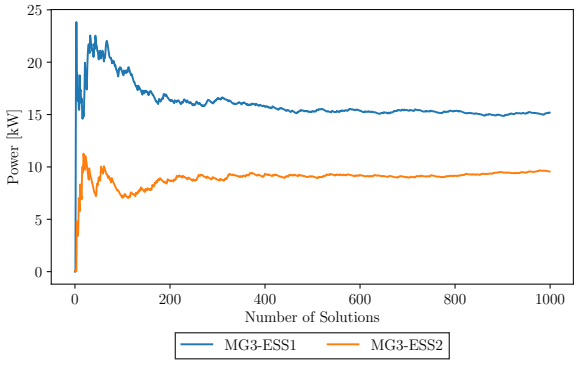

(f) Power dispatch of ESS units in MG3.

Figure 4.2: Convergence of power dispatch variables at hour 20 in MCS.

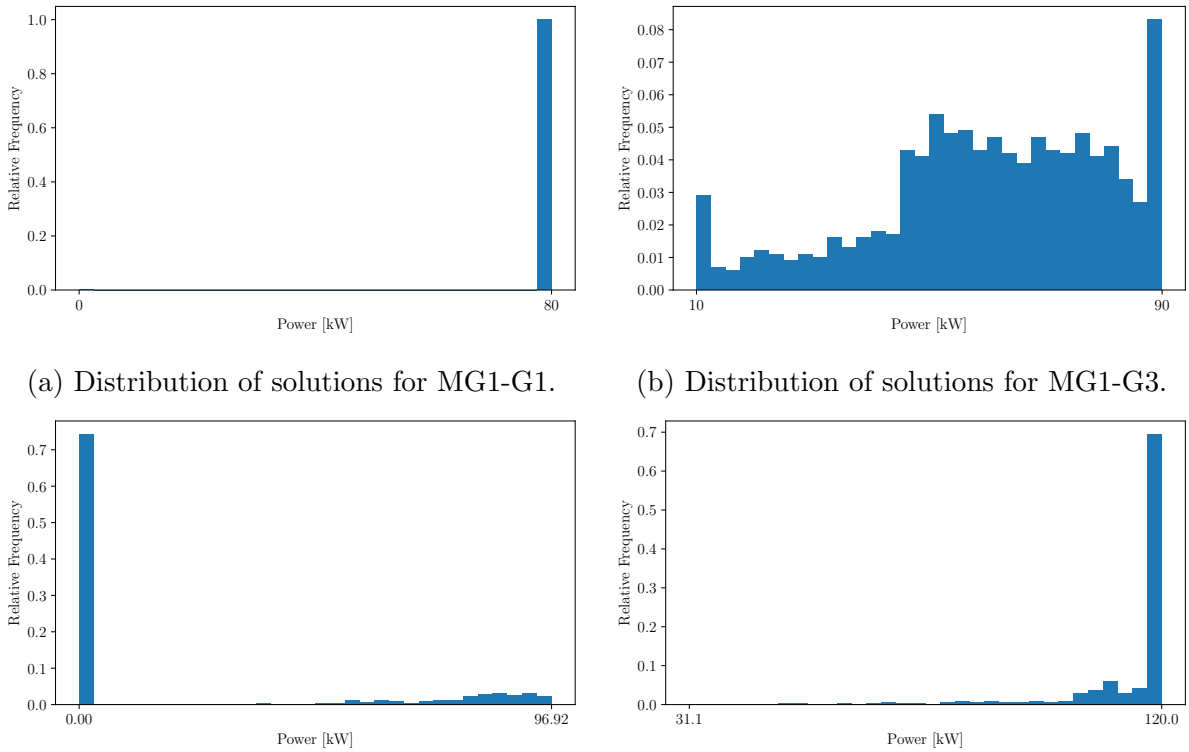

(a) Distribution of solutions for MG1-G1.

(b) Distribution of solutions for MG1-G3.

(c) Distribution of solutions for MG2-G3.

(d) Distribution of solutions for MG3-G2.

Figure 4.3: Distributions of power dispatch solutions at hour 20 in MCS.

defined bounds. On the other hand, the histogram of the power dispatch solutions for thermal unit G3 in MG1 at hour 20 (Figure 4.3b) shows a broader distribution of optimal values, indicating that the optimal dispatch varies according to the different demand and PV generation profiles.

To compare the output of MCS with the proposed AA model, intervals for each variable are obtained from the analysis of all solutions. A possible approach is to simply take the minimum and maximum values for each variable, which would result in the widest solution intervals. However, due to the binary variables and intertemporal constraints of the EMS problem, the combination of the extreme values of some variables at one hour with the extreme values at previous or subsequent hours may result in solution profiles that are infeasible in the original deterministic problem. Another approach involves the computation of confidence intervals from the obtained solutions, based on the mean, standard deviation, and number of samples; however, this method assumes that the solutions follow

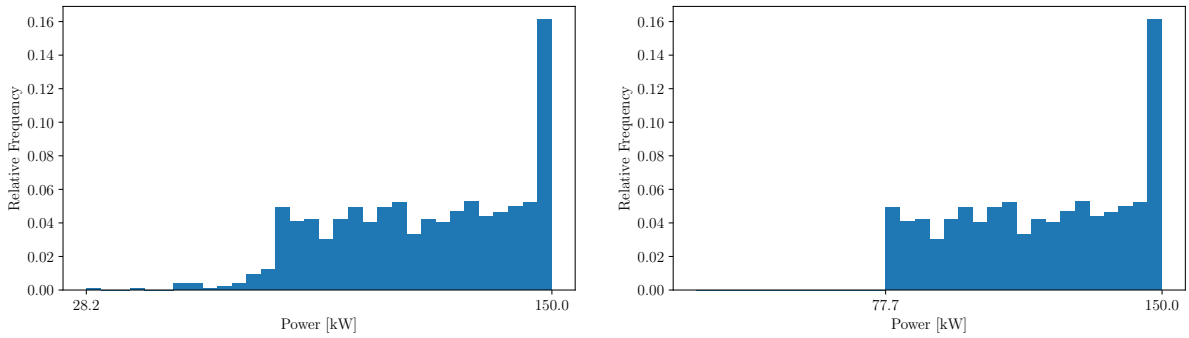

(a) Original distribution for MG2-G3.

(b) Reduced distribution for MG2-G3.

Figure 4.4: Distributions of power dispatch solutions at hour 19 in MCS.

a normal distribution, which is not the case for all variables, as can be seen in Figure 4.3. Thus, to overcome the need for assuming inaccurate solution distributions, and to obtain more significant solution intervals than those associated with the minimum and maximum values of each variable, a selection procedure based on the relative frequency of the solution distributions is implemented and described next.

First, a minimum relative frequency threshold is defined for each variable, based on a percentage of its highest interval, to ensure that the chosen minimum value is adequate for each variable. Then, the intervals with relative frequency lower than this threshold are discarded, which results in narrower and more significant intervals that do not rely on the assumption of normal distributions. For example, Figure 4.4a shows the original histogram of solutions for G3 in MG2 at hour 19, and Figure 4.4b shows the resulting interval after applying the described procedure, considering a percent value of 0.1 for the minimum relative frequency. Since the maximum relative frequency of this variable was approximately 0.16, all solutions with a relative frequency lower than $0.1 \times 0.16 = 0.016$ are discarded to produce the final interval, which is a reduced version of the original distribution. By removing the least probable solutions, the obtained intervals are a more significant representation of feasible solutions obtained from the MCS output.

AA Results

For the AA model, the partial deviations of all uncertain parameters must be specified. In this case, to match the input of MCS, the same upper and lower bounds are considered, i.e., the values of the partial deviations of the affine forms in (4.3) and (4.4) produce an

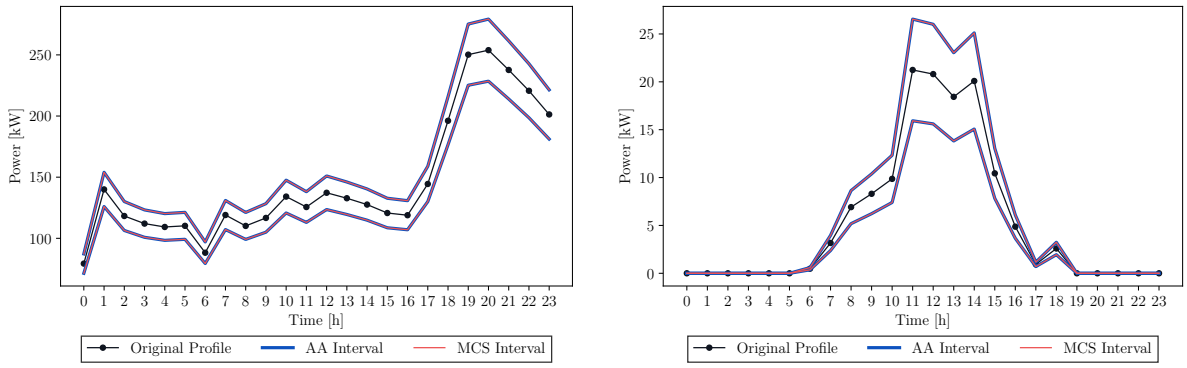

(a) Demand input intervals for MG1.

(b) PV generation input intervals for MG1.

Figure 4.5: Input intervals of uncertain parameters for AA model and MCS.

identical interval to the one defined by the upper and lower bounds of the random profiles used in MCS, defined by (4.69)–(4.72). For example, Figure 4.5 shows the original demand and PV generation profiles in MG1, with the corresponding input intervals used in the AA model and MCS, which overlap as intended. Similar profile intervals for each MG are generated. A weighting factor of $w = 0.9$ in (4.13) was chosen because it yields an objective function value close to the one obtained in the MCS solution, which also considers parameter uncertainties.

A comparison of the deterministic, MCS, and AA solutions is shown in Figure 4.6 for the power dispatches of thermal units G1 and G3 in each MG (profiles for units G2 are not shown because their power dispatch was zero at most hours in this case). Note that at certain hours there is no MCS interval, such as in the initial hours for unit G1 in MG2, shown in Figure 4.6c, which means that, for the random profiles considered, the optimal dispatch of that unit should follow the deterministic solution at those hours, regardless of the variations in the uncertain parameters. In all the dispatch profiles in Figure 4.6, it can be seen that the AA intervals do not always envelop the MCS intervals, nor the deterministic solution. This may seem counterintuitive, since the AA solution is robust for the full range of uncertainties considered, and is thus expected to be the most conservative and hence envelop both the deterministic and MCS solutions. However, in the MMG EMS model, the power generation and power exchanges of all MGs are coupled through the power balance constraints, and when the AA interval does not envelop the deterministic solution, that mismatch is compensated by the interval of another variable that results in a lower cost while satisfying the constraints of the problem. Furthermore, due to the formulation of the AA problem, which minimizes the magnitudes of the partial deviations,

the resulting intervals are as narrow as possible, while still ensuring the feasibility of the problem for any realization of the uncertain parameters. On the other hand, the MCS intervals are wider because they cover a range of solutions for each individual variable, while the AA solution gives the narrowest interval for all variables. A solution within the AA interval of a single variable may not be within the solution boundaries of MCS, due to the flexibility of the AA model to find the optimal solution contributing to minimizing the cost function. Based on this analysis, the resulting patterns of all variables are consistent with the AA formulation, which validates the proposed AA model.

Figure 4.7 shows the comparison of power dispatches of ESS units obtained from the deterministic, MCS and AA models, which are computed as the difference between discharging and charging powers at each hour. Thus, positive values indicate that the ESS unit is discharging, and negative values indicate that the ESS unit is charging. In this case, the optimal values of the partial deviations of both charging and discharging powers for all ESS units are zero at all hours because this results in the lowest operational cost according to the AA model, which produces the single-line "intervals" shown. This means that the optimal dispatch of ESS units in the AA model will be the same for any specific realization of the uncertain parameters within the input range considered.

The solution comparison for power exchanges between MGs and the main grid are shown in Figure 4.8. Similarly as before, the AA intervals follow a pattern that resembles the deterministic and MCS solutions, without enveloping the other solutions at all hours. This is a consequence of the coupling of power exchanges in the model, as previously explained. The power sold by the main grid to MG1 (Figure 4.8a) presents AA intervals with varying widths throughout the optimization period, which indicates that in these hours the power sold can take a range of values in the optimal solution, depending on the specific realization of uncertainties. Furthermore, the deterministic, MCS and AA models all indicate that no power should be bought by the main grid from MGs in the optimal solution, regardless of the variability in demand and PV generation.

To further clarify the validation of the solution intervals of the AA model, Figure 4.9 shows a comparison for MG1 of the demand profile with its corresponding input uncertainty range, and the solution intervals considering the total generation obtained from MCS and the AA model. Note that by taking into account the AA intervals for the aggregated generation in the MG, the total demand and its uncertainty interval are satisfied, thus demonstrating that the AA solution is in fact robust for any realization of the uncertain parameters when the whole system operation is considered. On the other hand, the MCS interval is wider than the AA interval at certain hours, which can be the case depending on the distribution of the solutions. A broader distribution of the MCS solutions results in larger intervals for the generation variables, which produces the wider aggregated interval

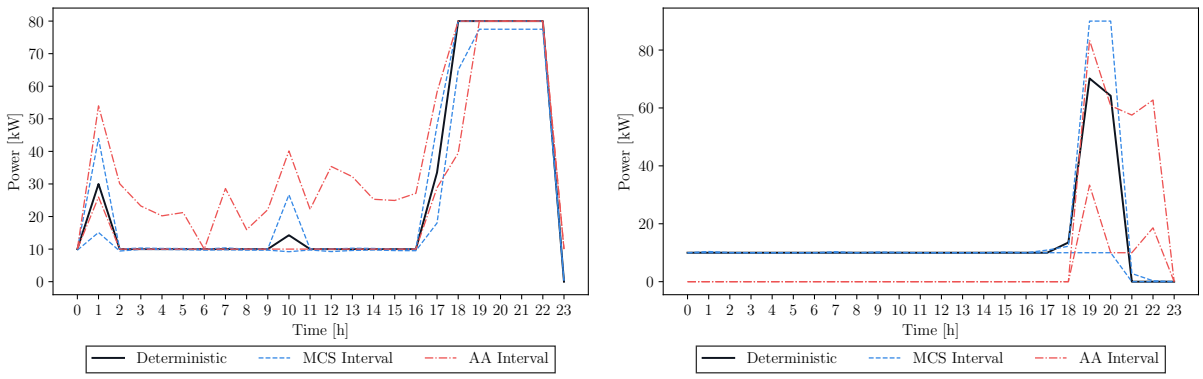

(a) MG1-G1.

(b) MG1-G3.

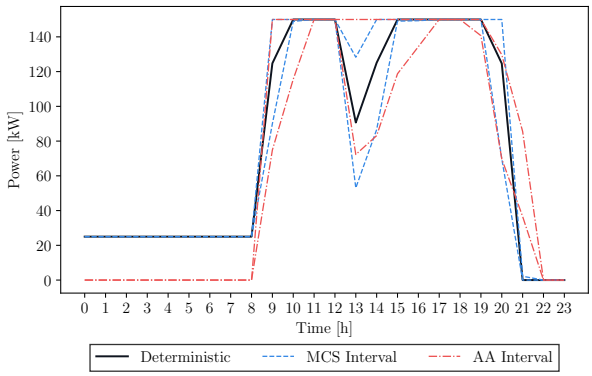

(c) MG2-G1.

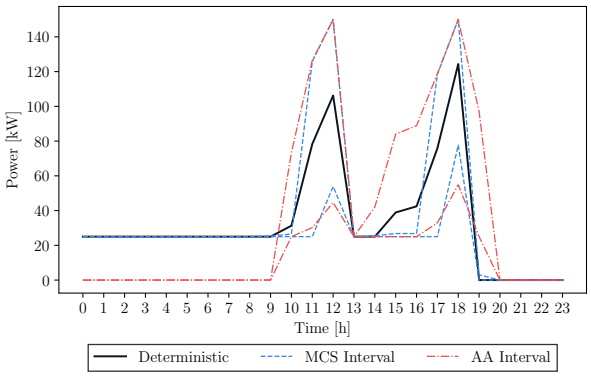

(d) MG2-G3.

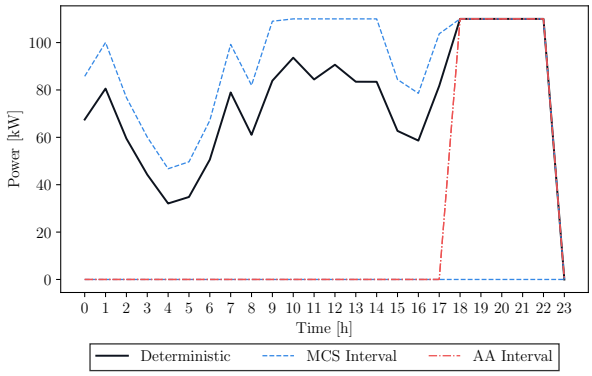

(e) MG3-G1.

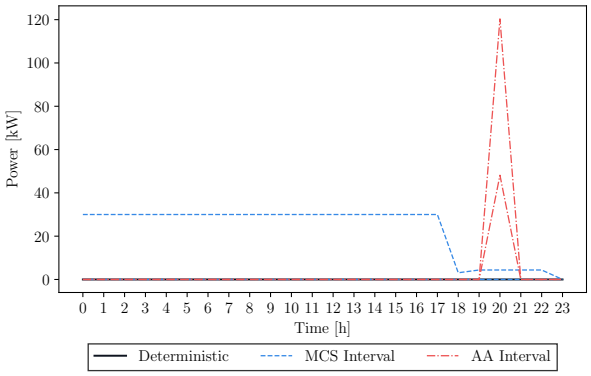

(f) MG3-G3.

Figure 4.6: Comparison of deterministic, MCS, and AA power dispatches for thermal units.

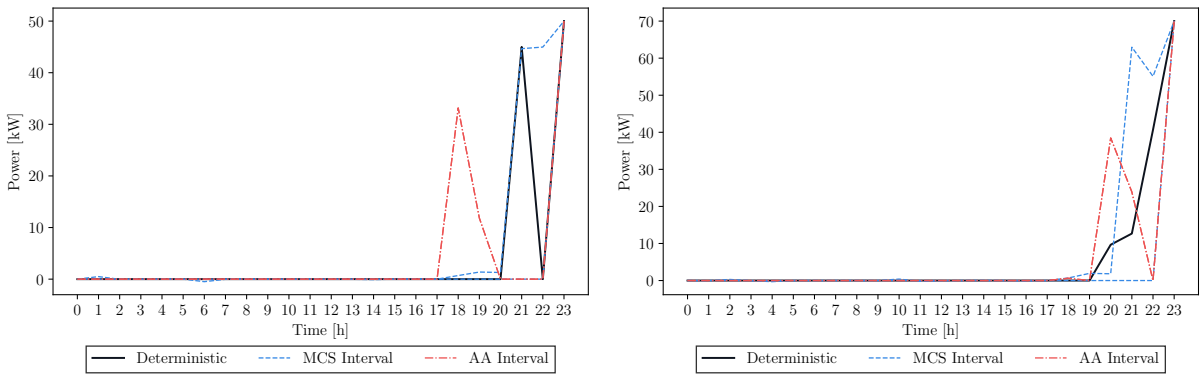

(a) MG1-ESS1.

(b) MG1-ESS2.

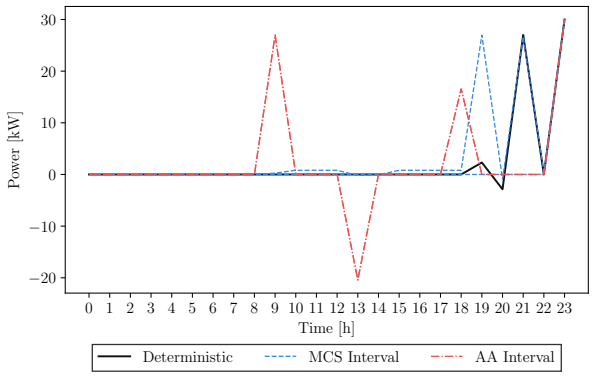

(c) MG2-ESS1.

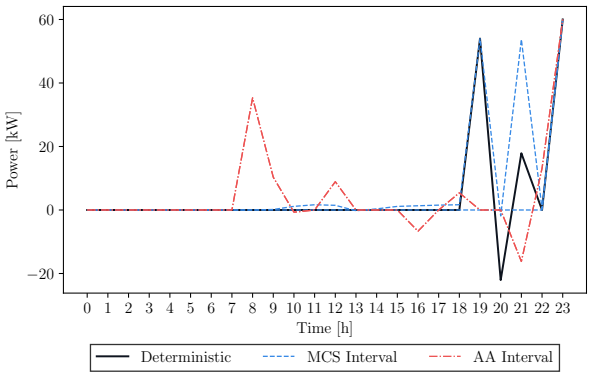

(d) MG2-ESS2.

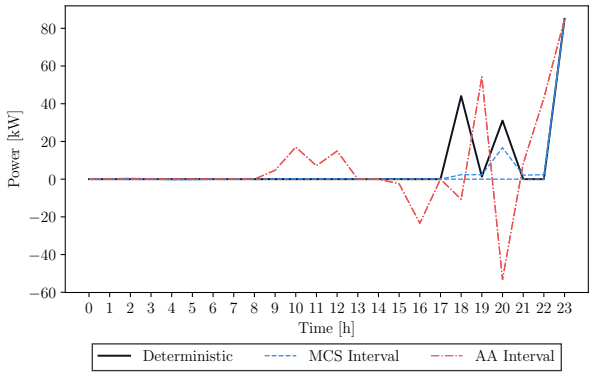

(e) MG3-ESS1.

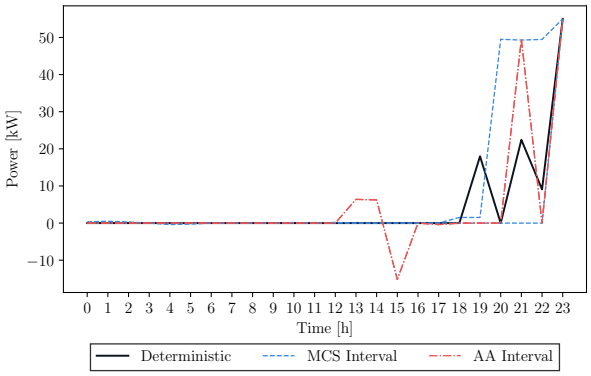

(f) MG3-ESS2.

Figure 4.7: Comparison of deterministic, MCS, and AA power dispatches for ESS units.

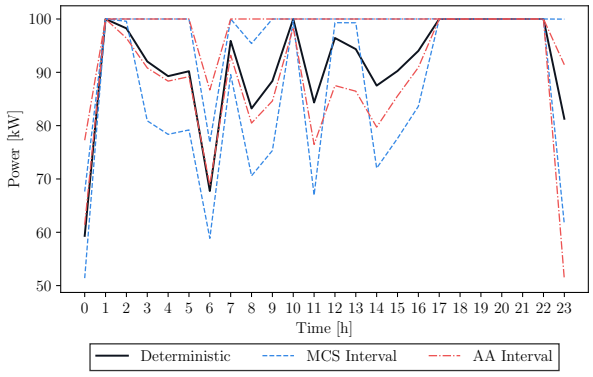

(a) Power sold by the main grid to MG1.

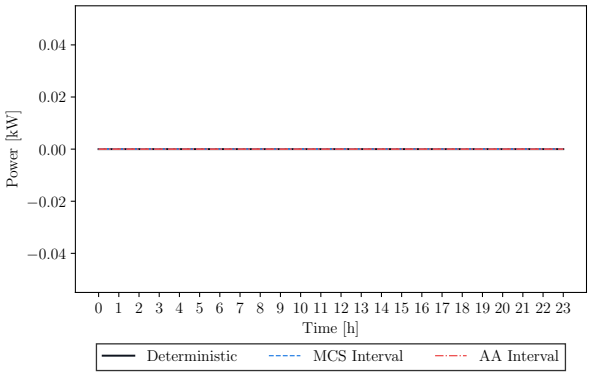

(b) Power bought by the main grid from MG1.

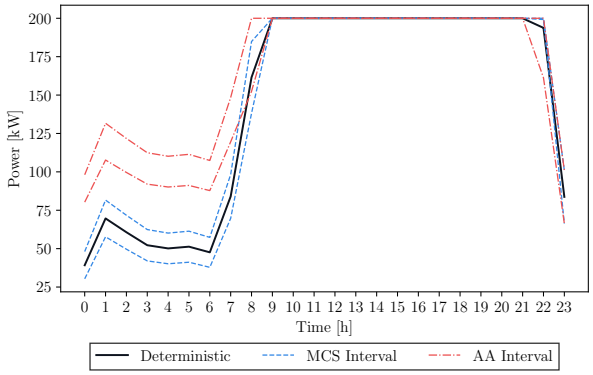

(c) Power sold by the main grid to MG2.

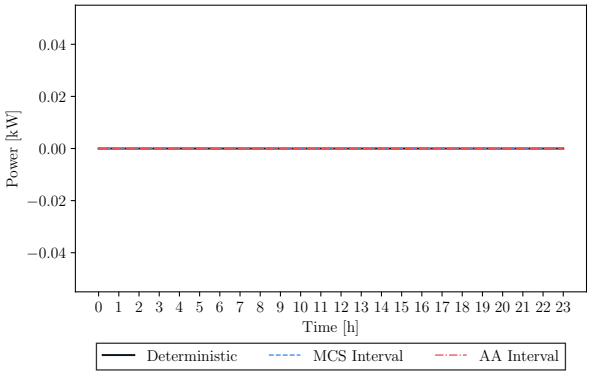

(d) Power bought by the main grid from MG2.

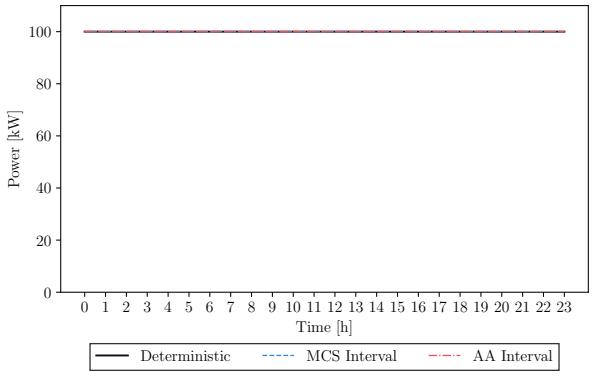

(e) Power sold by the main grid to MG3.

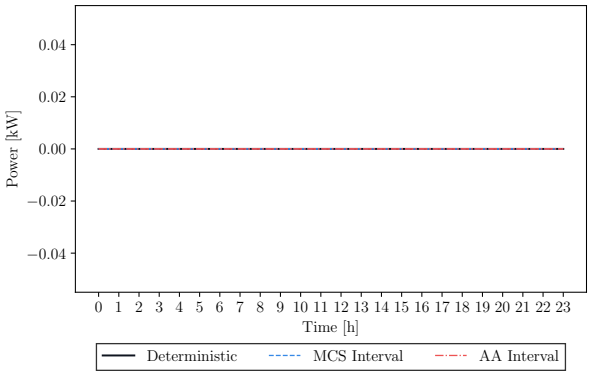

(f) Power bought by the main grid from MG3.

Figure 4.8: Comparison of deterministic, MCS, and AA solutions for power exchanges with the main grid.

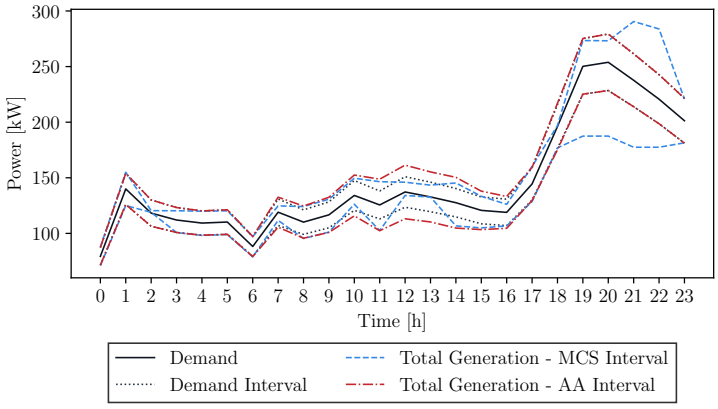

Figure 4.9: Comparison of demand and total generation intervals in MG1.

observed in Figure 4.9; the distribution of solutions is entirely determined by the problem parameters. This comparison further demonstrates that the AA model may yield a narrower solution interval because it is minimizing the magnitudes of the partial deviations, while still being robust under the range of uncertainties considered.

The execution time of the AA model for this case was approximately 3 min, while the execution time of the MCS was approximately 19 min; this significant reduction in computation time is a major advantage of the proposed AA model, which considers the same range of uncertainties. The objective function values of the deterministic, MCS, and AA models are \$6,470.1, \$6,536.6, and \$4,897.5, respectively; in this case, the value of the AA multi-objective function (4.13) is lower due to the weighting factor of the central and affine radius terms.

4.2.2 Dispatch from the AA Solution

To demonstrate the utility of the proposed AA model, a dispatch procedure can be implemented to convert the resulting affine forms to particular solutions for specific realizations of the uncertain parameters. This involves assigning values in the [-1, 1] interval to each noise symbol corresponding to the actual realization of the uncertainty when known, and substituting in the affine forms for finding a specific dispatch solution. To exemplify this, the noise symbols assignment can be made as follows:

$$\varepsilon^{D}_{m,t} = \frac{D_{m,t} - D_{0,m,t}}{D_{1,m,t}} \quad \forall\ m \in M,\ t \in t \tag{4.73}$$

$$\varepsilon^r_{m,t} = \frac{P^r_{m,t} - P^r_{0,m,t}}{P^r_{1,m,t}} \quad \forall\ m \in M,\ t \in t \tag{4.74}$$

where $D_{m,t}$ and $P^r_{m,t}$ are the realizations of the uncertain demand and renewable generation, $D_{0,m,t}$ and $P^r_{0,m,t}$ are the central values, and $D_{1,m,t}$ and $P^r_{1,m,t}$ are the corresponding partial deviations. Thus, assuming that a profile deviates from the deterministic hourly profiles, (4.73) and (4.74) can be used to compute all noise symbols associated with the two sources of uncertainty. For example, the affine form of the power output of generator G1 in MG1 at hour 11 is $\widehat{P}_{1,1,11} = 16.10 + 0.79\varepsilon^D_{1,11} - 5.31\varepsilon^r_{1,11}$. Note that this particular variable is more sensitive to renewable generation uncertainty than demand uncertainty, since the partial deviation corresponding to renewable generation has the largest absolute value. Similar affine forms of all the continuous variables in the problem are available from the optimal solution of the AA problem. Hence, substituting the values of noise symbols found from (4.73) and (4.74) for each uncertain parameter, in all affine variables, yields a particular dispatch solution.

To demonstrate this procedure, a realization of the uncertain parameters is chosen arbitrarily, assuming a deviation of +5% in demand and -5% in PV generation, for all MGs. Figure 4.10 shows the resulting power dispatches after applying the described dispatch procedure, as well as the corresponding deterministic and MCS solutions, for thermal units G1 and G3 in each MG. In some generators, the AA dispatch closely follows the deterministic and MCS solutions, as shown in Figure 4.10c. On the other hand, the other generators present significantly different dispatch profiles, which can be expected from the AA model, since the resulting profiles come from an optimal solution which is robust for a range of the uncertain parameters, resulting in an objective function value of $5,508.6. Therefore, note that the affine forms obtained from the solution of the AA model can be used to find the optimal dispatch for specific realizations of the parameters within the range of uncertainty considered, with no need for solving the problem again for different realizations, and with lower computational burden with respect to the MCS. Furthermore, the resulting affine forms provide valuable information regarding the sensitivity of variables to each source of uncertainty.

4.3 Summary

In this chapter, the centralized MMG EMS model was formulated as an AA-based optimization problem to consider uncertainties associated with electricity demand and renewable energy generation within each MG. Then, a detailed description of the procedure to linearize the absolute values introduced by the AA operators was presented. The proposed

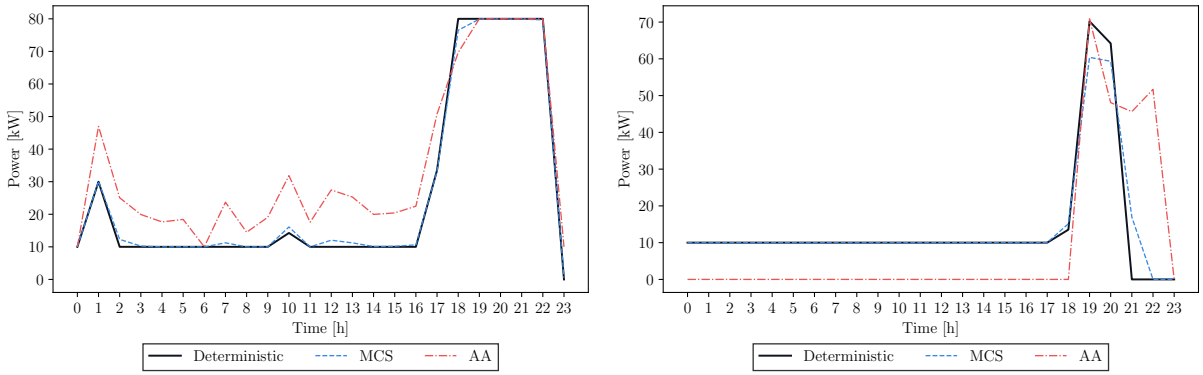

(a) MG1-G1.

(b) MG1-G3.

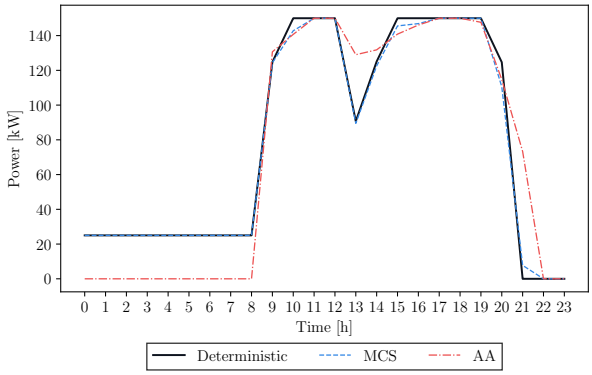

(c) MG2-G1.

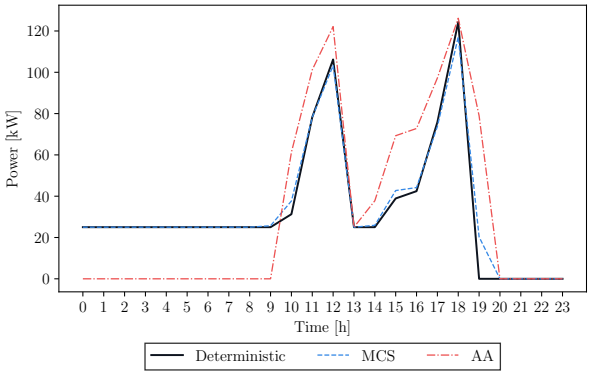

(d) MG2-G3.

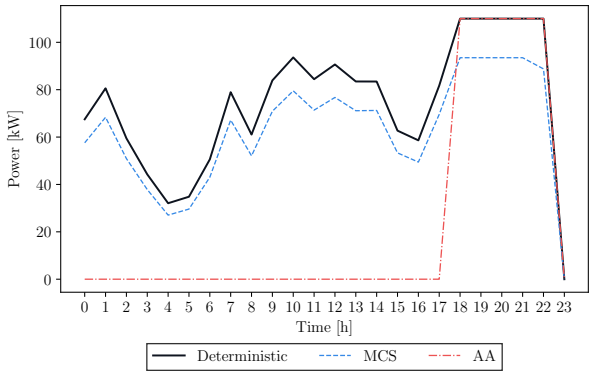

(e) MG3-G1.

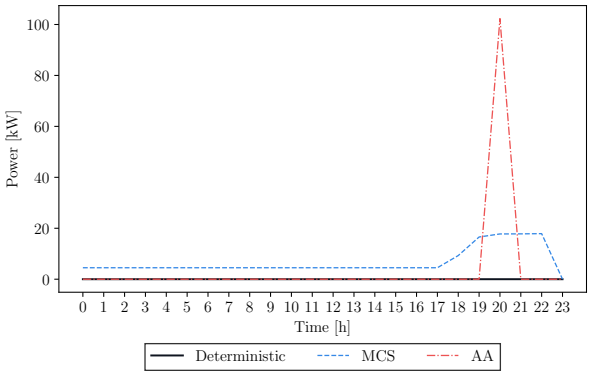

(f) MG3-G3.

Figure 4.10: AA power dispatch of thermal units for specific realizations of uncertain parameters.

AA model was compared with the deterministic and MCS solutions, and results showed that the AA model is capable of satisfying the range of uncertainty considered, and can be solved with relatively low computational burden and short execution time. Furthermore, an advantage of this approach is that the same affine forms can be used to find a dispatch for different realizations of the uncertain parameters, with no need to repeatedly solve the optimization problem.

Chapter 5

Conclusion

This chapter provides a summary of the models, solution methods, and results discussed in this thesis, highlighting the main conclusions and key takeaways from the presented research. Finally, the main contributions of the work described in the thesis and potential future research ideas are outlined.

5.1 Summary and Conclusions

The adoption of MGs enables the high penetration of DERs in existing electricity distribution networks, enhancing the reliability and efficiency of conventional power systems. More recently, the coordinated operation of multiple MGs has gained attention due to the associated economic and technical benefits. Thus, there is a need for developing adequate EMS models for MMGs, which can leverage the distributed nature of such systems while considering uncertainties in load and renewable generation in an efficient manner. In this context, a distributed EMS model and a centralized EMS model that considers uncertainties for the optimal coordinated operation of MMG systems were proposed in this thesis, considering detailed operational constraints of thermal generators and ESSs within each MG, as well as power exchanges among MGs and the main grid, and the corresponding power limits at the PCC.

In the first part of the thesis, the centralized MMG EMS model is formulated as an optimization problem that minimizes the operational cost of the overall system, over a 24-hour period. The model includes operational constraints of thermal generators such as power output limits, ramping limits, and minimum up and down time requirements,

as well as operational constraints of ESS units such as energy balance, SoC, and charging/discharging power limits. A system-wide supply-demand balance constraint ensures that the demand is satisfied in each MG at all times, considering power exchanges among MGs and the main grid. Furthermore, the PCC constraints restrict the total power outflow/inflow in each MG. The model was formulated to make it decomposable and thus suitable for the application of a distributed algorithm for its solution. Hence, the model was decomposed into a set of subproblems corresponding to each MG using Lagrangian relaxation, and solved using a distributed optimization approach based on the subgradient method. The distributed algorithm requires minimal information to coordinate the MGs operation, thus preserving the privacy of their local parameters and demand profiles. The model was tested using demand and solar irradiance data from a realistic ADN in São Paulo, Brazil, and results showed that the distributed algorithm converges to the optimal or near-optimal solution of the centralized model in a practical computational time, considering the time frame of the EMS problem, thus making the proposed model a viable alternative for the implementation of a distributed EMS in an MMG system. Finally, a comparison between individual and cooperative operation demonstrated that the operational cost of the MMG system significantly decreases when power exchanges are possible, as expected. For example, in the test system presented, the total operating cost decreased by around 17% as a consequence of the power exchanges.

In the second part of the thesis, the formulation of the centralized MMG EMS model in the AA domain was presented, to account for uncertainties associated with demand and renewable generation variability. The uncertain parameters were defined in affine form, considering independent and distinct noise symbols for each source of uncertainty. Then, all continuous variables in the model were redefined to include terms corresponding to each noise symbol of the uncertain parameters, and the objective function and constraints were reformulated according to previously defined AA operators and optimization framework. The linearization procedure of absolute values introduced by the AA formulation in the objective function and constraints was then described in detail; this procedure was necessary to be able to solve the model with existing optimization solvers. To validate the proposed AA-based MMG EMS model, comparisons with the deterministic solution and MCS were presented. To compare the output of the MCS with the AA model, intervals were generated from the distribution of the repeated solutions for each variable, applying a selection procedure that discarded the least likely solutions and did not rely on the assumption of normal distributions of the output variables. The proposed model was tested using the same data of the realistic ADN in São Paulo, Brazil, used in Chapter 3, with the results showing that the AA intervals for individual variables did not always envelope the MCS intervals, nor the deterministic solution. This occurs because the power generation and

exchanges of all MGs are coupled through the power balance constraints in the MMG EMS model, so that when the AA interval of one variable does not envelop the deterministic solution, the mismatch is compensated by the interval of another related variable. The optimal solution obtained from the AA model is robust under the same range of possible realizations of the uncertain parameters as an MCS approach, and can be solved with significantly lower computational burden. Finally, to demonstrate the practicality of the proposed AA model, a dispatch procedure to convert the resulting affine forms to particular solutions for specific realizations of the uncertain parameters was demonstrated.

The following are the main conclusions drawn from the development of this thesis:

- The implementation of MMGs enables optimal power exchanges that improve the overall operation of the system by enhancing its reliability and reducing its operation cost, thus mitigating the undesirable effects of high penetration of RESs.
- The inclusion of constraints that enforce power flow limits at the PCC of each MG significantly increases the complexity of the MMG EMS problem, particularly with regards to the applicability of distributed optimization algorithms.
- Alternative methods to update the multipliers in the subgradient method, such as the cutting plane method, were found to be less computationally efficient than the constant update step size. This is a consequence of the complexity of the problem, as each iteration requires the solution of an optimization problem with additional constraints.
- The proposed distributed optimization approach for solving the MMG EMS problem preserves the privacy of each MG by requiring minimal information to find the optimal solution. However, it should be noted that the multiplier update step still requires the collection of solutions of all MGs, which may be performed by the Distribution Network Operator (DNO).
- The distributed optimization approach reduces the complexity of the optimization problem solved by each MG, which facilitates the inclusion of new DERs without the need of updating a larger centralized model. However, the iterative distributed coordination algorithm also introduces a higher degree of mathematical complexity with respect to the centralized model, which should be taken into account when implementing an MMG EMS.
- The AA solution intervals were found to be less conservative than the MCS intervals. This is a consequence of the coupling of supply-demand balance constraints through

the power exchange variables, as well as the minimization of the affine radius in the objective function, which results in narrower AA intervals than those obtained with MCS that satisfy all constraints for the chosen uncertainty input ranges.

- The linearization of absolute values introduced by the AA formulation significantly increases the number of constraints in the optimization problem. While current optimization solvers can handle such constraints efficiently for relatively small systems, scaling the proposed AA model to consider a large number of MGs or several more sources of uncertainty may result in computational times that would be impractical when considering the operational time frame of the EMS.

- The solution intervals obtained from the AA model can be used to determine the optimal dispatch of MG resources and power exchanges for the range of uncertainty considered in the input parameters, without the need for repeated simulations.

- An AA-based approach for solving the MMG EMS problem presents key advantages over MCS approaches, mainly avoiding the need for statistical characterizations, and reducing the computational burden associated with repeated simulations, while considering the same range of uncertainties.

5.2 Contributions

The contributions of this thesis can be summarized as follows:

- A centralized and decomposable model for the optimal and coordinated operation of MMG systems was proposed, which enables power exchanges among individual MGs and the ADN, while realistically considering the power flow limits at the PCC of each MG. Furthermore, the proposed model includes detailed operational constraints of thermal generation units and ESSs.

- Based on the proposed centralized EMS model, a distributed solution method was implemented by applying a decomposition technique to the complete problem and implementing an iterative solution algorithm for the individual MG subproblems, which requires minimal information exchange, thus preserving the privacy of each MG. It was shown that the proposed distributed model converges to the centralized solution.

- The centralized MMG EMS model was formulated in the AA domain to account for uncertainties in electricity demand and renewable generation, including a detailed description of the procedure for linearizing absolute values to be able to solve the problem with existing optimization solvers.
- The proposed models were tested and validated with electricity demand and renewable generation data from an existing ADN in São Paulo, Brazil, showing that the proposed AA model provides solution intervals that are robust for the range of uncertainties considered, requiring significantly less computation time than an MCS approach. Furthermore, the dispatch procedure to determine the optimal power generation, energy storage, and power exchanges from the AA solution, for specific realizations of the uncertain parameters, was demonstrated.
- The benefits of the cooperative operation of MGs were confirmed with the proposed models, which are mainly reflected in significant operating cost reductions for the overall MMG system.

The results of a simplified version of the distributed model described in Chapter 3 were submitted for publication and presented at the 11^{th} Bulk Power Systems Dynamics and Control Symposium (IREP 2022) [108], and an article describing the extended model proposed in the thesis is being prepared for submission to a relevant journal. The proposed AA-based model and simulation results presented in Chapter 4 have been accepted for publication in the IEEE Transactions on Smart Grid journal [109].

5.3 Future Work

Based on the work presented in this thesis, the following issues could be addressed in the future:

- Enhance the proposed centralized MMG EMS model by considering nodal active and reactive power balance constraints in the optimization problem, as opposed to the single-bus model assumed in this work. As it was found throughout the development of this research, the distributed algorithm and the AA-based approach make the solution of the MMG EMS problem significantly complex. Therefore, the implementation of a more detailed model is a challenging and interesting research opportunity.
- Implement the execution of the proposed model for smaller intervals within the 1-hour periods assumed in the presented UC model, to better account for forecasting errors.

- Consider additional components in the individual MG EMS model. For example, a cost associated with the use of ESSs to represent their degradation, or a demand response scheme that would further enhance the flexibility of the model.
- Improve the distributed algorithm to achieve better convergence rates and reduced computation times. Modified decomposition techniques and subgradient methods may be explored in this case.
- Compare the performance of the AA-based MMG EMS with SP and RO models to further demonstrate its advantages.
- Apply the distributed solution algorithm to an MMG EMS model that considers uncertainties. Based on the experience with the proposed models, its implementation and solution with existing optimization solvers would be a significantly difficult task.

References

[1] International Energy Agency (IEA), *Energy Security and Climate Policy: Assessing Interactions*. OECD Publishing, 2007.

[2] F. Blaabjerg, Y. Yang, D. Yang, and X. Wang, "Distributed power-generation systems and protection," *Proceedings of the IEEE*, vol. 105, no. 7, pp. 1311–1331, July 2017.

[3] A. Khodaei, "Resiliency-oriented microgrid optimal scheduling," *IEEE Transactions on Smart Grid*, vol. 5, no. 4, pp. 1584–1591, July 2014.

[4] S. Mohamed, M. F. Shaaban, M. Ismail, E. Serpedin, and K. A. Qaraqe, "An efficient planning algorithm for hybrid remote microgrids," *IEEE Transactions on Sustainable Energy*, vol. 10, no. 1, pp. 257–267, January 2019.

[5] D. E. Olivares, A. Mehrizi-Sani, A. H. Etemadi, C. A. Cañizares, R. Iravani, M. Kazerani, A. H. Hajimiragha, O. Gomis-Bellmunt, M. Saeedifard, R. Palma-Behnke, G. A. Jiménez-Estévez, and N. D. Hatziargyriou, "Trends in microgrid control," *IEEE Transactions on Smart Grid*, vol. 5, no. 4, pp. 1905–1919, July 2014.

[6] G. Joos, J. Reilly, W. Bower, and R. Neal, "The need for standardization: The benefits to the core functions of the microgrid control system," *IEEE Power and Energy Magazine*, vol. 15, no. 4, pp. 32–40, July 2017.

[7] D. Ton and J. Reilly, "Microgrid controller initiatives: An overview of R&D by the U.S. Department of Energy," *IEEE Power and Energy Magazine*, vol. 15, no. 4, pp. 24–31, July 2017.

[8] E. O'Neill-Carrillo and A. Irizarry-Rivera, "How to harden Puerto Rico's grid against hurricanes," *IEEE Spectrum*, vol. 56, no. 11, pp. 42–48, November 2019.

[9] Puerto Rico Institute for Competitiveness and Sustainable Economy (ICSE-PR) and Rocky Mountain Institute (RMI), "Public collaborative for Puerto Rico's energy transformation," ICSE and RMI, Tech. Rep., October 2018.

[10] E. Wood, "Microgrids up and running despite earthquake and massive power outage in Puerto Rico," https://microgridknowledge.com/school-microgrids-up-and-running-despite-earthquake-and-massive-power-outage-in-puerto-rico/, January 2020, [Accessed: March 26, 2020].

[11] A. Mohammed, S. S. Refaat, S. Bayhan, and H. Abu-Rub, "AC microgrid control and management strategies: Evaluation and review," *IEEE Power Electronics Magazine*, vol. 6, no. 2, pp. 18–31, June 2019.

[12] G. Ma, J. Li, and X.-P. Zhang, "A review on optimal energy management of multi-microgrid system considering uncertainties," *IEEE Access*, vol. 10, pp. 77 081–77 098, July 2022.

[13] Z. Li, M. Shahidehpour, F. Aminifar, A. Alabdulwahab, and Y. Al-Turki, "Networked microgrids for enhancing the power system resilience," *Proceedings of the IEEE*, vol. 105, no. 7, pp. 1289–1310, July 2017.

[14] L. Che, X. Zhang, M. Shahidehpour, A. Alabdulwahab, and A. Abusorrah, "Optimal interconnection planning of community microgrids with renewable energy sources," *IEEE Transactions on Smart Grid*, vol. 8, no. 3, pp. 1054–1063, May 2017.

[15] J. A. P. Lopes, A. Madureira, N. Gil, and F. Resende, "Operation of Multi-Microgrids," in *Microgrids*, N. Hatziargyriou, Ed. Chichester, United Kingdom: John Wiley and Sons Ltd, December 2013, pp. 165–205.

[16] A. Ouammi, H. Dagdougui, and R. Sacile, "Optimal control of power flows and energy local storages in a network of microgrids modeled as a system of systems," *IEEE Transactions on Control Systems Technology*, vol. 23, no. 1, pp. 128–138, January 2015.

[17] X. Dong, X. Li, and S. Cheng, "Energy management optimization of microgrid cluster based on multi-agent-system and hierarchical Stackelberg game theory," *IEEE Access*, vol. 8, pp. 206 183–206 197, November 2020.

[18] C. Yuan, M. S. Illindala, and A. S. Khalsa, "Co-optimization scheme for distributed energy resource planning in community microgrids," *IEEE Transactions on Sustainable Energy*, vol. 8, no. 4, pp. 1351–1360, October 2017.

[19] H. Zou, S. Mao, Y. Wang, F. Zhang, X. Chen, and L. Cheng, "A survey of energy management in interconnected multi-microgrids," *IEEE Access*, vol. 7, pp. 72 158–72 169, May 2019.

[20] M. N. Alam, S. Chakrabarti, and A. Ghosh, "Networked microgrids: State-of-the-art and future perspectives," *IEEE Transactions on Industrial Informatics*, vol. 15, no. 3, pp. 1238–1250, March 2019.

[21] L. Ahmethodzic and M. Music, "Comprehensive review of trends in microgrid control," *Renewable Energy Focus*, vol. 38, pp. 84–96, September 2021.

[22] N. Nikmehr and S. Najafi Ravadanegh, "Reliability evaluation of multi-microgrids considering optimal operation of small scale energy zones under load-generation uncertainties," *International Journal of Electrical Power & Energy Systems*, vol. 78, pp. 80–87, June 2016.

[23] N.-O. Song, J.-H. Lee, H.-M. Kim, Y. H. Im, and J. Y. Lee, "Optimal energy management of multi-microgrids with sequentially coordinated operations," *Energies*, vol. 8, no. 8, pp. 8371–8390, August 2015.

[24] A. Ouammi, H. Dagdougui, L. Dessaint, and R. Sacile, "Coordinated model predictive-based power flows control in a cooperative network of smart microgrids," *IEEE Transactions on Smart Grid*, vol. 6, no. 5, pp. 2233–2244, September 2015.

[25] H. Farzin, M. Fotuhi-Firuzabad, and M. Moeini-Aghtaie, "Role of outage management strategy in reliability performance of multi-microgrid distribution systems," *IEEE Transactions on Power Systems*, vol. 33, no. 3, pp. 2359–2369, May 2018.

[26] Y. Wang, S. Mao, and R. M. Nelms, "On hierarchical power scheduling for the macrogrid and cooperative microgrids," *IEEE Transactions on Industrial Informatics*, vol. 11, no. 6, pp. 1574–1584, December 2015.

[27] P. Kou, D. Liang, and L. Gao, "Distributed EMPC of multiple microgrids for coordinated stochastic energy management," *Applied Energy*, vol. 185, pp. 939 – 952, January 2017.

[28] H. Dagdougui and R. Sacile, "Decentralized control of the power flows in a network of smart microgrids modeled as a team of cooperative agents," *IEEE Transactions on Control Systems Technology*, vol. 22, no. 2, pp. 510–519, March 2014.

[29] D. Gregoratti and J. Matamoros, "Distributed energy trading: The multiple-microgrid case," *IEEE Transactions on Industrial Electronics*, vol. 62, no. 4, pp. 2551–2559, April 2015.

[30] H. Wang and J. Huang, "Incentivizing energy trading for interconnected microgrids," *IEEE Transactions on Smart Grid*, vol. 9, no. 4, pp. 2647–2657, July 2018.

[31] Q. Xu, T. Zhao, Y. Xu, Z. Xu, P. Wang, and F. Blaabjerg, "A distributed and robust energy management system for networked hybrid AC/DC microgrids," *IEEE Transactions on Smart Grid*, vol. 11, no. 4, pp. 3496–3508, July 2020.

[32] Z. Liu, L. Wang, and L. Ma, "A transactive energy framework for coordinated energy management of networked microgrids with distributionally robust optimization," *IEEE Transactions on Power Systems*, vol. 35, no. 1, pp. 395–404, January 2020.

[33] A. Parisio, C. Wiezorek, T. Kyntaja, J. Elo, K. Strunz, and K. H. Johansson, "Cooperative MPC-based energy management for networked microgrids," *IEEE Transactions on Smart Grid*, vol. 8, no. 6, pp. 3066–3074, November 2017.

[34] Y. Du, J. Wu, S. Li, C. Long, and S. Onori, "Coordinated energy dispatch of autonomous microgrids with distributed MPC optimization," *IEEE Transactions on Industrial Informatics*, vol. 15, no. 9, pp. 5289–5298, September 2019.

[35] F. Luo, Z. Y. Dong, G. Liang, J. Murata, and Z. Xu, "A distributed electricity trading system in active distribution networks based on multi-agent coalition and blockchain," *IEEE Transactions on Power Systems*, vol. 34, no. 5, pp. 4097–4108, September 2019.

[36] J. Kim and Y. Dvorkin, "A P2P-dominant distribution system architecture," *IEEE Transactions on Power Systems*, vol. 35, no. 4, pp. 2716–2725, July 2020.

[37] A. Hussain, V. H. Bui, and H. M. Kim, "A resilient and privacy-preserving energy management strategy for networked microgrids," *IEEE Transactions on Smart Grid*, vol. 9, no. 3, pp. 2127–2139, May 2018.

[38] H. Gao, J. Liu, L. Wang, and Z. Wei, "Decentralized energy management for networked microgrids in future distribution systems," *IEEE Transactions on Power Systems*, vol. 33, no. 4, pp. 3599–3610, July 2018.

[39] Z. Wang, B. Chen, J. Wang, and J. Kim, "Decentralized energy management system for networked microgrids in grid-connected and islanded modes," *IEEE Transactions on Smart Grid*, vol. 7, no. 2, pp. 1097–1105, March 2016.

[40] A. Waqar, J. Hu, M. Awais, S. Xia, and X. Ai, "Distributed operation of multi-microgrids under censored communication," in *2021 4th International Conference on Energy, Electrical and Power Engineering (CEEPE)*. IEEE, April 2021.

[41] D. Tenfen and E. C. Finardi, "A mixed integer linear programming model for the energy management problem of microgrids," *Electric Power Systems Research*, vol. 122, pp. 19–28, May 2015.

[42] Y. Wen, C. Y. Chung, X. Liu, and L. Che, "Microgrid dispatch with frequency-aware islanding constraints," *IEEE Transactions on Power Systems*, vol. 34, no. 3, pp. 2465–2468, May 2019.

[43] D. E. Olivares, C. A. Cañizares, and M. Kazerani, "A centralized energy management system for isolated microgrids," *IEEE Transactions on Smart Grid*, vol. 5, no. 4, pp. 1864–1875, July 2014.

[44] E. Mayhorn, L. Xie, and K. Butler-Purry, "Multi-time scale coordination of distributed energy resources in isolated power systems," *IEEE Transactions on Smart Grid*, vol. 8, no. 2, pp. 998–1005, March 2017.

[45] W. Su, J. Wang, and J. Roh, "Stochastic energy scheduling in microgrids with intermittent renewable energy resources," *IEEE Transactions on Smart Grid*, vol. 5, no. 4, pp. 1876–1883, July 2014.

[46] S. Raychaudhuri, "Introduction to Monte Carlo simulation," in *Proceedings of the 40th Conference on Winter Simulation*, December 2008, pp. 91–100.

[47] D. Wang, X. Guan, J. Wu, P. Li, P. Zan, and H. Xu, "Integrated energy exchange scheduling for multimicrogrid system with electric vehicles," *IEEE Transactions on Smart Grid*, vol. 7, no. 4, pp. 1762–1774, July 2016.

[48] M. Mazidi, A. Zakariazadeh, S. Jadid, and P. Siano, "Integrated scheduling of renewable generation and demand response programs in a microgrid," *Energy Conversion and Management*, vol. 86, pp. 1118–1127, October 2014.

[49] E. G. Vera, C. A. Cañizares, M. Pirnia, T. P. Guedes, and J. D. M. Trujillo, "Two-stage stochastic optimization model for multi-microgrid planning," *IEEE Transactions on Smart Grid*, vol. 14, no. 3, pp. 1723–1735, May 2023.

[50] V. Gabrel, C. Murat, and A. Thiele, "Recent advances in robust optimization: An overview," *European Journal of Operational Research*, vol. 235, no. 3, pp. 471–483, June 2014.

[51] R. Gupta and N. K. Gupta, "A robust optimization based approach for microgrid operation in deregulated environment," *Energy Conversion and Management*, vol. 93, pp. 121–131, January 2015.

[52] A. Hussain, V.-H. Bui, and H.-M. Kim, "Robust optimal operation of AC/DC hybrid microgrids under market price uncertainties," *IEEE Access*, vol. 6, pp. 2654–2667, December 2017.

[53] J. D. Lara, D. E. Olivares, and C. A. Cañizares, "Robust energy management of isolated microgrids," *IEEE Systems Journal*, vol. 13, no. 1, pp. 680–691, March 2019.

[54] D. E. Olivares, J. D. Lara, C. A. Cañizares, and M. Kazerani, "Stochastic-predictive energy management system for isolated microgrids," *IEEE Transactions on Smart Grid*, vol. 6, no. 6, pp. 2681–2693, November 2015.

[55] Y. Zhang, F. Meng, R. Wang, W. Zhu, and X.-J. Zeng, "A stochastic MPC based approach to integrated energy management in microgrids," *Sustainable Cities and Society*, vol. 41, pp. 349 – 362, August 2018.

[56] M. Pirnia, C. A. Cañizares, K. Bhattacharya, and A. Vaccaro, "A novel affine arithmetic method to solve optimal power flow problems with uncertainties," *IEEE Transactions on Power Systems*, vol. 29, no. 6, pp. 2775–2783, November 2014.

[57] B. Thanigaivelan, A. Postula, and Y. Ding, "A self-validated computation approach to symbolic analysis of analog integrated circuits," in *Proceedings of the 9th International Workshop on Symbolic Methods and Applications to Circuit Design*, October 2006, pp. 1–6.

[58] J. Stolfi and L. H. de Figueiredo, "Self-validated numerical methods and applications," in *Proceedings of the 21st Brazilian Mathematics Colloquium*, vol. 5, 1997.

[59] ——, "An introduction to affine arithmetic," *TEMA-Tendências em Matemática Aplicada e Computacional*, vol. 4, no. 3, pp. 297–312, June 2003.

[60] L. H. de Figueiredo and J. Stolfi, "Affine Arithmetic: Concepts and Applications," *Numerical Algorithms*, vol. 37, pp. 147–158, December 2004.

[61] A. Vaccaro and C. A. Cañizares, "An affine arithmetic-based framework for uncertain power flow and optimal power flow studies," *IEEE Transactions on Power Systems*, vol. 32, no. 1, pp. 274–288, January 2017.

[62] M. Pirnia, C. Cañizares, K. Bhattacharya, and A. Vaccaro, "An affine arithmetic approach for microgrid dispatch with variable generation and load," in *2014 Power Systems Computation Conference*, August 2014, pp. 1–8.

[63] D. Romero-Quete and C. A. Cañizares, "An affine arithmetic-based energy management system for isolated microgrids," *IEEE Transactions on Smart Grid*, vol. 10, no. 3, pp. 2989–2998, May 2019.

[64] A. Vaccaro, M. Petrelli, and A. Berizzi, "Robust optimization and affine arithmetic for microgrid scheduling under uncertainty," in *2019 IEEE International Conference on Environment and Electrical Engineering and 2019 IEEE Industrial and Commercial Power Systems Europe (EEEIC / I&CPS Europe)*, June 2019, pp. 1–6.

[65] X. Wang and W. Zheng, "Optimal dispatch of multi-microgrids system based on affine arithmetic," in *2021 IEEE 2nd China International Youth Conference on Electrical Engineering (CIYCEE)*, December 2021, pp. 1–6.

[66] M. Barnes, J. Kondoh, H. Asano, J. Oyarzabal, G. Ventakaramanan, R. Lasseter, N. Hatziargyriou, and T. Green, "Real-world microgrids - an overview," in *2007 IEEE International Conference on System of Systems Engineering*, April 2007, pp. 1–8.

[67] M. H. Saeed, W. Fangzong, B. A. Kalwar, and S. Iqbal, "A review on microgrids' challenges & perspectives," *IEEE Access*, vol. 9, pp. 166 502–166 517, December 2021.

[68] J. M. Guerrero, J. C. Vásquez, and R. Teodorescu, "Hierarchical control of droop-controlled DC and AC microgrids — A general approach towards standardization," in *2009 35th Annual Conference of IEEE Industrial Electronics*, November 2009, pp. 4305–4310.

[69] A. Mehrizi-Sani and R. Iravani, "Potential-function based control of a microgrid in islanded and grid-connected modes," *IEEE Transactions on Power Systems*, vol. 25, no. 4, pp. 1883–1891, November 2010.

[70] P. Delgoshaei and J. D. Freihaut, "Development of a control platform for a building-scale hybrid solar PV-natural gas microgrid," *Energies*, vol. 12, no. 21, November 2019.

[71] A. D. Bintoudi, L. Zyglakis, T. Apostolos, D. Ioannidis, S. Al-Agtash, J. L. Martinez-Ramos, A. Onen, B. Azzopardi, L. Hadjidemetriou, N. Martensen, C. Demoulias, and D. Tzovaras, "Novel hybrid design for microgrid control," in *2017 IEEE PES Asia-Pacific Power and Energy Engineering Conference (APPEEC)*, November 2017, pp. 1–6.

[72] W. Su and J. Wang, "Energy management systems in microgrid operations," *The Electricity Journal*, vol. 25, no. 8, pp. 45 – 60, October 2012.

[73] A. Bani-Ahmed, M. Rashidi, A. Nasiri, and H. Hosseini, "Reliability analysis of a decentralized microgrid control architecture," *IEEE Transactions on Smart Grid*, vol. 10, no. 4, pp. 3910–3918, July 2019.

[74] D. Y. Yamashita, I. Vechiu, and J.-P. Gaubert, "A review of hierarchical control for building microgrids," *Renewable and Sustainable Energy Reviews*, vol. 118, p. 109523, February 2020.

[75] K. Hitchens, "Chula Vista solar microgrid to save school district $70 million," https://www.microgridknowledge.com/editors-choice/article/11436852/chula-vista-solar-microgrid-to-save-school-district-70-million, October 2022, [Accessed: January 15, 2023].

[76] Y. Ali, "New Siemens Microgrid Plans to Provide Flexibility for Vienna's Grid," https://www.microgridknowledge.com/regions/europe/article/11428237/new-siemens-microgrid-plans-to-provide-flexibility-for-viennas-grid, February 2021, [Accessed: January 15, 2023].

[77] G. Post, "Case study: How a DC microgrid helps over 10,000 Kenyan tea growers bring their product to market," https://www.microgridknowledge.com/resources/microgrid-case-studies/article/11437319/alencon-systems-case-study-how-a-dc-microgrid-helps-over-10000-kenyan-tea-growers-bring-their-product-to-market, October 2022, [Accessed: January 15, 2023].

[78] X. Zhou, L. Zhou, Y. Chen, J. M. Guerrero, A. Luo, W. Wu, and L. Yang, "A microgrid cluster structure and its autonomous coordination control strategy," *International Journal of Electrical Power & Energy Systems*, vol. 100, pp. 69–80, September 2018.

[79] F. Li, C. Cañizares, and Z. Lin, "Energy management system for DC microgrids considering battery degradation," in *2020 IEEE Power & Energy Society General Meeting (PESGM)*, August 2020, pp. 1–5.

[80] V. Amir, S. Jadid, and M. Ehsan, "Probabilistic optimal power dispatch in multi-carrier networked microgrids under uncertainties," *Energies*, vol. 10, no. 11, p. 1770, November 2017.

[81] B. Zhao, X. Wang, D. Lin, M. M. Calvin, J. C. Morgan, R. Qin, and C. Wang, "Energy management of multiple microgrids based on a system of systems architecture," *IEEE Transactions on Power Systems*, vol. 33, no. 6, pp. 6410–6421, November 2018.

[82] S. Wang, H. Gangammanavar, S. D. Ekşioğlu, and S. J. Mason, "Stochastic optimization for energy management in power systems with multiple microgrids," *IEEE Transactions on Smart Grid*, vol. 10, no. 1, pp. 1068–1079, January 2019.

[83] K. Rahbar, C. C. Chai, and R. Zhang, "Energy cooperation optimization in microgrids with renewable energy integration," *IEEE Transactions on Smart Grid*, vol. 9, no. 2, pp. 1482–1493, March 2018.

[84] E. Harmon, U. Ozgur, M. H. Cintuglu, R. de Azevedo, K. Akkaya, and O. A. Mohammed, "The internet of microgrids: A cloud-based framework for wide area networked microgrids," *IEEE Transactions on Industrial Informatics*, vol. 14, no. 3, pp. 1262–1274, March 2018.

[85] H. Qiu, W. Gu, Y. Xu, Z. Wu, S. Zhou, and G. Pan, "Robustly multi-microgrid scheduling: Stakeholder-parallelizing distributed optimization," *IEEE Transactions on Sustainable Energy*, vol. 11, no. 2, pp. 988–1001, April 2020.

[86] A. Kargarian and M. Rahmani, "Multi-microgrid energy systems operation incorporating distribution-interline power flow controller," *Electric Power Systems Research*, vol. 129, pp. 208–216, December 2015.

[87] Y. Zhang, T. Zhang, R. Wang, Y. Liu, B. Guo, and T. Zhang, "Dynamic dispatch of isolated neighboring multi-microgrids based on model predictive control," in *2016 International Conference on Smart Grid and Clean Energy Technologies (ICSGCE)*, October 2016, pp. 50–55.

[88] B. Zhou, J. Zou, C. Y. Chung, H. Wang, N. Liu, N. Voropai, and D. Xu, "Multi-microgrid energy management systems: Architecture, communication, and scheduling strategies," *Journal of Modern Power Systems and Clean Energy*, vol. 9, no. 3, pp. 463–476, May 2021.

[89] T. Yang, X. Yi, J. Wu, Y. Yuan, D. Wu, Z. Meng, Y. Hong, H. Wang, Z. Lin, and K. H. Johansson, "A survey of distributed optimization," *Annual Reviews in Control*, vol. 47, pp. 278–305, 2019.

[90] S. Marzal, R. Salas, R. González-Medina, G. Garcerá, and E. Figueres, "Current challenges and future trends in the field of communication architectures for microgrids," *Renewable and Sustainable Energy Reviews*, vol. 82, pp. 3610–3622, February 2018.

[91] M. Shahidehpour, Z. Li, S. Bahramirad, Z. Li, and W. Tian, "Networked microgrids: Exploring the possibilities of the IIT-Bronzeville grid," *IEEE Power and Energy Magazine*, vol. 15, no. 4, pp. 63–71, 2017.

[92] L. Cohn, "Here comes the future: Bronzeville 'microgrid cluster' set to begin operating this year," https://www.microgridknowledge.com/distributed-energy/article/11427478/here-comes-the-future-bronzeville-microgrid-cluster-set-to-begin-operating-this-year, January 2022, [Accessed: January 15, 2023].

[93] A. J. Conejo, E. Castillo, R. Mínguez, and R. García-Bertrand, *Decomposition Techniques in Mathematical Programming: Engineering and Science Applications*. Springer Science & Business Media, 2006.

[94] D. P. Bertsekas, "Chapter 1 - Introduction," in *Constrained Optimization and Lagrange Multiplier Methods*, D. P. Bertsekas, Ed. Academic Press, 1982, pp. 1–94.

[95] S. Boyd, N. Parikh, E. Chu, B. Peleato, and J. Eckstein, "Distributed optimization and statistical learning via the alternating direction method of multipliers," *Foundations and Trends in Machine Learning*, vol. 3, no. 1, pp. 1–122, 2010.

[96] J. Kazempour, "Distributed Optimization, Lecture 3: (Augmented) Lagrangian Relaxation," 2019, DTU CEE Summer School.

[97] M. L. Fisher, "The Lagrangian relaxation method for solving integer programming problems," *Management Science*, vol. 50, no. 12, pp. 1861–1871, December 2004.

[98] S. Boyd, L. Xiao, and A. Mutapcic, "Subgradient methods," *Lecture Notes of EE392o, Stanford University, Autumn Quarter*, 2003.

[99] B. V. Solanki, C. A. Cañizares, and K. Bhattacharya, "Practical energy management systems for isolated microgrids," *IEEE Transactions on Smart Grid*, vol. 10, no. 5, pp. 4762–4775, September 2019.

[100] M. Carrion and J. M. Arroyo, "A computationally efficient mixed-integer linear formulation for the thermal unit commitment problem," *IEEE Transactions on Power Systems*, vol. 21, no. 3, pp. 1371–1378, August 2006.

[101] G. P. McCormick, "Computability of global solutions to factorable nonconvex programs: Part I – Convex underestimating problems," *Mathematical Programming*, vol. 10, no. 1, pp. 147–175, December 1976.

[102] T. Lambert, P. Gilman, and P. Lilienthal, *Micropower System Modeling with HOMER*. John Wiley & Sons, Ltd, 2005, ch. 15, pp. 379–418.

[103] T. Xu, A. B. Birchfield, K. M. Gegner, K. S. Shetye, and T. J. Overbye, "Application of Large-Scale Synthetic Power System Models for Energy Economic Studies," in *50th Hawaii International Conference on System Sciences*, January 2017.

[104] "Brazil electricity prices, September 2022," https://www.globalpetrolprices.com/Brazil/electricity_prices/, October 2022, [Accessed: April 3, 2023].

[105] Gurobi Optimization, LLC, "Gurobi Optimizer Reference Manual," 2022. [Online]. Available: https://www.gurobi.com

[106] H. Ahmadi, J. R. Martí, and A. Moshref, "Piecewise linear approximation of generators cost functions using max-affine functions," in *2013 IEEE Power & Energy Society General Meeting (PESGM)*, July 2013, pp. 1–5.

[107] J. Bisschop, *AIMMS Optimization Modeling*. AIMMS B.V., July 2018.

[108] C. Ceja-Espinosa, M. Pirnia, and C. A. Cañizares, "A privacy-preserving energy management system for cooperative multi-microgrid networks," in *11th Bulk Power Systems Dynamics and Control Symposium (IREP 2022)*, July 2022. [Online]. Available: https://arxiv.org/abs/2207.04359

[109] ——, "An affine arithmetic-based energy management system for cooperative multi-microgrid networks," *IEEE Transactions on Smart Grid*, Accepted August 2023.